



Joanna Pawłat

Electrical discharges in humid environments

Generators, effects, application

MONOGRAPHIE

Electrical discharges in humid environments

Generators, effects, application

Monografie – Politechnika Lubelska



Politechnika Lubelska
Wydział Elektrotechniki i Informatyki
ul. Nadbystrzycka 38A
20-618 Lublin

Joanna Pawłat

Electrical discharges in humid environments

Generators, effects, application



Politechnika Lubelska
Lublin 2013

Reviewers:

Professor Mirosław Dors

Professor Zdenko Machala

This work was supported by National Science Centre in Poland,
grant no N N510 674540

Publication approved by the Rector of Lublin University of Technology

© Copyright by Lublin University of Technology 2013

ISBN: 978-83-63569-37-2

Publisher: Lublin University of Technology
ul. Nadbystrzycka 38D, 20-618 Lublin, Poland

Realization: Lublin University of Technology Library
ul. Nadbystrzycka 36A, 20-618 Lublin, Poland
tel. (81) 538-46-59, email: wydawca@pollub.pl
www.biblioteka.pollub.pl

Printed by : TOP Agencja Reklamowa Agnieszka Łuczak
www.agencjatop.pl

Impression: 100 copies

Contents:

Symbols	7
1. Introduction	9
2. Electrical discharges in humid environments	11
2.1. Electrical discharges in liquids: considerations on basic phenomena.....	11
2.2. Advanced oxidation processes	17
2.3. Non-thermal plasma reactors for humid environments	27
2.4. Foaming column.....	44
2.4.1. Foaming phenomena	46
2.4.2. Electrical discharge in foam	49
2.4.3. Formation of oxidants in foam	53
3. Removal of organic compounds using reactors working in humid environment.....	59
3.1. Selected examples of plasma treatment techniques employing liquids	62
3.1.1. Removal of phenol	62
3.1.2. Removal of dyes and pollutants from textile industry	73
3.2. Foaming system for abatement of organic compounds	81
4. Selected applications of plasmas and oxidative species for multi-phase environments	93
4.1. Plasma application for biomedical purposes	93
4.1.1. Methods of decontamination	94
4.1.2. Atmospheric pressure plasma jet.....	95
4.2. Application of oxidative species for treatment of soil.....	96
4.2.1. Ozone and soil properties	97
4.2.2. Oxidants in abatement of chemical pollutants in soil	101
4.2.3. Influence of ozone treatment on plants' growth and microorganisms in soil	105
5. Conclusions	111
6. References	113
Figures	131
Tables.....	137
Streszczenie	139

Symbols

A	- absorbance
A_i	- initial absorbance
A_t	- absorbance of solution treated for given time
a	- residual concentration
$C_p\rho$	- specific heat per unit volume
c	- concentration
c_0	- initial concentration at $t = 0$
c_t	- concentration at time t
C	- capacitance
D	- thermal diffusivity of water
d_{inEz}	- inside diameter of electrode
d_{outEw}	- outside diameter of electrode
d_{inR}	- inside diameter of reactor
E^0	- oxidation potential
E_a	- Arrhenius activation energy for the water conductivity
E_p	- pulse energy
E/n_0	- reduced electric field
ε	- molar absorbtivity
ε_0	- vacuum permittivity
ε_r	- relative permittivity
F_D	- decolourisation factor
f	- pulse repetition rate
G	- contaminant conversion yield
G_{50}	- G yield value at 50% of contaminant conversion
k	- reaction rate constant
L	- breakdown channel length
L_R	- length of reactor
l	- path length of the sample (path length of the cuvette in which the sample is contained)
λ	- wavelength
η	- efficiency
P	- discharge power
Q	- flow rate
R_0	- breakdown channel radius
RDR	- rate of the dye removal
σ	- conductivity of water
T_0	- temperature
t	- time
t_{50}	- time required for 50% pollutant's conversion
t_{eq}	- equivalence point
U	- voltage
V	- breakdown voltage
V_s	- volume of the sample

1. Introduction

Presently, escalation of consumer's demands associated with growth of population reflects in over-consumption, over-production and over-exploitation of natural resources. Ecological foot-print is one of the measures, which bound demands of population with the capital of natural resources and ability of the ecosystems to regenerate. Unfortunately, this measure, especially, in developed countries shows that to maintain present life style one planet's resources are simply not enough. Deterioration of quality of waters, soils and air due to the uncontrolled releases of not fully purified wastewaters and exhaust gases prove that ecological awareness of society, development of environmental standards and waste treatment technologies are not going in pair with the consumption growth.

There are many examples of chemical compounds of industrial or biological origin, which cause wastes to be classified as toxic, hardly-treatable or non-recyclable. Treatment technologies for them exist, but they are not implemented for several reasons, including the economical one (crucial in developing countries), system complexity and the operational difficulties. Removal of hazardous organic pollutants from groundwater, wastewater, soil and other multiphase environments in XXI century still remains one of the critical and urgent topics in environmental research. The aim of many research teams is to develop new, effective and possibly cheap techniques of the treatment to reduce environmental burden.

Plasma and Advanced Oxidation Processes (AOPs) are well known for excellent efficiency toward variety of pollutants as plasma comprises highly energetic species including charged particles, chemically reactive metastable species, free radicals, and UV photons. There are numbers of methods for generating active species, especially radicals that may be applied in AOP. However, a common feature of AOP is that the radical production involves a significant expense of the energy (either chemical, electrical or radiative).

Electrical discharges effecting in generation of non-thermal plasma, which can be used for the treatment of many types of pollutants are considered to be a relatively energy efficient method for production of active species. Plasma methods effectively combine the contributions of high electric fields, UV radiation and active chemicals, leading to higher treatment efficiency. Different designs of plasma reactors and variety of electrical discharge types (AC, DC, pulsed) generated either directly in water, in the gas introduced to water or above the water surface have been studied world-wide as possible methods for abatement of pollutants. Basic considerations on electrical breakdown in liquid are given in this book in order to understand the complexity of the process and number of factors, which should be addressed before

establishing the hybrid plasma reactors in the industrial field. Another important aspect on the edge of chemical and electrical engineering is knowledge of further interactions in gas-liquid systems.

This work also presents some chosen aspects of application of electrical discharges and oxidants in humid environment. The main goal is an introduction and popularization of hybrid plasma reactors (especially, the foaming system as potentially advantageous for conducting various technological processes) and presentation of their abilities for the generation of oxidants and pollutants' treatment. Moreover, basic chemical reactions initiated by the discharge and the effects of the physical processes on the promotion of desirable chemical reactions are introduced for selected reactors and model contaminants. Types of reactors studied by renowned research groups, selected pollutants, degradation processes, removal efficiency and oxidation products of model compounds are analyzed. Some miscellaneous applications of plasmas for multiphase environments, usually, not considered in main-stream research works but still worth attention are depicted.

2. Electrical discharges in humid environments

2.1. Electrical discharges in liquids: considerations on basic phenomena

The origin of interest in electrical discharges in liquids ranges eighties, when partial discharge, a localized dielectric breakdown in organic insulation fluids was studied by pulse power engineers. Partial discharges that occur in the organic liquids release by-products that have a lower molecular weight (lower vaporization temperature) and produce bubble impurities inside the medium affecting properties of original material. Problems related to the power engineering field mainly involved chemically induced ageing of the molecular liquid, which leads to a degradation of dielectric strength, electroosmotic flows, and tribo-charging (Beroual et al., 1998; Beroual and Aka-N'Gnui, 2002; Ceccato, 2009; Foffana and Beroual, 1998; Yang, 2011).

In the case of solid particles (or aggregation of particles) in electric field, two types of flow should be considered (Niewulis et al., 2007; Ristenpart et al., 2007; Zhao and Adamiak, 2009):

- electroosmotic flow (EOF) driven by the action of applied field on equilibrium diffuse charge layer near the particle. Many particles acquire a surface charge when in contact with the electrolyte. The immobile surface charge in turn attracts a cloud of free ions of opposite sign creating thin (1 - 10nm under typical conditions, e.g., univalent electrolyte at a concentration of 1 - 100mol/m³) Debye layer of mobile charges next to it. Thickness of this electric double layer is determined by a balance between the intensity of thermal (Brownian) fluctuations and the strength of electrostatic attraction to the substrate. In the presence of external electric field, fluid in this charged Debye layer acquires a momentum, which is then transmitted to adjacent layers of fluid through the effect of viscosity. If the fluid phase is mobile (such as in a packed bed of particles or in a narrow capillary), it would cause the fluid to flow (electroosmosis) (Castellanos, 1998; Ghosal, 2004; Kozlov et al., 2008);
- electrohydrodynamic (EHD) flow, which is the result of interaction between drifting ions and surrounding fluid (gas/liquid) molecules in applied electric field, which accelerates them.

Analytical calculations of two flow fields in the limits of infinitesimal double layers and slowly varying current indicate that the EOF and EHD flows are of comparable magnitude near the particle whereas in the far field, the EHD flow along the electrode is predominant. Moreover, dependence of EHD flow on the applied potential provides possible explanation for increased variability in aggregation velocities observed at higher field strengths.

Any low-conductivity liquid can be considered as a conductor or as an insulating medium depending on the timescale. Relevant time is Maxwell relaxation time that is the ratio of dielectric permittivity and electrical conductivity. From the practical point of view an insulating liquid is characterized by its dielectric strength. This strength quantifies voltage that medium is able to sustain without breakdown. It is a property related to the nature of liquid, applied voltage level and duration, and interelectrode gap. Due to dielectric behavior combined with large dielectric permittivity, high voltage pulse forming lines on microsecond timescale in many pulse power systems use distilled water as an insulating media. Power transformers or electrical distribution in industry working in AC modes usually are insulated with organic liquids such as castor oil, mineral oil, classical transformer oil, or recently ester liquids (Ceccato, 2009). Electrons in liquids are localized on molecule or molecular aggregates, or are solvated (trapped in bulk medium), but they are not free (Christophorou and Siomos, 1984).

Generally liquids can be divided into electrolytes (conductors, like acids, bases and salts) and non-electrolytes (alcohols, urea solution).

In electrolytes, electrical charge is conducted not by electrons but via ions. Decomposition of electrolytes in aqueous solutions onto the carrying charge is called electrolytic dissociation and was described by Arrhenius in 1887. Electrical current is not necessary for dissociation, but when to two electrodes in such a solution DC voltage is applied, the current appears due to flow of anions to anode and cations to cathode. After the charge transfer, neutral atoms are eventually set off from the solution. Above phenomena are known as electrolysis.

Water is highly polar (relative permittivity of $\epsilon_r=80$), low molecular weight liquid and, as mentioned before, the conductivity is in competition with the dielectric behavior of medium. Electrical conductivity of water ranges from about $1\mu\text{S}/\text{cm}$ for distilled water to several thousand $\mu\text{S}/\text{cm}$ for cooling water, depending on the amount of dissolved ions in water. When concentration of the solution increases, conductivity also increases to certain maximum limiting value. Further increasing of concentration brings up to decreasing conductivity.

Given that a specific water is exposed to the electric pulse with duration of Δt , when $\Delta t \gg \epsilon_r \epsilon_0 / \sigma_0$, where ϵ_0 is vacuum permittivity and σ_0 is the conductivity of water, the aqueous solution can be considered a resistive medium. For long pulse, oxygen and hydrogen production takes place due to electrolysis. For short pulse duration $\Delta t \ll \epsilon_r \epsilon_0 / \sigma_0$ water behaves as dielectric medium and high applied voltage will lead to the breakdown of the solution (Sunka, 2001; Yang, 2011; Yang et al., 2012). In order to obtain electrical breakdown in liquid it is necessary to fulfill following condition:

$$V \geq [(DC_p \rho T_0^2) / (\sigma_0 E_a)]^{1/2} (L/R_0)$$

where:

V - breakdown voltage,

D - thermal diffusivity of water (ca. $1.5e^{-7} \text{m}^2/\text{s}$),

$C_p \rho$ - specific heat per unit volume,

T_0 - temperature,

σ_0 - water conductivity,

E_a - Arrhenius activation energy for the water conductivity,

L - breakdown channel length,

R_0 - breakdown channel radius.

On the other hand, water differs strongly from the liquefied noble gases at high pressure, and also from other insulating liquids from the electronic state point of view (Ceccato, 2009). High density of liquids and a short mean free path of electrons, requiring very high electric field E/n_0 are limiting factors for the discharges in liquid. High density of such liquids prevents electrons to accelerate and undergo dissociative collisions unless the electric field is several orders of magnitude higher compared to plasmas at atmospheric pressures. The critical breakdown condition for gas can be described by the Paschen curve, from which one can calculate the breakdown voltage. A value of 30kV/cm is a well-accepted breakdown voltage of air at 1atm. When one attempts to produce direct plasma discharge in water, a much higher breakdown voltage on the order of 30MV/cm is needed based on the Paschen curve due to the density difference between air and water. However, it was also proven that the breakdown of liquids can be performed not at the extremely high electric fields required by the Paschen curve but at those that only slightly exceed the breakdown electric fields in atmospheric pressure molecular gases (Yang, 2011).

Electron avalanches are almost impossible inside liquid because of low mobility and high recombination rate. One needs to explain why plasma discharge occurs whereas the electronic state of the liquid is unfavorable. A phase change can be required prior to electron avalanches. Thus thermodynamics can play a role and can be coupled to gas discharge physics.

Breakdown of liquids seems to have more in common with the breakdown of solids than gases (Atrazhev and Timoshkin, 1998; Ceccato, 2009; Elles et al., 2007; Ihara et al., 1997; Joshi et al., 2003; 2004; Li et al., 2011; Mikula et al, 1997; Tajima et al., 2000; Ushakov V., 2007).

Two basic mechanisms of liquid rupture can be distinguished:

- Specific (usually investigated in very thin liquid layers. Emission from cathode is the electrons' source. Near the surface of cathode, local, very strong electric fields are created ($100\text{kV}/\text{cm}^2$) because of some inhomogeneity of its external structure and several positive ions. Electrons from cathode collide with liquid particles, causing their oscillation (with energy 0.3eV),

or less probable dissociation (energy: 5.1eV) and ionization (energy: 10eV). Due to this fact, local temperature increases and gas bubbles can occur because of liquid evaporation. The last part of the process is similar to the breakdown in the gases);

- Non-specific (proceeds in liquids, which consists of some impurities (solid particles, water or gas)):

A) Cavitation theory (main reason of the rupture is presence of solid impurities in liquid. In the strong electric field, due to the electrostatic force, repulsion of liquid from conducting surface occurs and vacuum layer is created. At this point emission from the cathode takes place. Liquid is evaporated and the micro-bubble of gas occurs. Further processes can be compared to those in the gas, the micro-bubble elongates and gas channel is increasing its length till the electrodes are connected by one).

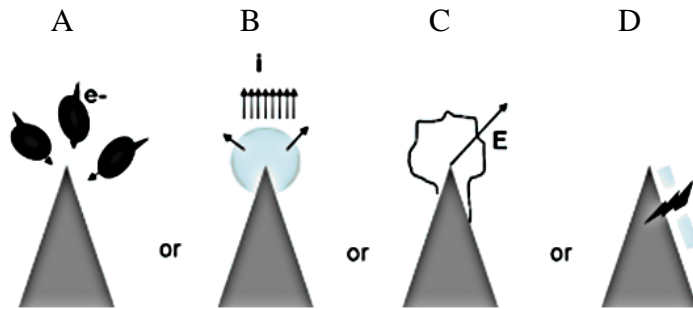


Fig. 2.1. Possible initiation mechanisms at the metal/liquid interface: avalanches in the liquid phase (A), ion conduction and nucleation by joule heating (B), cavity or crack created by electrostatic pressure (C), breakdown of an oxide layer or local electrode melting and plasma spot formation (D) (Ceccato, 2009)

B) Bridge theory (impurities and particles change their position due to the direction of electric field (depending on liquid viscosity, too). If they are transferred to strong electric field area, the impurities bridge is created. It increases electric field and again gas micro-bubble is formed).

Group of Atrazhev stated that high-mobility liquid breakdown is governed by electron ionization mechanism. The ionization mechanism development time is about several nanoseconds and bubble mechanism requires more than 1 μ s (Atrazhev et al., 1991). The energy per single photon ranges from 3.1eV to 6.2eV.

Transient absorption spectroscopy performed by (Elles et al., 2007) revealed the relative yields of ionization and dissociation following two-photon excitation of liquid water at 8.3 and 9.3eV. Two decay channels occurred with nearly equal

probability at the higher energy, but for 8.3eV excitation - the dissociation channel dominated.

Ceccato summarized possible following initiation mechanism of the discharge in liquid phase (Fig. 2.1) with potential transition states among them for instance: the electron avalanches in the liquid phase, solvated ion conduction and local heat conduction followed by a microbubble nucleation, charge injection, electrostatic stress and crack formation, and formation of plasma spot at the electrode due to the local melting or the oxide layer breakdown.

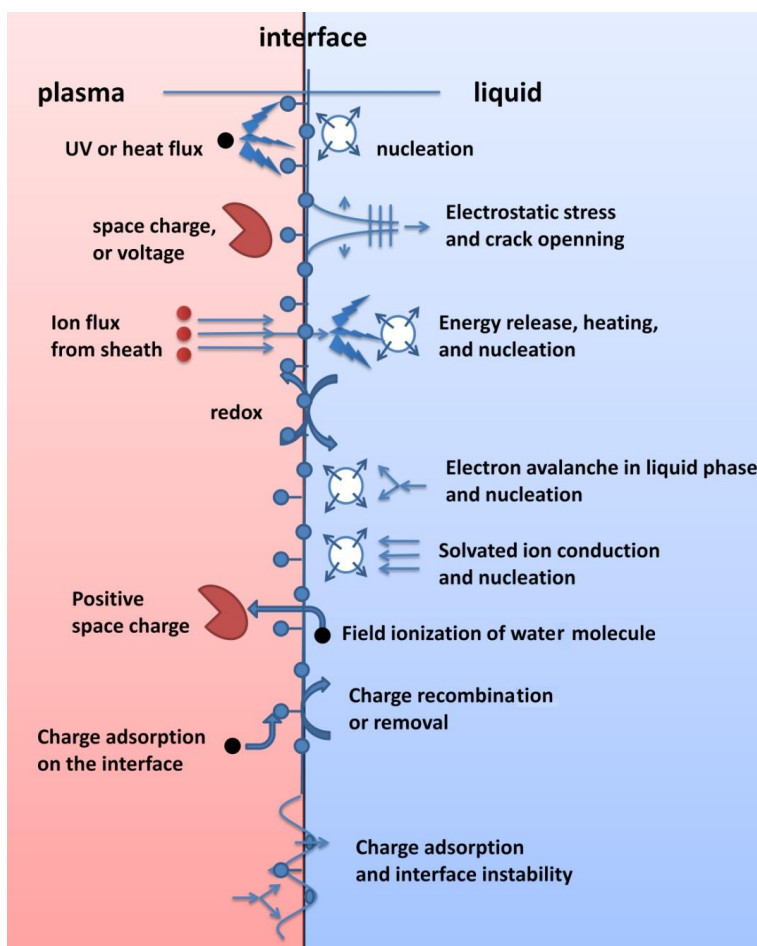


Fig. 2.2. Summary of the physical processes at the plasma/liquid interface (Ceccato, 2009)

Tab. 2.1. Summary of the characteristics of pulsed corona, pulsed arc and pulsed spark discharge in water (Yang, 2011; Yang et al., 2012)

Pulsed corona	Pulsed arc	Pulsed spark
<ul style="list-style-type: none"> - Non-thermal plasma. - High operating frequency (100 - 1000Hz). - Current transferred by slow ions. - Partial discharge: (streamer filaments do not propagate across electrode gap). - Streamer length: order of cm, channel width 10 - 20μm). - Energy per pulse: often less than 1J. - Weak to moderate UV generation. - Weak to moderate shockwave. - Relatively low current, i.e., peak current less than 100A. - A fast rising voltage. - Operating frequency 100 - 1000Hz. - Electric field intensity at the tip of electrode is 100 - 10000kV/cm. - Treatment area is limited at a narrow region near the corona discharge. 	<ul style="list-style-type: none"> - Quasi-thermal plasma. - Low operating frequency (<1Hz). - Current transferred by electrons. - High current filament channel bridges electrode gap. - Smaller gap between electrodes is needed about 5mm. - Large energy of discharges, greater than 1kJ/pulse. - Strong but short-lived UV emission. - Strong shockwave with cavitation zone. - Large current of 100A order with peak value greater than 1000A. - Voltage rise time 1 - 10μs. - Pulse duration about 10ms. - Light pulse from the spark includes 200nm wavelength. - Time delay between voltage pulse increase and spark formation depends on capacitance size and the electric conductivity of water. - Temperature of arc greater than 10000K. - Gas inside channel is ionized. 	<ul style="list-style-type: none"> - Similar to pulsed arc, except for short pulse duration and low temperature. - Pulsed spark is faster than pulsed arc, i.e., strong shockwaves are produced. - Plasma temperature in the spark is around a few thousand K.

Those processes need to establish a volume with suitable conditions for the propagation of a plasma cavity or a plasma filament. Among the mechanisms, contributing to formation of above phenomena are interface charging and repulsion, interface instability, interface etching by ion bombardment, sheath at the filament head, density lowering, avalanches, filamentation and electrostatic crack. Physical processes at the plasma/liquid interface were depicted by (Ceccato, 2009) in Fig. 2.2.

An interesting review on liquid-phase non-equilibrium plasma in water was given by group of Yang and Friedman from Drexel University. The basic characteristics of most common discharge types for underwater plasmas are presented in Tab. 2.1. Yang used a pulsed power system with 32 - 112kV pulse amplitude, 0.5 - 12ns pulse duration and 150ps rise time. Measurement with 4Picos ICCD camera with a minimum gate time of 200ps revealed that discharge in liquid water formed in a picosecond time scale, and the propagation velocity of the streamers was about 5000km/s. The reduced electric field E/n_0 at the tip of the streamer was about 200Td. Both, the propagation velocity and the reduced electric field in the test were similar to the streamer propagation in the gas phase, indicating that plasma could be formed in liquid phase without the phase change (Yang, 2011).

2.2. Advanced oxidation processes

Ozone in gaseous form is a well known oxidant. Industrially, ozone is generated in dry oxygen or air as a result of electrical discharge between two electrodes (at least one is covered by dielectric layer), using the devices called ozonizers (Eliasson and Kogelschatz, 1991; Kogelschatz, 1992). Ozone is utilized in treatment of gas, waters, wastewaters, and in many technological processes. This oxidant is able to improve water properties by removal of color, smell, and inactivation of pathogens. Ozone reacts with macromolecular organic pollutants, improves flocculation and successive removal of these substances. It can also increase the biological accessibility of organic pollutants when toxic substances are present, which otherwise inhibit the activity of microorganisms. In high doses ozone can even cause a complete wet oxidation, in which all present organic matter is wholly mineralized (Janknecht et al., 2001; Langlais et al., 1991; Maier, 1991; Morvova et al., 2004; Ozonek, 1993; 1996; Pollo, 1999; Pollo et al., 1981; Pschera, 1997; Takahashi et al., 1997).

Ozone half life period in air ranges 12 hours so it cannot be stored or transported and must be produced from oxygen or oxygen containing gases like air at the place and the time of consumption. To produce ozone, energy in a form of ultraviolet radiation or electrical discharges is applied to molecular oxygen (O_2). However, relatively small portion of oxygen can be transformed to ozone so it is always a mixture of ozone and carrying gas (ranging to 90% of the mass of the mixture). Usually in the case of application of gaseous ozone

to liquid, it needs to be transferred from the gas phase mixture into the liquid phase. Usually it is realized using contacting methods such as bubble columns, impellers, injectors, etc. Diffusion coefficient of ozone in water is relatively low; however, the transfer performance can be and in technical application often is considerably increased by mechanical agitation creating shear forces on the liquid boundary layer close to the surface, thus overlaying a fast convective transport with the slow diffusion (Janknecht et al., 2001).

Tab. 2.2. Advanced oxidation processes (Anotai et al., 2010; Bremner et al., 1996; Kwon et al., 2009; Nawrocki, 1999; Venkatadri and Peters, 1993)

Phase	UV presence	Process
Homogenic	+	O ₃ /UV H ₂ O ₂ /UV Electron beam Ultrasound
	-	O ₃ /H ₂ O ₂ O ₃ /OH ⁻ H ₂ O ₂ /Fe ²⁺
Heterogenic	+	TiO ₂ /O ₂ /UV TiO ₂ /H ₂ O ₂ /UV Fenton-electron beam Fenton-ultrasound
	-	Electro-Fenton Fluidized bed Fenton

Decomposition of ozone is much more rapid in water, depending on conditions; it takes from few seconds to few hours. High pH value, high temperature, organic matter and carbonates shorten the presence of ozone in water in its molecular form. Ozone reacts with pollutants directly or decomposes via catalytic reaction with other species (such as metal oxides) present in the environment to form the secondary oxidizing agents: omnipotent hydroxyl radicals, ozonide radicals, hydrogen peroxide, perhydroxyl, superoxide, and singlet oxygen (Glaze and Kang, 1988; Gordon and Bubnis, 1999; Staehelin and Hoigne, 1985; Voloshin et al., 1986). Each intrusion in gas and liquid matrix can affect physical, chemical and biological properties because many unstable and rapid chemical reactions can be expected after applying ozone.

AOPs employ several kinds of environmental friendly oxidants during one treatment cycle, giving a superposition effect. Thus, they are considered the most efficient way of the impurities' removal (De Laat et al., 1997; Gehringer et al., 1997; Karmi et al., 1997; Sentek et al., 2010; Schmidt-Szałowski et al., 2011; Tuhkanen et al., 1994).

Tab. 2.3. Basic reactions involving oxidative compounds in humid environment (Dors et al., 2005; Chen et al., 2002; 2009; Grymonpre et al., 2001; Mok et al., 2008)

Chemical reaction	Reaction rate constant [M ⁻¹ s ⁻¹]
$\text{H}_2\text{O}=\text{H}\cdot+\cdot\text{OH}$	1.7×10^{-7}
$2\text{H}_2\text{O}=\text{H}_2\text{O}_2+\text{H}_2$	3.9×10^{-6}
$\text{H}_2\text{O}=\text{H}^++\text{e}_{\text{aq}}+\cdot\text{OH}$	4.2×10^{-7}
$\text{e}_{\text{aq}}+\text{H}\cdot=\text{H}_2+\text{OH}^-$	2.5×10^{10}
$\text{e}_{\text{aq}}+\cdot\text{OH}=\text{OH}^-$	3.01×10^{10}
$\text{e}_{\text{aq}}+\text{HO}_2\cdot=\text{HO}_2^-$	2.01×10^{10}
$\text{e}_{\text{aq}}+\text{O}_2^{\cdot-}=\text{HO}_2^-+\text{OH}^-$	1.3×10^{10}
$\text{e}_{\text{aq}}+\text{H}_2\text{O}_2=\cdot\text{OH}+\text{OH}^-$	1.2×10^{10}
$\text{e}_{\text{aq}}+\text{HO}_2^{\cdot-}=\text{O}^-+\text{OH}^-$	3.51×10^9
$\text{e}_{\text{aq}}+\text{O}_2=\text{O}_2^{\cdot-}$	1.8×10^{10}
$\text{e}_{\text{aq}}+\text{H}^+=\text{H}\cdot$	2.31×10^{10}
$\text{e}_{\text{aq}}+\text{H}_2\text{O}=\text{OH}^-+\text{H}\cdot$	1.00×10^3
$2\text{e}_{\text{aq}}=\text{H}_2+2\text{OH}^-$	4.99×10^9
$2\text{H}\cdot=\text{H}_2$	7.82×10^9
$\text{H}\cdot+\cdot\text{OH}=\text{H}_2\text{O}$	2.51×10^{10}
$\text{H}\cdot+\text{HO}_2\cdot=\text{H}_2\text{O}_2$	2.01×10^{10}
$\text{H}\cdot+\text{O}_2^{\cdot-}=\text{HO}_2^-$	2.01×10^{10}
$\text{H}\cdot+\text{H}_2\text{O}_2=\text{H}_2\text{O}+\cdot\text{OH}$	8.44×10^6
$\text{H}\cdot+\text{O}_2=\text{HO}_2\cdot$	2.11×10^{10}
$\text{OH}^-+\text{H}\cdot=\text{e}_{\text{aq}}+\text{H}_2\text{O}$	2.21×10^7
$\cdot\text{OH}+\cdot\text{OH}=\text{H}_2\text{O}_2$	5.51×10^9
$\cdot\text{OH}+\text{O}^{\cdot-}=\text{HO}_2^-$	2.01×10^{10}
$\cdot\text{OH}+\text{HO}_2\cdot=\text{O}_2+\text{H}_2\text{O}$	6.32×10^9
$\cdot\text{OH}+\text{O}_2^{\cdot-}=\text{O}_2+\text{OH}^-$	8.22×10^9
$\cdot\text{OH}+\text{H}_2\text{O}_2=\text{HO}_2\cdot+\text{H}_2\text{O}$	4.07×10^7
$\cdot\text{OH}+\text{HO}_2^{\cdot-}=\text{HO}_2\cdot+\text{OH}^-$	7.52×10^7
$\cdot\text{OH}+\text{H}_2=\text{H}\cdot+\text{H}_2\text{O}$	3.82×10^7
$\cdot\text{OH}+\text{OH}^{\cdot-}=\text{O}^-+\text{H}_2\text{O}$	1.2×10^{10}
$2\text{O}^{\cdot-}=\text{OH}^-+\text{HO}_2^-$	1.0×10^9
$\text{O}_2^{\cdot-}+\text{O}^{\cdot-}=\text{O}_2+2\text{OH}^-$	6.02×10^8
$\text{O}^-+\text{H}_2\text{O}_2=\text{O}_2^{\cdot-}+\text{H}_2\text{O}$	5.01×10^8
$\text{O}^-+\text{HO}_2^{\cdot-}=\text{O}_2^{\cdot-}+\text{OH}^-$	4.01×10^8
$\text{O}^-+\text{H}_2=\text{H}\cdot+\text{OH}^-$	8.02×10^7
$\text{O}^-+\text{H}_2\text{O}=\text{OH}\cdot+\text{OH}^-$	1.76×10^6
$2\text{HO}_2\cdot=\text{O}_2+\text{H}_2\text{O}_2$	8.34×10^5
$\text{HO}_2\cdot+\text{H}_2\text{O}_2=\cdot\text{OH}+\text{O}_2+\text{H}_2\text{O}$	2.01×10^{-1}

Chemical reaction	Reaction rate constant [M ⁻¹ s ⁻¹]
$O_2^- + HO_2 \bullet = HO_2^- + O_2$	9.72×10^7
$HO_2 \bullet = H^+ + O_2^-$	7.52×10^5
$2O_2^- = H_2O_2 + O_2 + 2OH^-$	3.01×10^{-1}
$O_2^- + H_2O_2 = \bullet OH + O_2 + OH^-$	1.31×10^{-1}
$O_2^- + HO_2^- = O^- + O_2 + OH^-$	1.31×10^{-1}
$H^+ + O_2^- = HO_2 \bullet$	5.11×10^{10}
$H_2O_2 = 2 \bullet OH$	3.18×10^{-7}
$H_2O_2 + OH^- = HO_2^- + H_2O$	1.0×10^{10}
$HO_2^- + H_2O = H_2O_2 + OH^-$	1.13×10^6
$HO_2^- + H^+ = H_2O_2$	2.01×10^{10}
$H^+ + OH^- = H_2O$	1.4×10^{11}
$H_2O = H^+ + OH^-$	2.54×10^{-5}
$O^- + O_2 = O_3^-$	3.0×10^9
$O^- + O_3^- = 2O_2^-$	7.0×10^9
$H_2O_2 + O_3^- = O_2^- + O_2 + H_2O$	1.6×10^6
$HO_2^- + O_3^- = O_2^- + O_2 + OH^-$	8.9×10^5
$O_3^- = O_2 + O^-$	3.0×10^2
$H_2 + O_3^- = H \bullet + O_2 + OH^-$	2.5×10^5
$O^- + H^+ = OH^-$	1.0×10^{10}
$HO_2 \bullet + OH^- = O_2^- + H_2O$	1.0×10^{10}

At present, the electrical discharges, Fenton and Fenton-like processes, ozonation, TiO₂ photocatalysis, electron-beam and γ -beam irradiation, radiolysis and sonochemistry, electrochemical and wet oxidation, and photolysis in various combinations are considered the effective AOPs, utilizing non-selective and active OH radicals as oxidants to attack organic contaminants (Chen, 2004; Gierzatowicz and Pawłowski, 1996; Kusic et al., 2005; Shi et al., 2009). Examples of known AOPs are summarized in Tab. 2.2. Electrical discharge occurring directly within the liquid or addition of several types of separately produced oxidative species is also a good example of AOP. Chemical reactions employing oxidative compounds used in advanced oxidation technologies for humid environments are stated in Tab. 2.3. (Dors et al., 2005; Grymonpre et al., 2001). Properties of selected species are summarized in Tab. 2.4.

From the chemical point of view, underwater and liquid-interacting plasmas besides oxidative species are able to produce: flux of charged or heavy particles, pulsed electric field, UV irradiation, shock waves and thermal effects. Those different effects play simultaneously a role in the global chemical yield of the discharge and synergy has been observed especially in hybrid reactors (Ceccato, 2009; Feng et al., 2009).

Tab. 2.4. Properties of selected species involved in AOPs (Buxton et al., 1988; Lide, 2006; Petri et al., 2011)

Species	Formula	Standard electrochemical potential, [V]	pH where present	Role
Hydroxyl radical	$\bullet\text{OH}$	+2.59	pH<11.9	Strong oxidant
Hydrogen peroxide	H_2O_2	+1.77	pH<11.6	Strong oxidant, week reductant
Superoxide anion	O_2^-	-0.33	pH>4.8	Weak reductant
Perhydroxyl radical	$\text{HO}_2\bullet$	+1.49	pH<4.8	Strong oxidant
Hydroperoxide anion	HO_2^-	+0.88	pH>11.6	Week oxidant, week reductant
Singlet oxygen	$^1\text{O}_2$			
Ozone gas	O_3	+2.07		Strong oxidant
Atmospheric oxygen (normal triplet form)	O_2	+1.23		Week oxidant
Solvated electrons	$e_{(\text{aq})}^-$	-2.77	pH>7.85	Strong reductant

Influence of some of above effects is summarized in Tab. 2.5. Emission of ultraviolet and visible photons suggests that incorporation of photocatalysis into the electrical discharge system enhances the overall performance, especially in the terms of selectivity toward total oxidation/mineralization (Ceccato, 2009; Kim et al., 2003; Mok et al., 2008; Zhang et al., 2006).

Catalyst can be incorporated into the system in suspended or porous solid form, respectively. The usual catalysts are: photocatalyst such as TiO_2 ceramics or zeolites, activated carbon, metal particles or nano particles of noble metals used also in wet oxidation processes such as Ru, Rh, Pd, Ir, and Pt as well as oxides of Cr, Mn, Fe, Co, Ni, Cu, Zn, Mo, Al and Ce (Kim and Ihm, 2011). Similar as in gas discharges, the introduction of catalyst to a hybrid plasma reactor can influence the final chemical yield due to the porosity effect (that concentrates the pollutant in a localized region of liquid, or increases the residence time of the pollutant by adsorption on the pollutant), activation (that converts by-products or the pollutant itself) and modification of the discharge properties and thus modification of the discharge's chemical reactivity (Ceccato, 2009).

Tab. 2.5. Selected chemical and physical phenomena due to the electrical discharge in dense medium

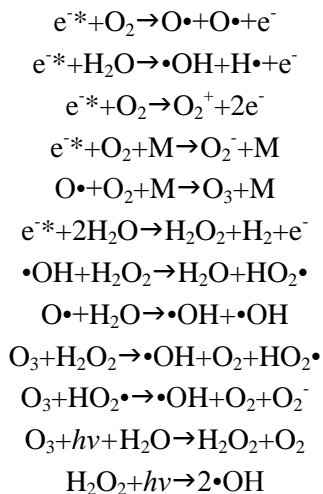
Phenomena	Effect	Ref.
UV emission	<ul style="list-style-type: none"> – initiates chemical reactions – oxidizes pollutants via direct photochemical attack or by water molecule dissociation – damages DNA, cell membranes, initiates apoptosis – low efficiency if produced only by plasma (the most efficient is hot arc discharge (black body radiation instead of discrete line emission)) 	(Anpilov et al., 2002; Hancock et al., 2003; Ceccato, 2009; Lukes, 2001)
Shock waves	<ul style="list-style-type: none"> – strong- produced by arc discharges and moderate- by corona-like discharges rather with direct excitation – in case of resonance and formation of thermal plasma may lead to sonoluminescence 	(Ceccato, 2009; Sunka et al., 2002)
Thermal effect	<ul style="list-style-type: none"> – mainly in the arc discharge – may lead to pyrolysis of the pollutant in the discharge region 	(Ceccato, 2009)

When discharge occurs in multiphase environment, the nature of activated species strongly depends on that of the liquid and gas.

Chemical processes that take place in the electrical discharges in water include direct formation of reactive radicals such as hydroxyl, hydrogen, superoxide, perhydroxyl and oxide anions, and molecular species such as hydrogen peroxide and ozone (Grymonpre et al., 2001). Ozone can oxidize contaminants in water in two ways (Kurniawan et al., 2006; Rosenfeldt et al., 2006):

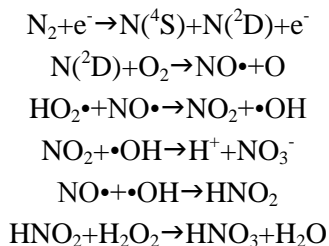
- direct reaction of gaseous ozone and dissolved ozone with the contaminants at the gas-liquid interface and in the bulk phase,
- decomposition of dissolved ozone and formation of powerful hydroxyl radicals, which further quickly react with the contaminants.

Additional reactions involving formation of oxidative species in water are cited by (Dojcinovic et al., 2011; Malik et al., 2001):



Group of Brisset (Abdelmalek et al., 2004; Depenyon et al., 2008; Njoyim-Tamungang et al., 2011) investigated humid air plasmas and electrical discharges on the surface of liquids. In such an environment, oxidative species derive from N_2 , O_2 and H_2O and therefore hydrogen peroxide, ozone or nitrogen oxides NO_x are expected, although O_3 is not favored by the occurrence of water. Emission spectroscopy measurements on a gliding arc plasma in humid air revealed that OH radicals and NO radicals are simultaneously present in the discharge, with much higher density for strongly oxidizing OH radicals than for NO radicals, which are known as parent molecules for acid derivatives HNO_2 , HNO_3 , inducing a steep pH lowering of the solution. Thus, presence of both types of radicals can enhance the treatment process (Abdelmalek et al., 2004; Benstaali et al., 1998; 1999; 2002; Chang, 1989; 1992; Matzing, 1994; Peyrous et al., 1987; Tsagou-Sobze et al., 2008).

Reactions employing nitrogen compounds in humid environments (Abdelmalek et al., 2008; Marouf-Khelifa et al., 2006) are as follows:



Plasma formed compounds are mainly considered with solute/plasma interactions and induce acid and oxidation reactions (Fig. 2.3).

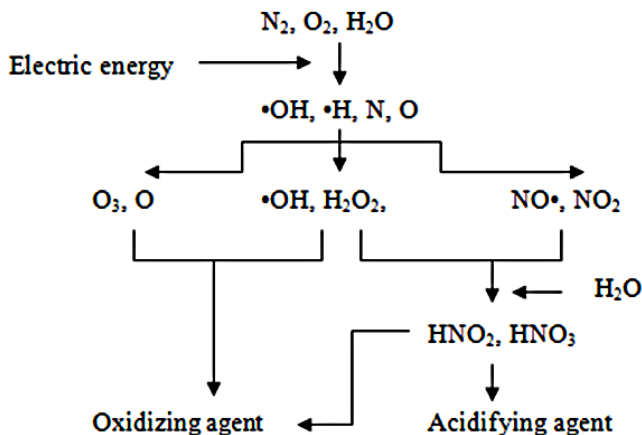


Fig. 2.3. Main molecular species in humid air plasma (Doubla et al., 2008)

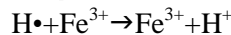
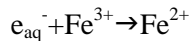
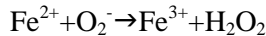
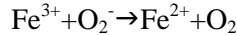
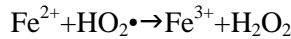
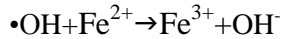
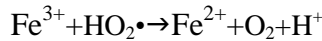
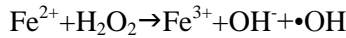
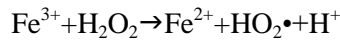
The acid effect is related to the formation of transient nitrous acid, ONOH (which disproportionates into NO and nitric acid for $\text{pH} < 6$) and stable nitric acid. Peroxynitrous acid is a weak acid ($\text{pK}_a = 6.8$). Oxidizing character is attributed to $\bullet\text{OH}$, H_2O_2 and ONO_2H .

Apart from these basic reactions, peroxynitrous acid and its matching salt, peroxynitrite, react as nitrosating and nitrating agents on double bonds and carboxylic acids. That makes them the key agents for bacterial inactivation because of their chemical attack at the microorganisms' membranes (Doubla et al., 2008; Njoyim-Tamungang et al., 2011).

Antelman summarized normal potential values (V/NHE), such as $E^0(\bullet\text{OH}/\text{H}_2\text{O}) = 2.72$; $E^0(\text{O}_3/\text{O}_2) = 2.07$; $E^0(\text{H}_2\text{O}_2/\text{H}_2\text{O}) = 1.76$; $E^0(\text{HO}_2\bullet/\text{H}_2\text{O}_2) = 1.5$ for the most popular systems (Antelman, 1982). Normal Hydrogen Electrode (NHE, potential of a platinum electrode in 1N acid solution) is a historical standard, sometimes still used.

Current standard for zero potential, e.g. the 0.0V thermodynamic reference point for all potential measurements at all temperatures is Standard Hydrogen Electrode (SHE, potential of a platinum electrode in a theoretical solution). The examples of standard oxidation potentials (V/SHE), of $E^0(\text{H}_2\text{O}_2/\text{H}_2\text{O}) = 1.68$; $E^0(\bullet\text{OH}/\text{H}_2\text{O}) = 2.85$ and $E^0(\text{ONOOH}/\text{NO}_2) = 2.05$ are noticeably higher than that of the oxygen system $E^0(\text{O}_2/\text{H}_2\text{O})$ and most of organic waste compounds are close to 0.5V/SHE. Thus, species present in the plasma are thermodynamically able to oxidize organic solutes. General degradation mechanism of large molecules involves the previous addition of $\bullet\text{OH}$ or $\text{NO}\bullet$ radicals on unsaturated bonds. Usually, in radical reactions, formation of organic radical, electrophilic addition and electron transfer are mentioned. OH radical is a very powerful, nonselective oxidant with 402.8MJ/mol energy, which can destruct the C–C,

when using electrodes containing iron. The primary active chemical radical produced by plasma discharge in water is OH and the stable form of OH is H₂O₂ which is also very good non selective oxidant. Unfortunately, the oxidation potential of H₂O₂ is lower than OH and not all pollutants are destroyed by H₂O₂. However, when ferrous ions are introduced in the liquid, Fenton reaction occurs: ferrous ion reacts with H₂O₂ to give back OH. Thus, it is a kind of catalytic regeneration process, which can increase the yield tenfold. Ferrous ion can originate from electrode redox dissolution or erosion in the liquid. This fact must be taken into account when performing chemical measurement. Ferrous ion can be manually added to the liquid as well. To use Fenton process more efficiently it is necessary to optimize the primary radical production by generating electrical discharge with higher reduced field and thus higher electron velocity. Discharge duration and volume should allow proper use of produced radicals instead of their recombination. Reactants should be distributed in the reaction chamber homogenously via enhancing of diffusion process and the reaction path should be recognized and optimized (Ceccato, 2009). Main chemical reactions involved in Fenton process are as follows:



Combination of active species mentioned in this chapter can impart energies as high as 10eV. Therefore, plasma can support abatement of many chemical contaminants and inactivate most of pathogens: Gram-negative and Gram-positive bacteria, microbial spores, molds and fungi, viruses and maybe even prions.

2.3. Non-thermal plasma reactors for humid environments

When considering environmental application of plasmas, the main share of the market goes to ozone generators of various constructions, where ozone is produced as an effect of electrical discharges in the gas phase. This well known technology is constantly developed and improved for more than 150 years. Gaseous ozone generated in ozonizer is usually further transported to medium, which requires treatment; for instance: to water, exhaust gas or sewage.

In the end of XX century some research groups started investigating a different approach: generation of electrical discharges and producing oxidants directly in polluted medium. This solution can possibly bring up to some economical savings due to smaller amount of required equipment, lack of additional tubing and contact tanks, saving space, simplification of set-up's control and maintenance, and limiting losses of oxidant during the transport. However, it has also some drawbacks as it is much easier and cheaper to generate electrical discharge in dry gas than in humid environment.

The aim of this part of book is introduction of the basic ideas related to the construction of plasma reactors, which are able to work in humid environments and presentation of designs proposed by various research groups including the original foaming plasma reactor.

Traditionally, the combination of plasma over and inside liquid at the same time can be performed in a hybrid reactor. Sometimes "hybrid" is used in the wider sense, when electrical discharges develop and proceed within at least two phases: gas and/or liquid and/or solid.

There are many attempts around the world to improve and further commercialize hybrid reactors.

Main trends can be recognized as follows:

- generation of active species directly in bulk liquid,
- generation of active species in gas bubbles introduced to the liquid,
- generation of active species during the surface processes at the electrode/liquid interface,
- generation of the electrical discharge above the surface of liquid,
- generation of active species in aerosols or wet gases.

In general, geometries of discharge reactors working in humid environment could be classified as:

- needle-plate,
- wire-cylinder,
- point-point,
- ring-cylinder reactor,
- plate-to-plate,
- pinhole, capillary, etc.

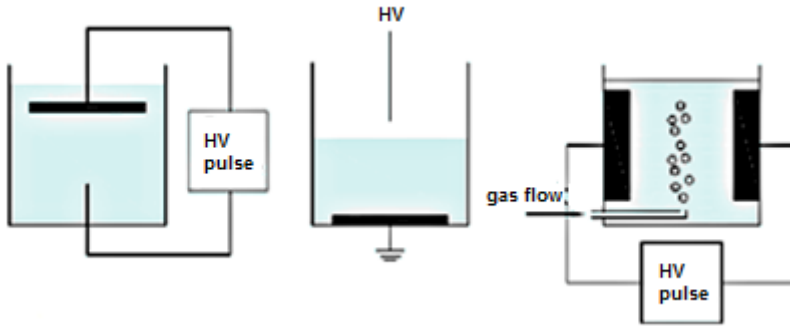


Fig. 2.5. Plasma underwater, overwater, inside bubbles (Bruggeman and Leys, 2009; Ceccato, 2009)

One can distinguish between breakdown in homogenous electric field (difficult to achieve for long (cm) gaps) with symmetrical electrode configuration, and breakdown in inhomogeneous electric field with strongly asymmetric electrode configuration such as point to plane.

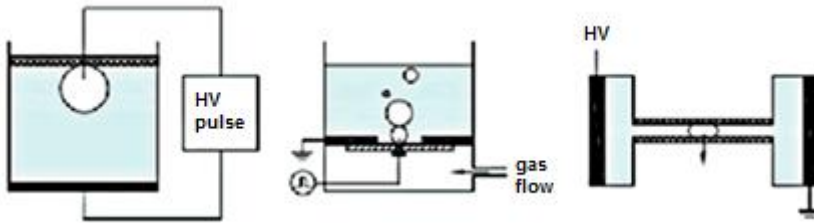


Fig. 2.6. Capillary discharge reactor configurations (Bruggeman and Leys, 2009; Ceccato, 2009)

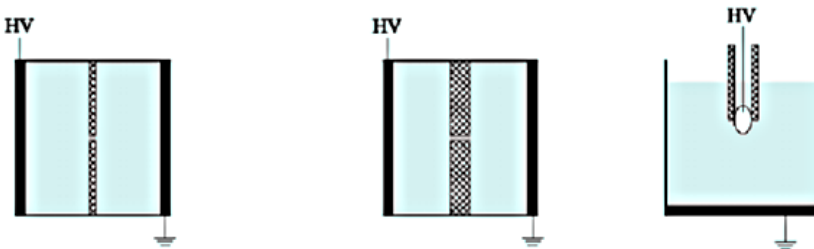


Fig. 2.7. Diaphragm discharge reactor configuration (Bruggeman and Leys, 2009; Ceccato, 2009; Neagoe et al. 2008)

However, short gaps in the range of hundreds of micrometers (often reported in literature as homogenous field case) also lead to a different phenomenology compared to that observed in larger gaps (cm).

The most exhaustive classification of presently used reactors from the presence of gas, discharge geometry, type and electrode configuration points of view was given by (Bruggeman and Leys, 2009) and cited by (Ceccato, 2009). Summary is presented in Figs. 2.5 - 2.10.

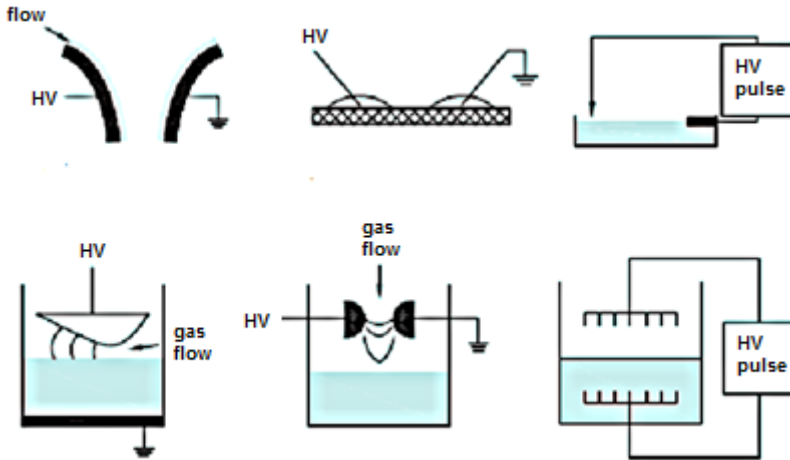


Fig. 2.8. Configurations of plasma overwater reactor (Bruggeman and Leys, 2009; Ceccato, 2009)

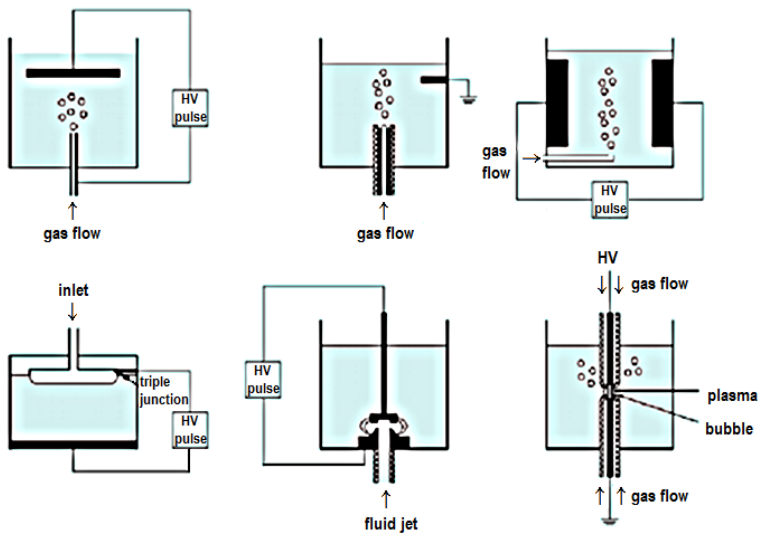


Fig. 2.9. Gas injection reactor configuration (Bruggeman and Leys, 2009; Ceccato, 2009)

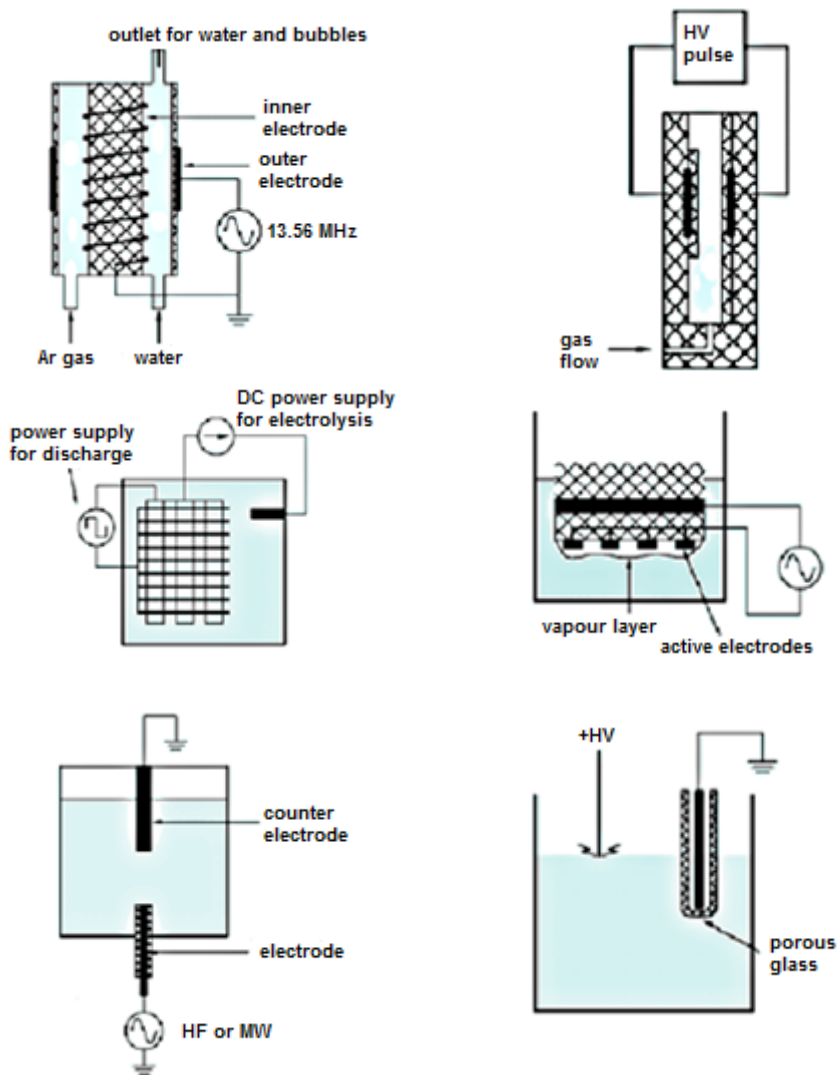


Fig. 2.10. Glow discharge electrolysis reactors (Bruggeman and Leys, 2009; Ceccato, 2009)

The glidarc discharge belongs to the group of non-thermal plasmas, although it is formed from an electric arc. It is actually a quenched plasma operated at atmospheric pressure; the macroscopic temperature exceeds ambient temperature only by few degrees (Abdelmalek et al., 2004; Burlica et al., 2006; Czernichowski, 1994; Diatczyk et al., 2011; Komarzyniec et al., 2011; Pawlat et al., 2011; Stryczewska, 2009; Stryczewska et al., 2011; Zhang et al., 2009).

In the case of (Burlica et al, 2006), the electrodes in the glidarc reactor were supplied from AC high-voltage transformer with a magnetic shunt (maximum power 700W, maximum voltage 12kV).

The discharge current was approximately 100mA and the dissipated power of the discharge was approximately 500W. Energy transfer from the electric field to the ambient gas leads to the formation of activated species which are raised to some excited energy levels, and this induces vibration, rotational and electronic transitions, which further can be transferred to the liquid part. Examples of gliding arc water reactors, quite well investigated, are presented in Fig. 2.11.

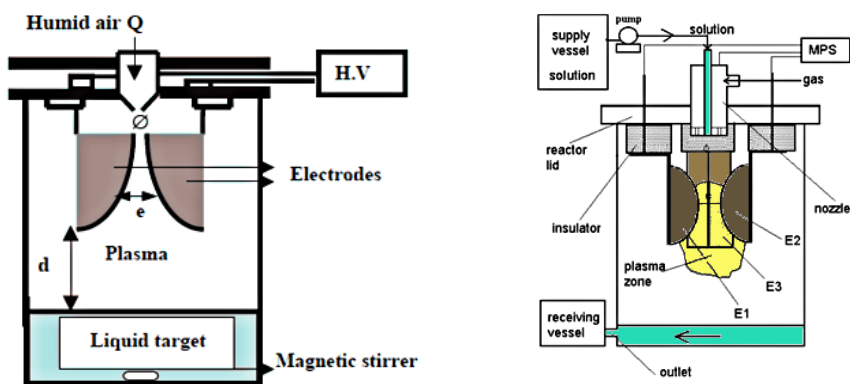


Fig. 2.11. Experimental set-ups of the glidarc plasma (E-electrodes) (Abdelmalek, 2003; Abdelmalek et al., 2004; Burlica et al, 2006)

Group of (Choi et al., 2006a) studied the action of atmospheric pressure air glow discharge with aqueous electrolyte cathode onto the surface of polyethylene (PE) films. Distilled water and aqueous solutions of KCl and HCl were utilized as a cathode. Modification processes were able to improve the surface free energy of PE. The experimental set up is presented in Fig. 2.12.

Contact glow discharge electrolysis (CGDE) is a different case (Liu, 2009; Schaper et al., 2008; Sengupta et al., 1997; Yerokhin et al., 1999; Wüthrich and Mandin, 2009), where thermal plasma layer around the immersed electrode in highly conductive electrolyte (saline) is formed. Electrochemical processes occur in the glow discharges at the plasma-electrolyte interface. Phenomena develop spontaneously at the electrode during conventional electrolysis whenever the applied voltage is sufficiently high irrespective of the electrolyte being aqueous, non-aqueous or molten. The onset of CGDE is marked by a steep drop in the current with the simultaneous appearance of a luminous sheath of gas at either the cathode or the anode caused by a film of solvent vaporized locally due to Joule heating and redox reactions (Sengupta et al., 1997).

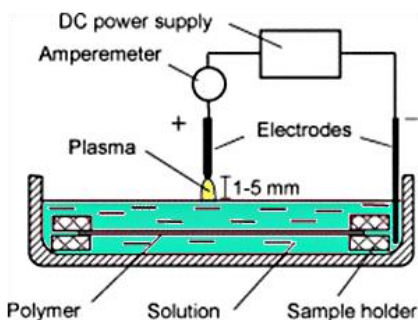


Fig. 2.12. Glow discharge electrolysis (GDE) (Choi et al., 2006a)

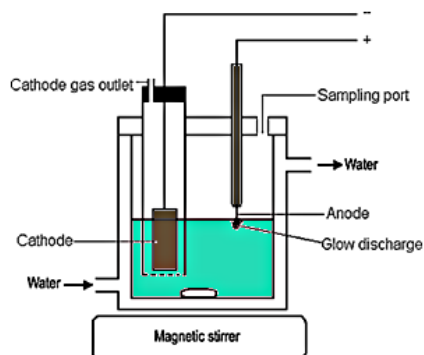


Fig. 2.13. Contact glow discharge electrolysis (CGDE) (Wang, 2009)

The electrode where the current density is larger, electrolyte resistivity is higher or electrolyte surface tension is lower tends to be the centre of CGDE. A remarkable feature of CGDE is that its chemical yield at the glow discharge electrode is several times the Faraday law value.

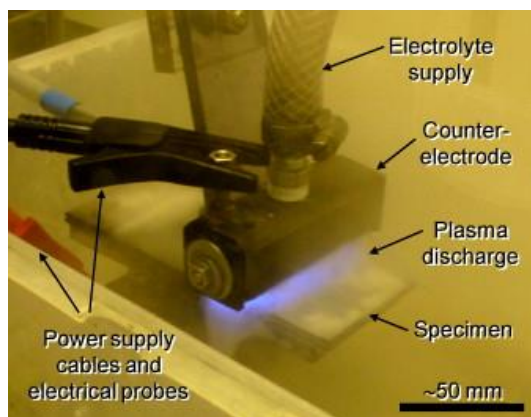


Fig. 2.14. Typical appearance of plasma discharge during EPP treatment. The optical emission from the discharge is characteristic of electrolyte composition (e.g. Zn^{2+} in this illustration) (Yerokhin et al., 2010)

Wang investigated contact glow discharge electrolysis in set up depicted in Fig. 2.13. The platinum wire anode was sealed into a glass tube and only slightly protruding from the glass body. The cathode was a stainless steel plate immersed in the electrolyte and separated from the anodic compartment by a glass tube with a glass frit of medium porosity at the bottom (Wang, 2009). Similar

reactor was used by (Yang and Tezuka, 2011) for mineralization of pentachlorophenolate ion (PCP) in phosphate buffer as a good alternative for other processes, for instance for electron beam proposed by (Kwon et al., 2009). Group of (Yerokhin et al., 2010) described electrolytic plasma process (EPP) (Fig. 2.14) for cleaning AISI 4340 steel, performed in 10% solution of sodium bicarbonate and operated at 70°C. Compared to the conventional DC process, the pulsed EPP cleaning resulted in reduced surface roughness and compressive residual stress at the surface.

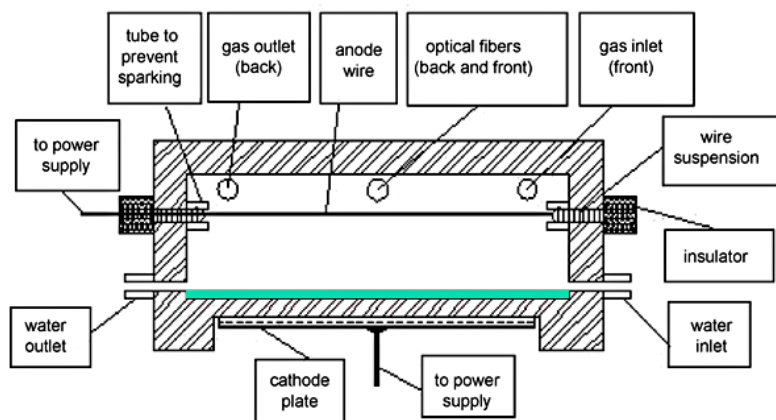


Fig. 2.15. The schematic diagram of corona above water reactor (Bian et al., 2009; Grabowski et al., 2006)

Corona discharge, occurring at high voltage (25 - 40kV), and having a pulse width of approximately 200ns, which saves the power (in the case of longer pulse width, power is wasted also on ionic migration because the mobility of ions is much less than that of electrons) is popular method of plasma generation at the presence of liquid. In the corona reactor, electrical discharge is produced in gaseous phase. In the corona above water reactor (CAW), which is depicted in Fig. 2.15, the discharge electrode made from stainless steel was placed in the upper part and the ground electrode was placed at the bottom side outside the reactor and covered with water. Reactor worked in DC mode but pulse regime is also used. However, in the case of pulse, there are still some problems to be solved, such as metal electrode corrosion, and the necessity of low initial solution conductivity (Shi et al., 2009). Thus, many improvements in reactor designs and in power source design are made to overcome this problem.

Group of (Dors et al., 2006) used positive DC corona discharge with pulse rate of 50kHz, which was generated between a stainless steel hollow needle electrode and the surface of pure water or water contaminated with phenol. A grounded flat stainless-steel mesh electrode was set 10 mm below the water surface (Fig. 2.16).

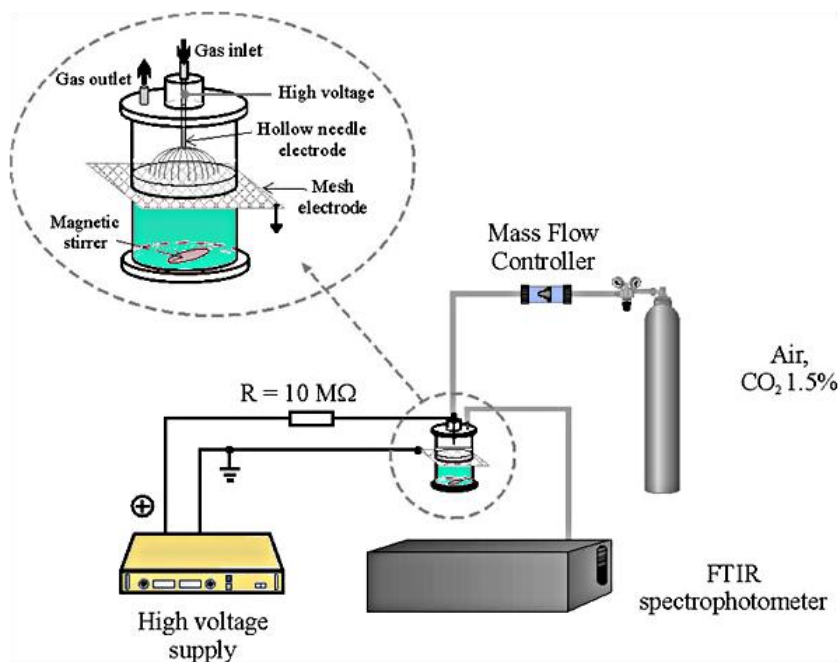


Fig. 2.16. Experimental set-up with corona-liquid reactor (Dors et al., 2006)

The electrostatically atomized ring-mesh reactor consisted of electrostatic atomization part and corona discharge part (Fig. 2.17). The flow of liquid was atomized in DC electric field before entering the discharge area to reduce gas-liquid mass transfer resistance and the impact of high conductivity in liquid-phase discharge process (Njatawidjaja et al., 2005; Shi et al., 2009).

An interesting example is cylindrical wetted-wall reactor designed from wire-cylinder reactor, which is presented in Fig. 2.18. Gas was fed either upwards or downwards through the reactor, in which water was circulated as a falling thin film on the inner wall of the cylindrical ground electrode (Sano et al., 2003; Shi et al., 2009).

Group of (Chen et al., 2009) presented reactor with the pulse power supplied brush electrode in the gas phase (Fig. 2.19). Plate-type electrode was submerged in the liquid. The distance between two electrodes was 20mm, and the closest gap between the gas-phase electrode and the water surface was about 1mm.

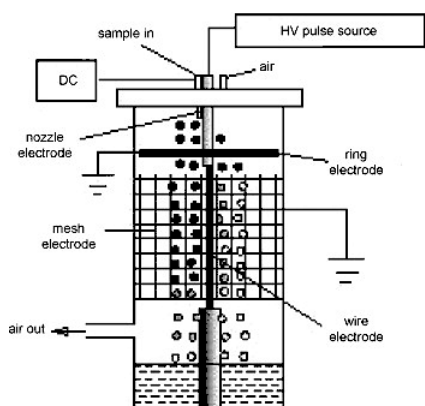


Fig. 2.17. The schematic diagram of electrostatically atomized ring-mesh reactor (Njatawidjaja et al., 2005; Shi et al., 2009)

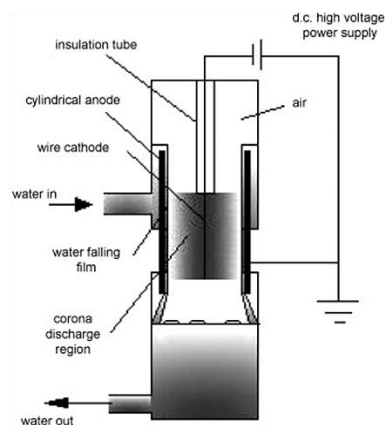


Fig. 2.18. The schematic diagram of cylindrical wetted-wall reactor (Sano et al., 2003; Shi et al., 2009)

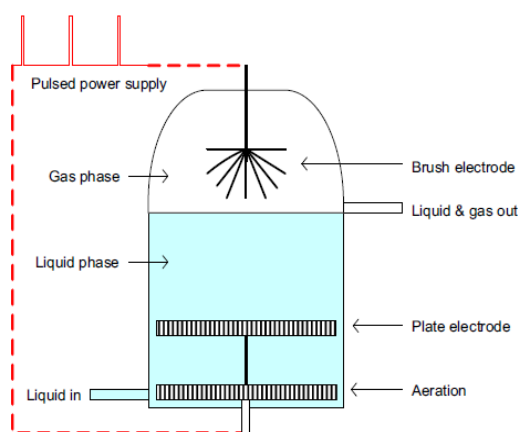


Fig. 2.19. Illustration of brush-plate electrical discharge reactor (Chen et al., 2009)

Dielectric barrier discharge reactor, the most common for industrial ozone generation (Jodzis, 2012; Jodzis et al., 2011; Kogelschatz, 2003), can be also applied for liquids as well. Mok used immersed DBD reactor, (shown in Fig. 2.20) which was powered from AC high voltage via copper rod. Wastewater was over the ground electrode and as it was electrically conductive, it elongated the ground electrode up to the outer surface of the quartz tube. Electrical discharge occurred in the space between the copper electrode

and the inner surface of the quartz tube, where gas flew and ozone and UV were generated (Mok, 2008).

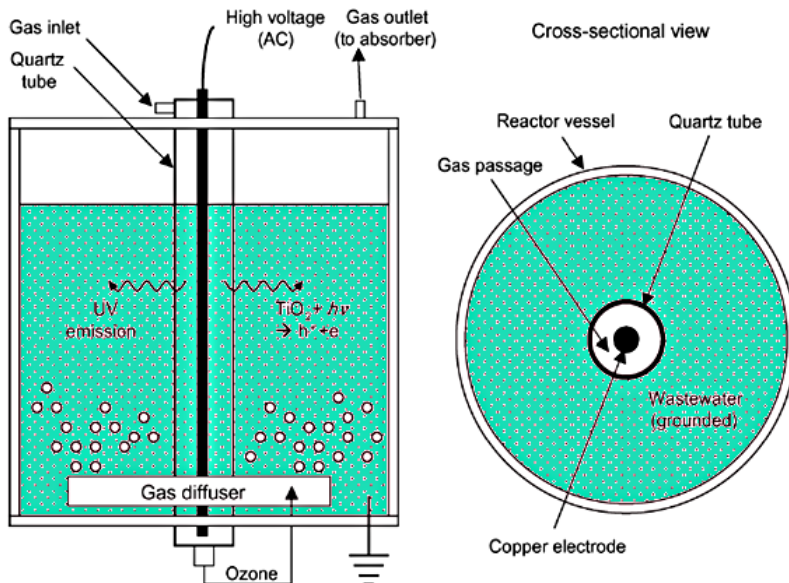


Fig. 2.20. Diagram of DBD experimental apparatus (Mok et al., 2008)

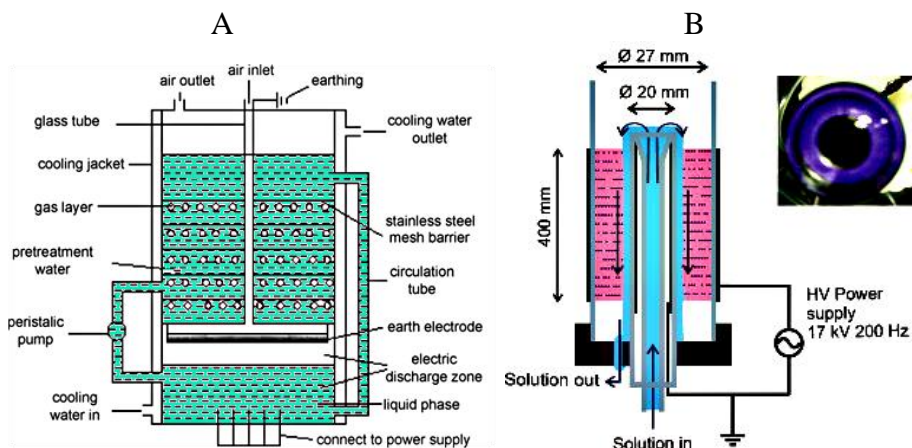


Fig. 2.21. The schematic diagram of dielectric barrier gas-liquid discharge reactors: DBD with mesh (A) and water falling DBD (B) (Zhang et al., 2008; Dojcinovic et al., 2011)

Other design was mesh barrier gas-liquid discharge reactor, presented in Fig. 2.21A. In this case, high-voltage electrode was submerged in liquid phase

and the ground electrode was suspended in the gas. Electric discharge formed in the aqueous phase, in the gas-liquid interface and the gas phase above the solution (Shi et al., 2009; Zhang et al., 2008). Group of (Dojcinovic et al., 2011) experimented on DBD discharge source, which worked as a falling film reactor presented in Fig. 2.21B.

Water flew up through a vertical hollow glass tube and flew down making a thin dielectric film over the electrode. The optimum of pulse frequency was found at 200Hz. Discharge was generated within 3.5mm gap between glass and water layer by applying voltage of 17kV.

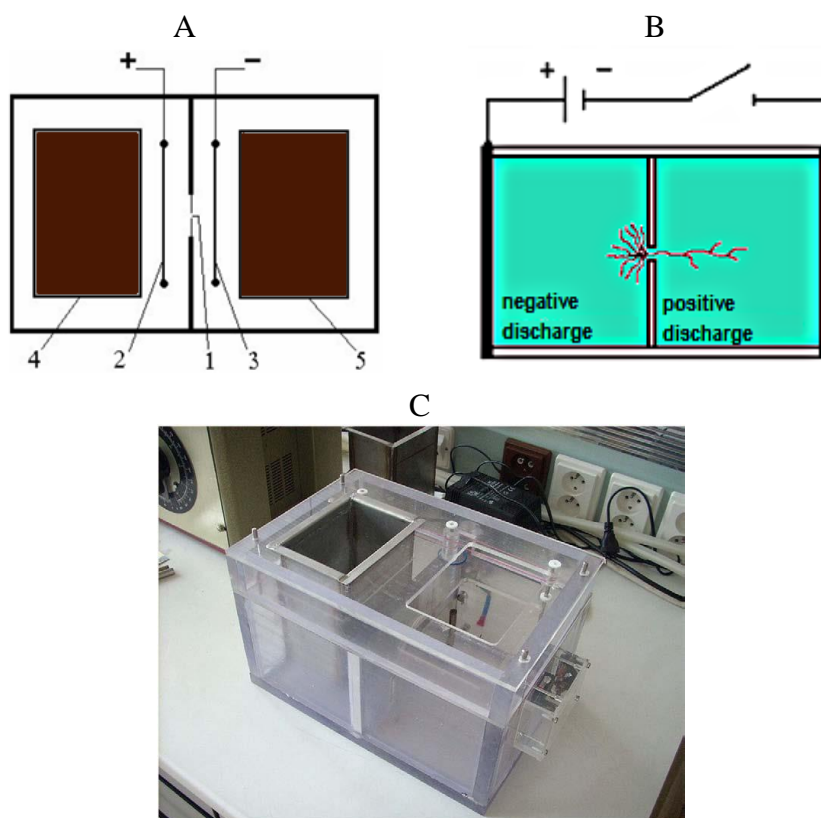


Fig. 2.22. Configuration of diaphragm discharge. Schema of set-up (1 - dielectric diaphragm with the pin-hole, 2 - anode, 3 - cathode, 4, 5 - cooling) (A), ideogram of process (B), reactor (C) (Kozakova et al., 2010; Stara et al., 2009)

In the diaphragm discharge shown in Figs. 2.7 and 2.22, a small diameter, chemically inert dielectric opening separated the electrodes and discharge was not in contact with any metal electrode (Kozakova et al., 2010; Neagoe et al. 2008; Stara et al., 2009). When voltage was applied on the electrodes, high electric field

between two planar electrodes was concentrated just in the pinhole. If the electric field was sufficiently high, and strong current flew through this opening then joule heating nucleated a gas bubble. The discharge was formed in the bubbles of evaporated water in and/or near the pin-hole made in the diaphragm. Two kinds of plasma streamers of the opposite polarity were created in two parts of the reactor separated from each other by an insulating wall containing the diaphragm. The difference in properties of plasma channels propagating toward the electrodes in this case is not only in their shape, but also foremost in the velocity of electrons accelerated by the applied electric field and the energy dissipation in channels. For a better understanding of streamer propagation, there is the analogy between generation of the diaphragm discharge and corona discharge in point-to-plate electrode configuration. The pin-hole behaves as a point electrode of both polarities each one for two separated parts of the reactor. In the part with the plane cathode, electrons are accelerated toward the positively charged pin-hole (like to the point anode) and the remaining positive space charge at the end of the streamer is further enhancing electrons' velocity. Created streamers represent long plasma channels. This form of plasma is referred to herein as "positive discharge". On the contrary, electrons propagating from the negatively charged pin-hole (as from the point cathode) toward the plane anode are dragged by the positive space charge and their velocity decreases. The final shape of negative streamers is represented by shorter bush-like plasma channels having a spherical shape, referred to as "negative discharge" (Kuzhekin, 1995; Stara et al., 2009). The bubble expands or grows, then it is further expelled from the opening and the discharge is quenched.

The operating mode of such a discharge is always pulsed from the plasma point of view but can be obtained with DC voltage (Kozakova et al, 2010; Stara et al., 2009) or in pulsed regime. The main advantage of DC non-pulsed voltage, comparing to the pulsed regimes, is relatively simpler HV source and substantially lower voltage magnitude required for the discharge ignition (approximately 2kV comparing to 20 - 30kV in the pulsed regime). Moreover, high voltage in the range of tens of kV generates much stronger electromagnetic field and shock waves while these processes are only negligible if lower non-pulsed voltage is used and they do not disturb surrounding environment, (Kozakova et al., 2010). Group of (Zhang et al., 2009a) proposed pin-hole discharge type reactor made from two Plexiglas cylinders, which were separated by an insulating plate with single, 1mm size pinhole. Two planar stainless steel electrodes located in the cylinders were placed at a distance of 27mm and operated in pulse mode. Air, oxygen or nitrogen at atmospheric pressure were bubbled into the reactor from the bottom, flowed through the pinhole and flowed out from the above. The electrical conductivity of the solution was adjusted by the KCl solution. Photograph of the discharge in dependence on applied voltage is depicted in Fig. 2.23.

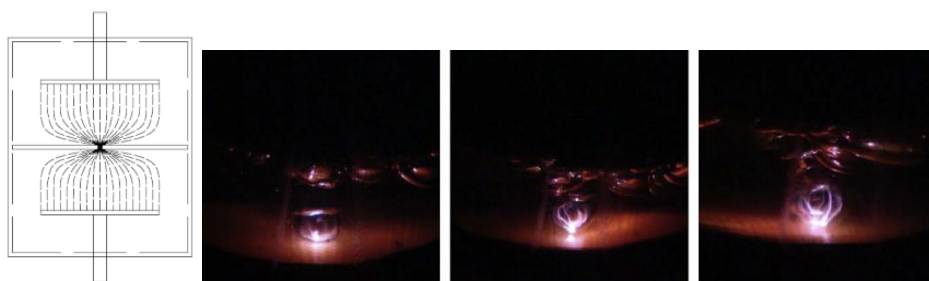


Fig. 2.23. Photographs of liquid phase discharge at different voltage. From left to right, the peak voltages are 22, 24, 26kV, Q_{air} 200ml/min (Zhang et al., 2009a)

Many researchers try to compare the efficiency of various discharge types using similar geometry of reaction vessel.

Zhang studied several different discharge modes, such as streamer corona discharge, spark discharge, and arc discharge with a variety of electrode geometries (e.g., point-point, needle-plate and wire-cylinder), which are presented in Fig. 2.24.

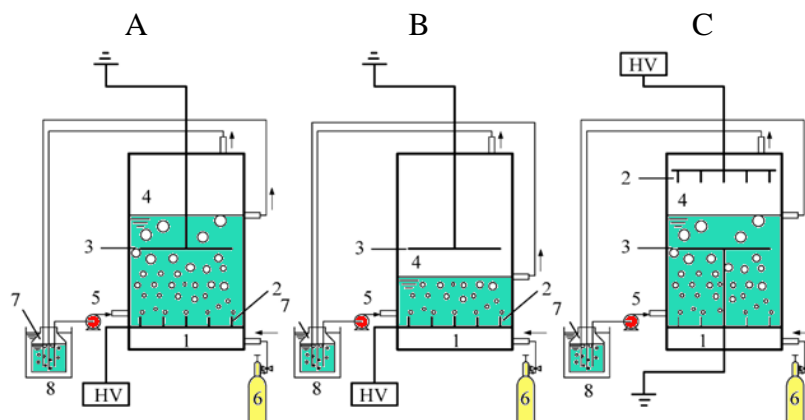


Fig. 2.24. Schematic diagram of HDBW reactor (A), HDAW reactor (B) and GD reactor (C). 1 - Oxygen room, 2 - high voltage electrode, 3 - ground electrode, 4 - liquid surface, 5 - peristaltic pump, 6 - cylinder, 7 - solution tank, 8 - cooling water (Zhang et al., 2007; 2007a). HDBW-reactor with both electrodes submerged into liquid phase, HDAW-reactor with high voltage hollow electrodes immersed in water whereas the ground electrode placed over water, GD-reactor with pulsed high voltage electrodes in the gas phase above water level and the ground electrode submerged into liquid

Electrical energy was formed from large pulse-forming capacitance (4nF) and released as a pulsed electrical discharge using double rotating spark gap. Applied voltage was 16kV and pulse repetition rate was 100Hz. In HDBW

reactor spark discharge was produced between high voltage discharge electrodes and ground electrode with bright light emission.

In HDAW reactor, the intense plasma channels appeared more similar to the arc-like discharge, which was formed between the liquid surface and the ground electrode in the gas phase. Additionally, spark discharge occurred in liquid phase. In GD reactor each high voltage discharge electrode could produce plenty of gas phase non-thermal plasma channels above the water surface. The discharge regions in HDAW and HDBW reactors were both between high voltage discharge electrodes and ground electrode, but the discharge region in GD reactor was only in the gas phase from high voltage discharge electrodes to the liquid surface, so the discharge region in GD reactor was smaller than in HD reactors (Fig. 2.25). Hybrid gas/liquid electrical discharge corona reactors presented in Fig. 2.26 (hybrid-series and hybrid-parallel) and a standard reference corona discharge reactor for degradation of phenol in the presence and absence of zeolites were compared by (Kusic et al., 2005).

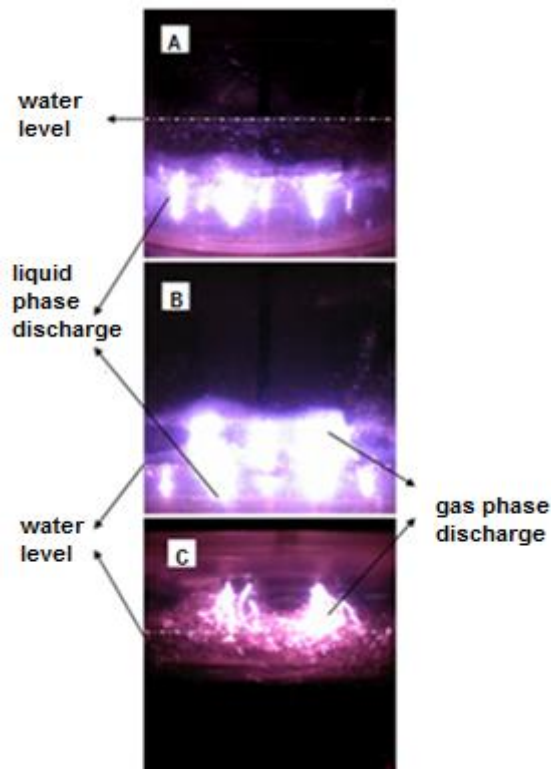


Fig. 2.25. Discharge modes in HDBW reactor (A), HDAW reactor (B) and GD reactor (C) (Zhang et al., 2007; 2007a)

Researchers Sugiarto and Sato observed that in water, for a given pulse duration in the set up shown in Fig. 2.27, one can obtain various discharge types from pulse: streamer or spark. Moreover, they can coexist at the same time.

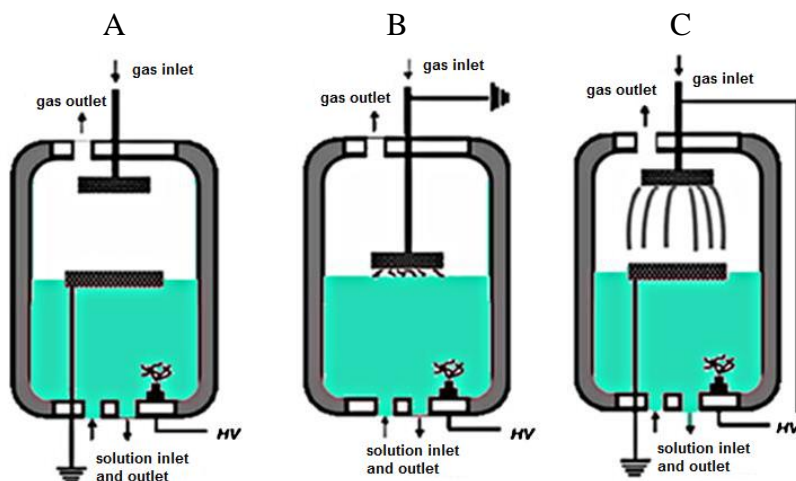


Fig. 2.26. Schemat of reactor configurations: (A) reference reactor, (B) series reactor and (C) parallel reactor (Kusic et al., 2005)

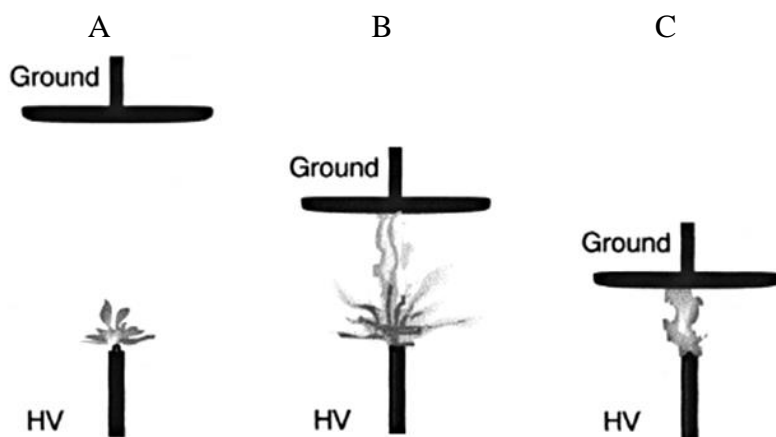


Fig. 2.27. Streamer discharge with electrode gap 45mm (A), spark with streamer discharge with electrode gap 15mm (B) spark discharge with electrode gap 6mm (C) (Sugiarto and Sato, 2001) cited by (Ceccato, 2009; Locke et al., 2006)

Plasma in water grows as a partial discharge starting from the electrode and can be described as corona-like. The discharge is partial because it does not bridge the gap and is not a full breakdown of the gap. If the plasma is able to reach the opposite electrode, a conductive channel bridges the interelectrode gap and the power supply begins to supply as much current as it can. It will lead to a spark or an arc depending on the power supply. This spark is transient and thermalize into an arc only if spark duration is long enough to allow time for the plasma channel to fully thermalize (typically some microseconds) (Ceccato, 2009; Locke et al., 2006; Sugiarto and Sato, 2001; Sugiarto et al., 2003).

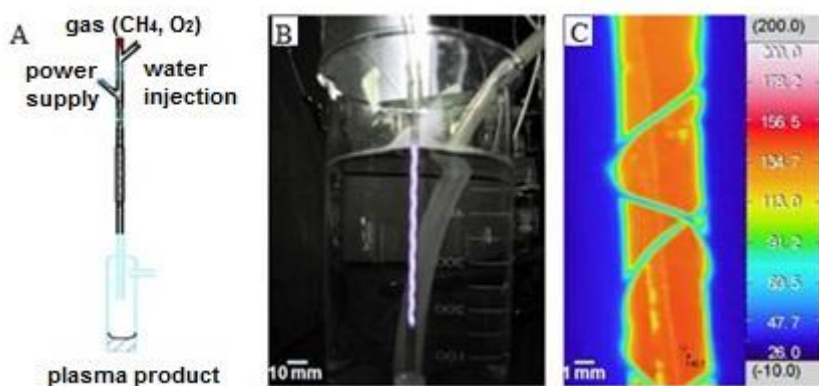


Fig. 2.28. Schematic representation of the plasma microreactor (A), microplasma generated in the glass tube (B), thermal image of the reactor during reaction conditions without external cooling (C) (Agiral et al., 2011)

Recently, microplasmas are gaining a lot of interests. For the humid environments there are examples of utilization of microplasma reactors, especially, in the field of material science and fuel conversion. A multi-phase flow non-thermal plasma microreactor based on dielectric barrier discharge has been developed for partial oxidation of methane with oxygen to liquid oxygenates carried at atmospheric pressure by (Agiral et al., 2011). A pulsed water injection method has been used to remove condensable liquid components from the active discharge region. Microreactor presented in Fig. 2.28 consisted of a quartz glass tube (i.d. 1.5mm, o.d. 4.5mm) and a twisted metallic wire inside the tube. Bipolar pulsed high-voltage with peak intensity of 10kV and fixed frequency at 10kHz was applied between the twisted metallic wire and a grounded aluminum foil electrode wrapped on external side of the glass tube. The principle of generating atmospheric non-thermal plasma is similar to dielectric barrier discharge (DBD). The peak temperature was up to 145°C, which is detrimental for the yield of oxygenates so the cooling at near 0°C was necessary. Under these conditions,

liquid components were condensed to form aerosol drops that eventually precipitated on the cooled microreactor wall. Furthermore, pulsed water injection was applied to remove liquid oxygenates condensed on the wall. The combination of a plasma microreactor and pulsed water injection enabled efficient product separation from the active plasma region, which increased product selectivity. Streamer corona discharge in artificial cloud of charged aerosol was also investigated by (Temnikov et al., 2008).

A gas-to-liquids process for direct and selective synthesis of oxygenates by partial oxidation of methane in a multi-phase flow non-thermal plasma microreactor (Fig. 2.29A) was described by (Nozaki et al., 2011). Intermediate oxidation products were stimulated to condense on the cooled microreactor walls and pulsed water injection removed liquid products from active discharge region before further oxidation might take place. At similar methane conversions, pulsed water injection increased the carbon balance and oxygenates yield comparing to experiments carried out without any water injection. Hydrogen peroxide was formed as a partial oxidation product and it has been found as key component which oxidizes formaldehyde in the post-discharge liquid. Alternative catalyst-supported plasma decomposition of formaldehyde was investigated by (Hensel et al., 2003, 2003a, 2003b).

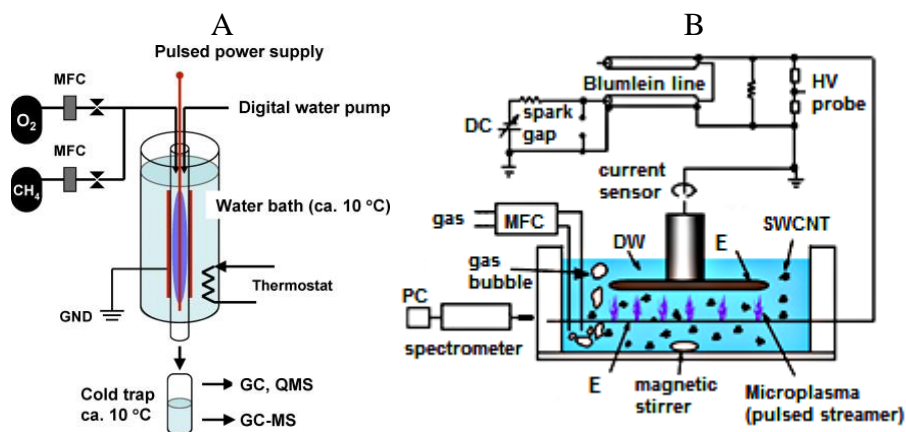


Fig. 2.29. Examples of microplasma reactors working in humid environments, (A) - (Nozaki et al., 2011), (B) - (Imasaka et al., 2008) (DW-deionised water, E- electrodes)

(Imasaka et al., 2008) studied influence of gas bubbling (O_2 , Ar, N_2 and CO_2) on water-solubility of single-walled carbon nanotubes (SWCNTs) and found out that solubility increased twice after microplasma treatment in water (Fig. 2.29B). It was the weakest in the case of CO_2 because CO_3^{2-} ion is radicals' scavenger.

2.4. Foaming column

First experiments concerning obtaining electrical discharge and generation of active species in flat foaming column (Fig. 2.30) were summarized in (Pawłat, 2001; Pawłat et al., 1999; 2000). Research on the electrical discharges in foams including modified reactor (Fig. 2.31), generation of oxidants and application for removal of contaminants were presented in (Pawłat, 2004; 2005; Pawłat et al., 2002; 2002a - h; 2003; 2003a - h; 2004; 2004a - h; 2005; 2005a - b; 2006; 2006a - c; 2007; 2007a; 2008; 2008a - c). Oxidants such as hydrogen peroxide, gaseous ozone, dissolved ozone and hydroxyl radicals were produced by the discharge in dynamic foam generated in one compact reactor without the addition of surfactants.

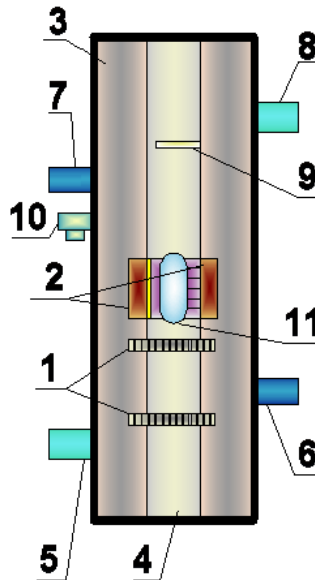


Fig. 2.30. Foaming column (1 - diffusers; 2 - electrodes (NP for the needle-to-metal plate electrode, ND for the needle-to-dielectric covered metal plate electrode, PP for the metal plate-to-metal plate electrode, and PD for the metal plate-to-dielectric covered metal plate electrode); 3 - housing; 4 - spacer; 5 - gas inlet; 6 - liquid inlet; 7 - liquid outlet; 8 - gas outlet; 9 - drops' grabber, 10 - overflow, 11 - quartz glass window)

Foaming leads to the intensification of processes between the gas and liquid phase, especially of those, which proceed on the interphase surfaces. Bistrón mentioned that in the dynamic foam conditions, increasing of the inter-phase surface leads to significant increase of mass and heat exchange coefficients

(in comparison to the typical bubbling process) (Bistroń et al., 1978; Pozin et al., 1962). Thus, very specific environment, possibly enhancing the treatment processes may be created in foam.

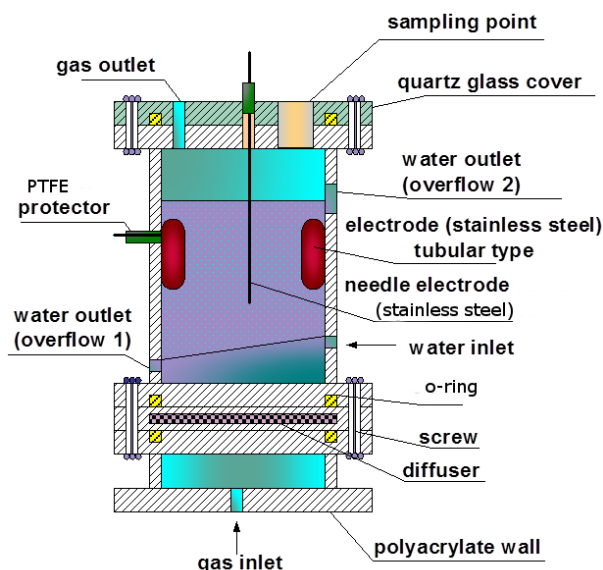


Fig. 2.31. Cylindrical foaming column

Cylindrical, single-diffuser (type IA-500 of mainly aluminum oxide) foaming column ($d_{inR}=50\text{mm}$, $L_R=200\text{mm}$) made of polyacrylate is depicted in Fig. 2.31. Inner electrode (stainless steel tube $d_{outEw}=1.5\text{mm}$) was placed inside the outer electrode (stainless steel ring $d_{inEz}=40\text{mm}$, $l=30\text{mm}$) above the diffuser. Quartz glass window for the discharge observation was put on the top of the apparatus.

The diagrams of electric power supply are presented in Fig. 2.32. Electrical set-up consisted of pulse power source operated at variable frequencies, which was connected to the voltage and current measurement system. In the most frequent case, multi-stage pulse power source made from RG/8-U coaxial cable as a capacitance was used for the electrical discharge generation. Total capacitance of single 5m length line was 484pF. Device operated in a single shot mode or repetition mode with repetition rate depending on the used switch (thyatron or open gap switch, where frequency was regulated by an oscillator). Discharge was triggered by the triggering system connected to the switch and to the Blumlein serially. Alternatively, electrical circuit with rotary spark-gap was used.

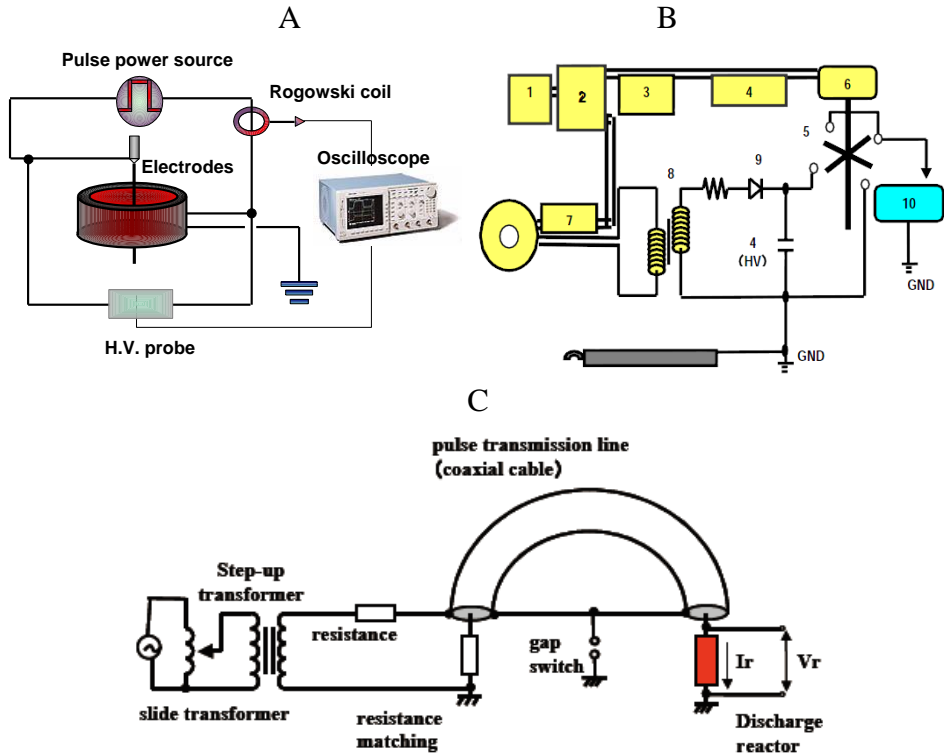


Fig. 2.32. Pulse power sources: schematic wiring (A), set-up with rotary spark-gap (B) (1 - AC 100V, 2 - breaker, 3 - switch, 4 - capacitor, 5 - rotary spark gap, 6 - motor, 7 - switch, 8 - transformer, 9 - diode (10kΩ), 10 - reactor), set-up with coaxial cable (C)

Discharge voltage and current were measured by the high voltage probe Tektronix model P6015A and the Rogowski coil Pearson model 110 with Tektronix model TDS 380 oscilloscope, respectively.

2.4.1. Foaming phenomena

Foams are thermodynamically unstable colloidal structures. They might be described as highly concentrated dispersions of gas in two-phase system with a gas phase as dispersed phase and the liquid matrix (Dickenson, 1992; Patino et al., 1995). Foams contain more than 90% of gas, so amount of water is relatively small. Thin liquid films are known as lamellae (Kovscek et al., 1995).

Several kinds of foam, with different properties and hydraulic parameters exist. Many transition structures ranging from spherical to polyhedral ones can occur during the foam production. Foams can be easily created using

the dispersion technique, with shaking or whipping liquid with gas, which is immiscible in that liquid. Without continuous flow such kind of foam is decomposed in very short time.

Foams can be divided into homogenous and pneumatic in dependence on the method of generation (Bhakta and Ruckenstein, 1997). In the case of pneumatic foams, there is a certain gas velocity level beyond which, the steady state height will not be attained. The origin of this kind of foaming process is a bubbling technique (introduction of gas to a liquid layer). The most well known are foams created by the surface-active substances. However, unstable dynamic foams without the surfactant's addition, generated using only kinetic energy of the gas flow, keeping the strict conditions of media's flow and using the diffusers in the apparatus of a special construction cannot be neglected (Bistroń et al., 1978; Hobler, 1978).

Gas behavior (the uprising velocity and the diameter of bubbles) in liquid depends on the gas velocity (Hobler, 1978). General rules concerning gas flow rate and the apparatus' construction limits for creation of foams are presented below:

- linear velocity of substrate gas for whole apparatus cross-section: 0.1 - 4.0m/s,
- gas velocity in the diffuser hole: 10 - 20m/s,
- diffuser's perforation level: 5 - 20% of whole shelf area.

Velocity, that is too high, causes formation of the splashing zone. Too low velocity is the reason of water accumulation and bubbling instead of foaming during the operation of foaming column.

Dynamic foams formed without addition of foaming agent are totally harmless from an environmental point of view. Therefore, this type was chosen as a model medium in the presented experiments. Co-current flow (gas and liquid flow through the same diffuser's hole) allowed for the efficient usage of the inside area (Bistroń et al., 1978).

On the basis of observations with flat type reactor (Fig. 2.30), the uniform foam zone was generated above the second diffuser. It was also noticed that too large and too small widths of the diffuser and spacer had a negative influence on the foam formation and rather bubbling conditions occurred than foaming. Bubbles of small diameter tended to share their films, which became big lamellae, connected to the wall in the case of small widths and diameters (10mm and below). It caused the edge effect promoted by the adhesion of bubbles to the walls, leading to bubbling conditions and the separation of liquid and gaseous phase. On the other hand, in the case of too large diffuser's width it was difficult to achieve the expected foam level and the higher gas flow rate had to be applied to keep the foaming conditions. For the most ideal condition from the foam creation point of view, the diffuser's width should be wider

than 4mm. Thus, simplified cylindrical column was designed to maintain this condition (Fig. 2.31). This type of reactor was tested for investigating properties of electrical discharge in various flow regimes:

- water filled reactor without gas flow (Fig. 2.33A),
- bubbling environment as depicted in Fig. 2.33B,
- foaming (Fig. 2.33C).

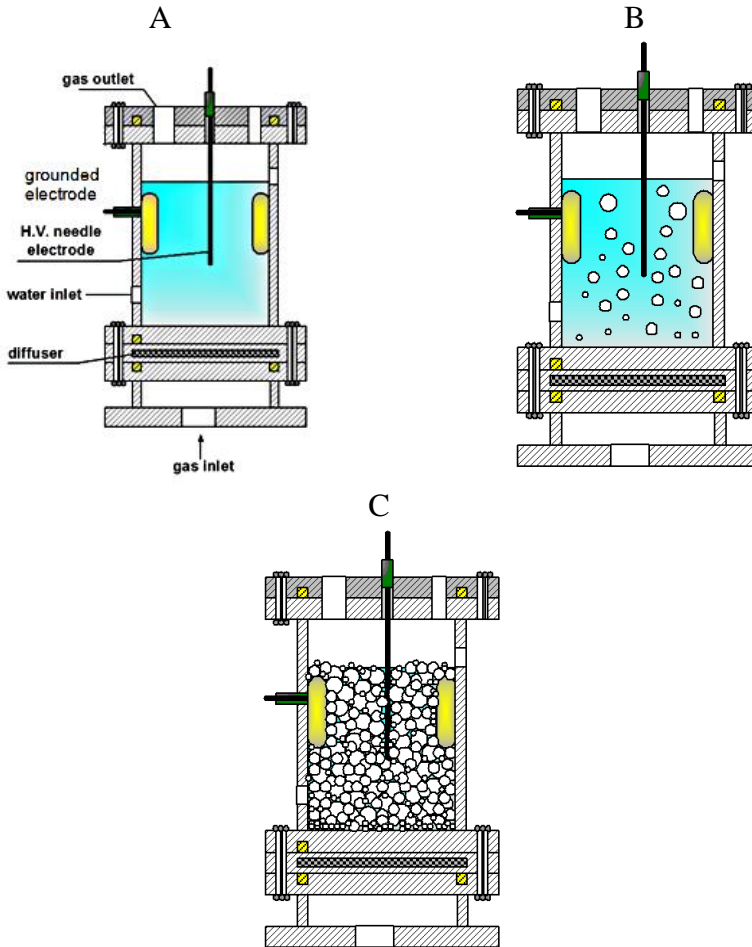


Fig. 2.33. Regimes of cylindrical plasma reactor: (A) - for discharge in water (submerged electrodes), (B) - bubbling, (C) - foaming

The average diameter of single bubble in foam ranged from 1 to 5mm. In the case of bubbling, diameters increased to 4 - 12mm. The diameters of bubbles tended to be bigger (connecting to each other and then sharing their

lamella) with increasing of the distance from the diffuser, as shown in Fig. 2.34, and with increasing of gas flow rate as well.

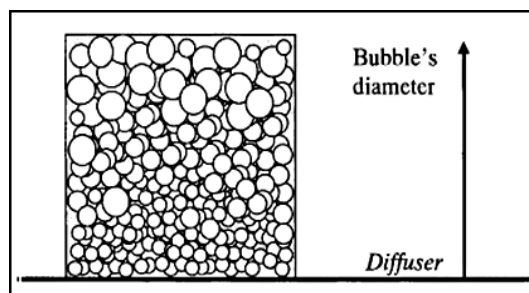


Fig. 2.34. The bubble structure while departing from the diffuser

2.4.2. Electrical discharge in foam

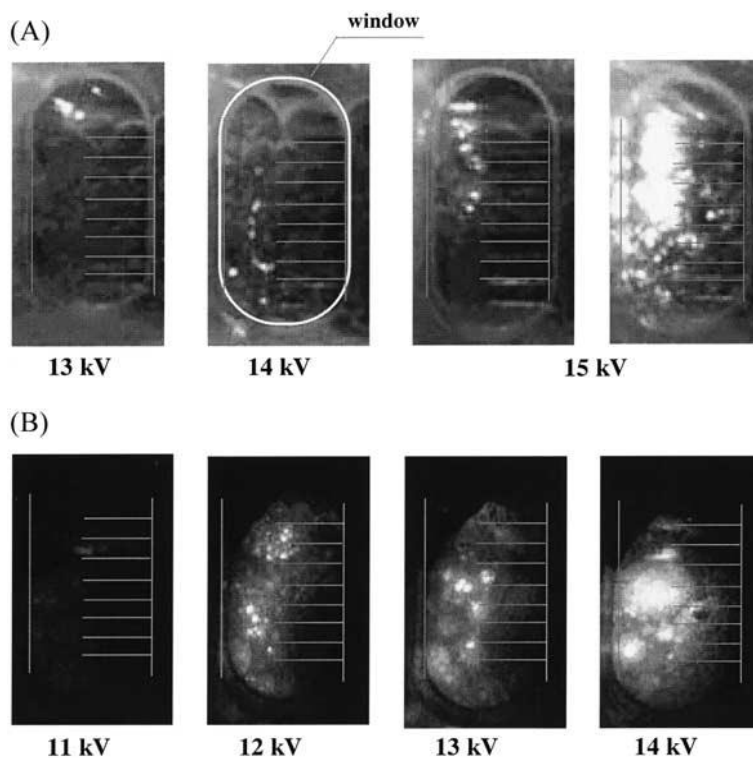


Fig. 2.35. Photographs of spatial development of the discharge in flat foaming column taken by ICCD camera in dependence on charging voltage for the NP electrode (A) and ND electrode (B), airflow rate 10l/min

Generally, several types of discharges were obtained in the dynamic foam. Visible discharge appeared at about 11 - 12kV of applied voltage in not transparent, white color medium. At the lower voltage some faint discharge proceeded what was confirmed by low concentrations of oxidants. The discharges, however, were not totally uniform in all mentioned cases. Discharge pictures were taken by ICCD camera with the minimal shutter speed 10ns and the minimal duration time 50ns.

The most common types of the discharges, appearing in flat foaming reactor are presented in Fig. 2.35.

Spatial distribution of the discharge light emission was observed to establish the influence of the value of applied voltage on the discharge in foam. Two main patterns were noted in dependence on the presence of dielectric in the electrode setup. The dependence of discharge area on applied voltage was clear in the case of metal plate-to-metal plate and the needle-to-metal plate electrode.

The upper parts of foam (large diameter of bubbles) and its surface area were the most preferable places for discharge occurring at relatively lower applied voltage. Increase of the applied voltage brought the system to more homogenous spatial distribution of the discharge and discharge occurred in the entire area within the electrodes as presented in Fig. 2.35A. The oval-shaped structure, which is seen in the figure, was the quartz glass window for the spectroscopic measurement.

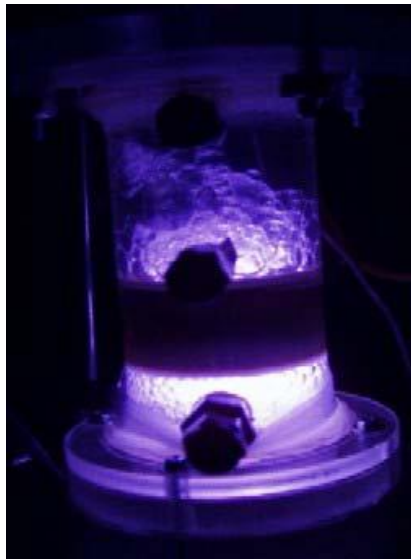


Fig. 2.36. Digital photo of the electrical discharge in cylindrical foaming column

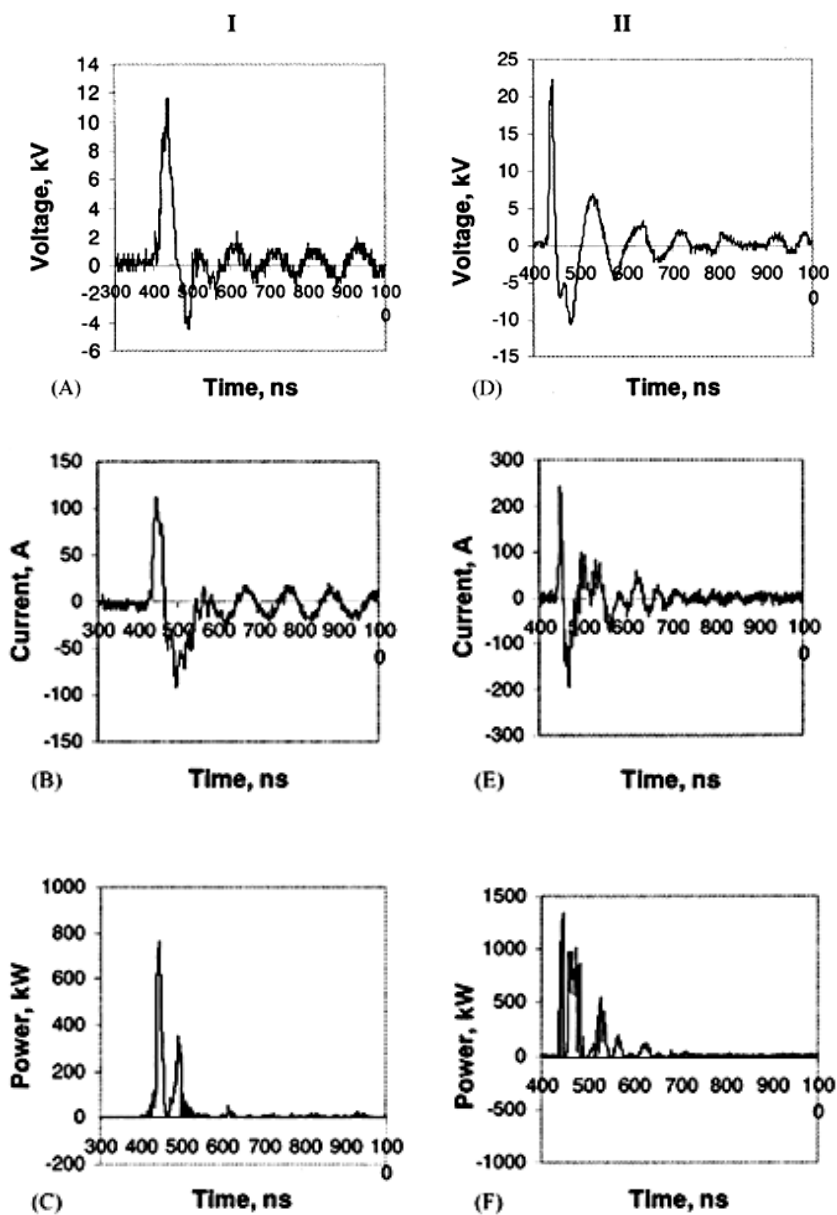


Fig. 2.37. The electrical waveforms (A, B, D, E) and instantaneous power (C, F) of the discharges in the NP (I) and ND electrode (II) set-ups. Airflow rate: 8l/min, 14kV of applied voltage

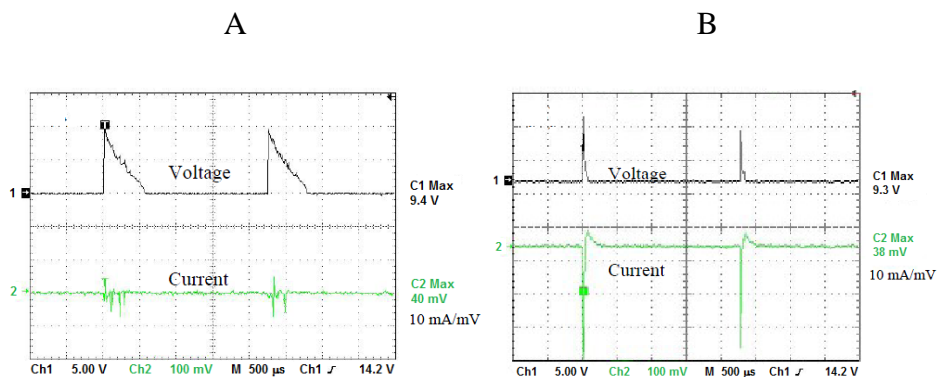


Fig. 2.38. Typical applied voltage and current waveforms of the discharge in oxygen (A), air (B). Electrical supply with rotary spark gap, gas flow rate 5l/min, input power 40W

Positive influence of dielectric layer on the spatial distribution of the discharge development was observed in the case of metal plate-to-dielectric plate and the needle-to-dielectric plate electrodes. The discharge was more uniform and single-channel discharges occurred only sporadically (5-10%). Even at lower applied voltage, the spatial uniformity could be achieved (Fig. 2.35B). As expected, discharge intensity increased with the applied voltage increase. Photograph of the discharge in the cylindrical reactor is presented in Fig. 2.36.

Electrical discharge development in foam was usually very rapid: the first peak of applied voltage was about 50ns and strong light emission from the discharge took place. Typical applied voltage and current waveforms with calculated power for the most frequent case of the discharge in flat type reactor and the NP (needle-to-plate) and ND (needle-to-dielectric) electrode set-ups are presented in Fig. 2.37A - C. Comparable characteristics were observed for the ND electrodes. Some weak oscillations and micropeaks of the current and voltage curves were observed due to the increased capacitance in the case of dielectric coating (Fig. 2.37D - F).

Observed characteristics were response to the trigger: self-attenuating pulse discharge was induced with the spark-gap. Current micropeaks that indicated propagation of multiple discharges in foam are noticeable in the oscillograms. Very strong ringing effect caused by both: RLC components in the circuit and proceeding of multiple discharges can be also observed. Only the first peaks in voltage and current characteristic were taken into consideration for estimation of instantaneous power (error of was not calculated). Fig. 2.38 depicts electrical parameters of discharges obtained in the cylindrical foaming column using power source from Fig. 2.32.

2.4.3. Formation of oxidants in foam

Proceeding of various reactions' chains, which may lead to the formation of several oxidants, was expected in the humid environment (Beltran, 1997). Generation of hydrogen peroxide, hydroxyl radicals, gaseous and dissolved ozone was possible in foam, during the competitive and sequential reactions in the gaseous bulk, liquid films and on their interfaces (Fig. 2.39).

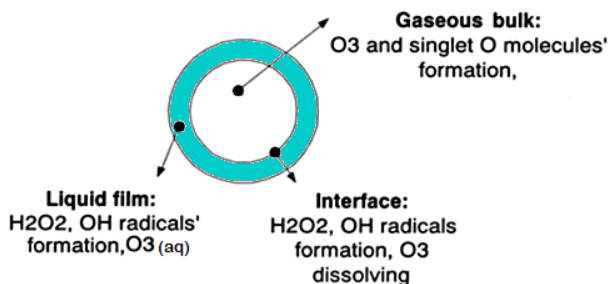


Fig. 2.39. Cross section of the single foam bubble with the proceeding processes

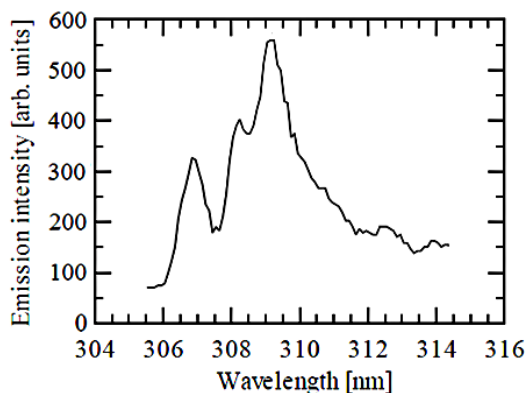


Fig. 2.40. Emission intensity in foam, applied voltage: 15kV, substrates: argon and pure water

Foam was generated using pure water as substrate liquid and air or oxygen as the substrate gases. Presence of oxidative species such as gaseous ozone (O₃), dissolved ozone (O_{3(aq)}), hydrogen peroxide (H₂O₂) and detection of hydroxyl radicals (OH) were performed.

Generation of OH radicals was confirmed. The emission band of OH (A²Σ⁺ - X²Π) ranges from 300 to 335nm (Ohgiyama et al., 1991; Vinogradov and Wiesemann, 1998). In the case of air, an emission of OH radicals' transition cannot be distinguished because of the overlap

of the intense nitrogen emission. Thus, argon had to be used instead of air during the OH radicals' detection. The discharge light start-time was obtained by a signal cable terminated with 50Ω resistor.

Intensity of the emission in the respective wavelengths is also changing during the discharge development. OH ($A^2\Sigma^+$) and OH($X^2\Pi$) radicals in the foaming conditions can be generated by the electron collisions with water molecules and by the ozone decomposition and its further reaction with water molecules. UV emission spectra from the discharge region, taken with argon and oxygen as the substrate gases and pure water as a substrate liquid were captured.

In both cases, peaks corresponding to the OH radicals' emission were resolved in the spectral range from 306 to 313, with the main peak around 310nm as shown in Fig. 2.40. Spectrum observed in argon gas at 15kV of applied voltage is presented. Generally, the emission intensity increased significantly with the increasing of applied voltage.

The comparison of oxidants' generation in time for cylindrical reactor was made for 3 cases:

- submerged electrodes (130ml of pure water),
- bubbling environment (130ml of pure water, gas flow rate: 4l/min),
- foaming (60ml of pure water, gas flow rate: 4l/min).

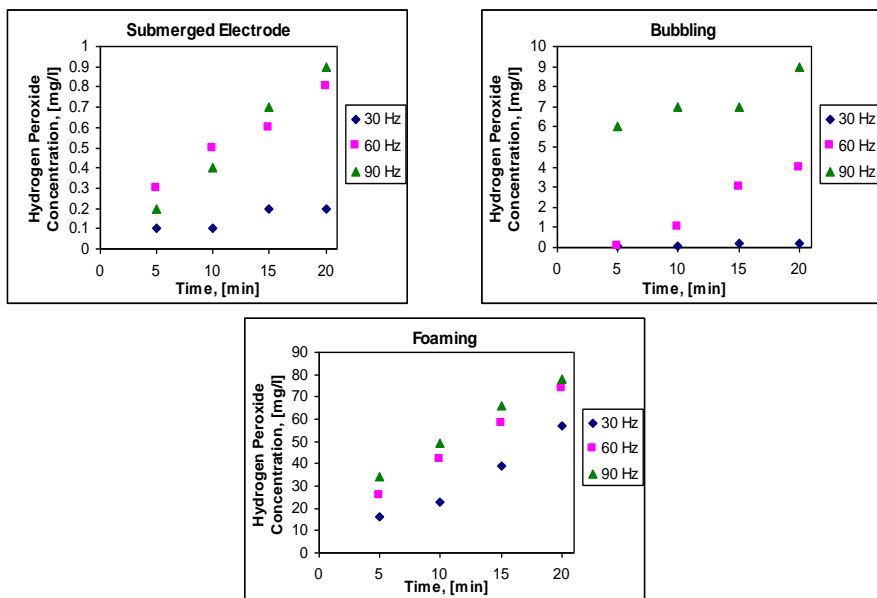


Fig. 2.41. Hydrogen peroxide concentration in dependence on frequency and time (for water submerged electrodes, bubbling and foaming)

Hydrogen peroxide concentration was determined using Hydrogen Peroxide Test Kit (HACH, Model HYP-1). Thiosulfate titration of the sample (liquid after the discharge application, mixed with specially formulated starch-iodide reagent used in the hydrogen peroxide tests and with ammonium molybdate reagent) was performed at a low pH (3.5) condition. Summarized results for cylindrical column are presented in Fig. 2.41.

Dissolved ozone concentration was determined using a spectrophotometer (HACH, DR/4000) and indigo method in an acidic (pH 2.5) environment. Indigo method is based on the specific reaction of ozonizing of double bound C=C in indigo di- or trisulfonate molecule and on the formation of colorless isatin. The blue indigo color is bleached in proportion to the amount of ozone, which is present in the sample. Results are depicted in Fig. 2.42.

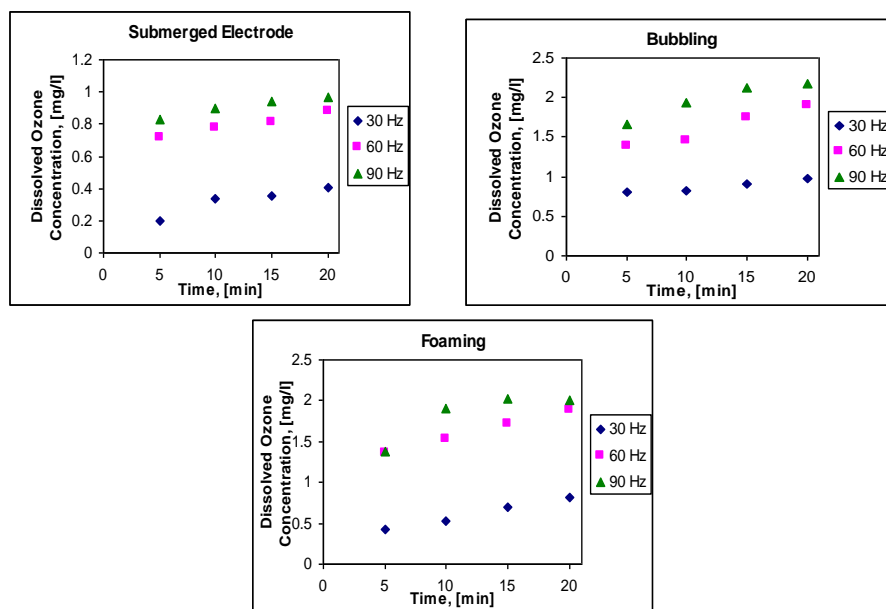


Fig. 2.42. Dissolved ozone concentration in dependence on frequency and time (water submerged electrodes, bubbling and foaming)

Standard titration method was used to determine ozone concentration in the outlet gas. Tested medium was gas after the decomposition of foam taken from its outlet placed in the upper part of apparatus and introduced into the sample with pure water and KI solution. KI solution with starch indicator was titrated in acidic environment with the sodium thiosulfate solution. Moreover, outlet gas

was collected in the gasbags and sampled with GASTEC and KITAGAWA ozone gas probes. Gaseous ozone concentration for cylindrical column is shown in Fig.2.43.

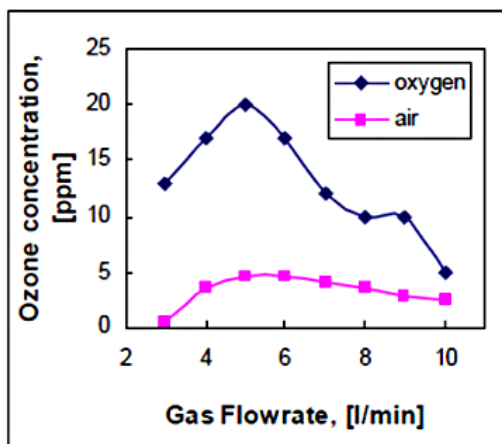


Fig. 2.43. Gaseous ozone concentration in cylindrical foaming column in dependence on the gas flow. Total power 40W

In cylindrical foaming column, concentrations of oxidants increased with the increasing of pulse repetition rate and applied voltage as expected. The highest concentration of dissolved ozone was 1.38mg/l (at 60Hz after first 5min) and it was obtained in the bubbling system. However, similar results were achieved in foam (1.36mg/l). In the case of submerged electrodes, the amount of dissolved ozone was much lower and it ranged 0.72mg/l. Foaming system was definitely the most efficient one for hydrogen peroxide production. It was possible to generate 74mg/l of H_2O_2 in 20min at 60Hz. It was more than 10 times higher than in the case of bubbling and 100 times higher than with submerged electrodes. In all regimes slight increase of active species' concentration was observed with time. Due to high water conductivity for submerged electrodes energy provided to the reaction zone was obviously not sufficient to generate oxidants. In this case different type of electrical power supply should be applied.

For flat foaming reactor, the dominance of the needle-to-dielectric covered plate electrode was recognized. In this set-up, higher values of discharge current and voltage and higher values of instantaneous power were achieved. Additionally, the micropeaks in the oscillograms (Fig. 2.37) could indicate high number of generated discharge microchannels. Quantity of all oxidizing agents for this electrode type increased when applied voltage increased. At lower gas flow rate, it was easier to generate the multi-channel discharges. Thus,

the volume, where active species were generated, was more extended than in the case of one discharge channel and their concentration was higher. However, foam could not be created in regard to the strict limits of foam formation at too low gas flow rate. On the other hand, the excessive gas velocity caused inhomogeneous increase of diameter of the gas bubbles and flow became turbulent. That made the discharge development more difficult.

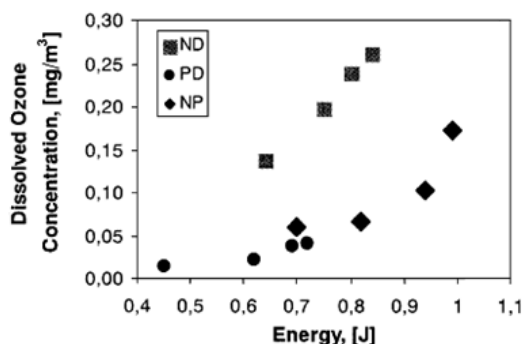


Fig. 2.44. The comparison of the instantaneous input energy versus $O_{3(aq)}$ concentration obtained in the flat type reactor in dependence on electrode configuration at 8l/min oxygen flow rate (NP - needle-to-metal plate electrode, ND - needle-to-dielectric covered metal plate electrode, PD - metal plate-to-dielectric covered metal plate electrode)

Number of effective electron impacts decreased. In such a case, the discharge occurred mainly at the surface area of foam, where molecules were carried out by a high-speed gas. In consequence, reduction of oxidants' concentration was observed. Visible single channel discharges occurred when the bubbles recombined and formed large diameter ones, which further merged into the channel between electrodes.

The highest energies of the discharge were achieved for the NP electrode. Though, the concentrations of oxidants obtained in this case were average (Fig. 2.44). Positive influence of dielectric layer on the discharge development and formation of oxidants was observed. In dielectric barrier discharge reactors, due to charge build-up at the dielectric surface, within a few ns after breakdown, the electric field at the location of a microdischarge is reduced to such an extent that the current flow at this position is interrupted. Because of short duration and the limited charge transport and energy dissipation this normally results in little gas heating. In a microdischarge, a large fraction of the electron energy can be utilized for exciting atoms or molecules in the background gas, thus, initiating chemical reactions and/or emission of radiation (Kogelschatz et al., 1999). In foaming column, dielectric barrier limited the duration

of a discharge promoting development of microdischarges instead of one single discharge channel. Microdischarges also tended to cover larger area than single filament and their further collective motion resulted in increase of uniformity.

Concentrations of oxidants in the foaming system are influenced not only by the parameters of the electrical discharge but they are also strongly inclined by the geometry of the gap space and flow regime so generation of oxidants must be always a compromise of several factors.

Almost all of hybrid reactors, presented in chapter 2.3 have limited abilities of treatment of huge amount of contaminants in both gaseous and liquid phase. Many of them are *stricte* plug-flow type. To sustain dynamic foam small amount of liquid is necessary but relatively high gas flows are required. This fact broadens possible application field to industrial treatment of humid gases and aerosols in foaming column in the future.

3. Removal of organic compounds using reactors working in humid environment

Plasma techniques for removal of contaminants from effluent gases and liquids are known for few decades and number of research papers related to this topic is increasing every year (Diatczyk et al., 2011; Doubla et al., 2007; Guo et al., 2008; Hermann et al., 1999; Kim et al., 2002; Malik et al., 2011; Magureanu et al., 2011; Pawłat, 2004; 2005; Pawłat et al., 2002; 2002a-h; 2003; 2003a-h; 2004; 2004a-h; 2005; 2005a-b; 2006; 2006a-c; 2007; 2007a; 2008; 2008a-c; 2009; Pawłat, 2009), etc.

For removal of organic compounds, non-thermal plasma can be produced during the electrical discharges in gas, liquid or hybrid liquid-gas phase. The experimental reactors employ pulsed spark discharge, pulsed streamer corona discharge, pulseless corona discharge within liquids; corona, arc, glow discharge on the surface of liquid, and many others as it was presented in chapter 2. Plasma methods allow employing various species such as $\bullet\text{OH}$, $\bullet\text{H}$, $\bullet\text{O}$, $^1\text{O}_2$, $\bullet\text{HO}_2$, H_2O_2 , O_3 , etc. In addition, pyrolysis, thermal oxidation within the plasma channel, vacuum UV photolysis, visible photons at the surface of the plasma channel, electrohydraulic cavitation and supercritical oxidation with the subsequent bubble occur in the immediate vicinity of the plasma channel. All of these species and effects can oxidize organic pollutants effectively (Busca et al., 2008; Braun and Oliveiros, 1997; Grymonpre et al., 2004; Kim et al., 2003; Yamatake et al., 2006; Zhang et al., 2006).

Proposed reactors for the abatement of organic compounds operate in flow or steady-state modes in dependence on the purpose of investigation (chemical efficiency, reaction parameters). Variety of methods is used for the quantitative and qualitative analysis of decontamination process. Basic ones are measurements of pH, conductometry and colorimetric titration. Analytical methods employ gas and liquid chromatography and spectroscopic measurements. Backgrounds of pollutants' removal in selected hybrid plasma reactors will be described in this chapter.

Evaluation of dye concentration in the solution is often calculated from absorbance data at selected wavelength by the Lambert-Beer formula during UV-visible absorption spectrometry. According to the Lambert-Beer law, described by equation 3.1, the absorbance of a solution is proportional to the concentration of the absorbing species and the length of the path the light (Meek, 1998). The optimal wavelength for measuring absorbance is that one, which is most absorbed by the compound (Tab. 3.1). To evaluate the correlation between concentration and absorbance calibration curves are prepared.

$$A = \epsilon lc \quad (3.1)$$

where:

A - absorbance, [-],

ϵ - molar absorptivity, [$\text{dm}^3/\text{mol cm}$],

l - path length of the sample (path length of the cuvette in which the sample is contained), [cm],

c - concentration of the compound in solution, [mol/dm^3].

Tab. 3.1. Examples of most absorbed wavelengths for selected dyes (saujanya.com; stainsfile.info; Stara et al., 2009; Van der Zee et al., 2001)

Dye	Class	Maximum absorption wavelength, [nm]
Acid Orange 7	Azo-dyes	484
Acid Red 266		492
Acid Yellow 23		428
Acid Yellow 137		456
Acid Yellow 159		362
Basic Red 23		526
Direct Black 19		675
Direct Black 22		484
Direct Blue 53		608
Direct Blue 71		579
Direct Blue 106		608
Direct Red 79		506
Direct Red 81		509
Direct Yellow 4		402
Direct Yellow 12		401
Direct Yellow 29		392
Direct Yellow 50		402
Mordant Orange 1		373
Mordant Yellow 10		355
Reactive Black 5		595
Reactive Orange 14		433
Reactive Orange 16		492
Reactive Red 2		539
Reactive Red 4	521	
Reactive Yellow 2	405	
Direct Blue 53	Disazo-dye	592
Basic Blue 9	Thiazine	576
Acid Blue 74	Indigoid	608
Acid Red 87	Fluorone	516

The extent of decolourisation can be calculated according to:

$$F_D = (A_i - A_t) / A_i \quad (3.2)$$

where:

F_D - decolourisation factor, [-],

A_i - initial absorbance, [-],

A_t - absorbance of solution treated for a given time, [-].

The time dependence of each treated dye concentration can be fitted by the exponential form:

$$c(t) = c_0 \exp[-k, t] + a \quad (3.3)$$

where:

$c(t)$ - concentration at time t ,

c_0 - initial concentration,

k - reaction rate constant of decolourisation,

a - residual concentration.

The existence of residual concentration can be attributed to several factors (Doubla et al., 2008; Stara et al., 2009):

- the existence of non-decomposed dye,
- absorption of final products absorbing at the used wave length,
- absorption caused by hydrogen peroxide (formed by the electrical discharge in water, absorption maximum is approximately at 296nm).

The rate of the dye removal can be measured and calculated as a derivation of concentration in time,

$$RDR = dc/dt = f(t) \quad (3.4)$$

where:

dc/dt - a time derivative of concentration, [mg/l min].

Chemical yield of the discharge can be quantified as a function of electrical parameters, electrode configuration, duty cycle, molecule concentration, mixing of molecules, etc. Power input of the discharge can be measured with electrical diagnostics and compared to the mineralization efficiency (Ceccato, 2009; Lukes, 2001).

The measured data of RDR can be used for the expression of energy efficiency of decolourisation η , (Stara et al., 2009):

$$\eta = (RDR V_s) / 60 P, \text{ [mg/J]} \quad (3.5)$$

where:

V_s - volume of treated solution, [dm³],

P - discharge power, [W].

In order to compare the discharge energy efficiency of contaminants' removal or ozone and hydrogen peroxide formation, G yield values are calculated, using the number of converted pollutants' molecules or the amount of formed ozone and hydrogen peroxide molecules divided by the required

energy input (Dors et al., 2007; Hoeben et al., 2000; Mok, 2000; Yang et al., 2005; Zhang et al., 2007).

$$G = |c_0 - c_t| V_s E_p f t, \text{ [mol/J]} \quad (3.6)$$

$$E_p = \frac{1}{2} C U^2, \text{ [J/pulse]} \quad (3.7)$$

where:

c_0 - initial concentration at $t=0$, [M],

c_t - concentration at t time, [M],

f - pulse repetition rate, [Hz],

E_p - pulse energy from pulse-forming capacitance,

C - capacitance of the pulse-forming,

U - voltage from the pulse-forming capacitance,

t - time, [min].

G_{50} yield value - G yield value at 50% of contaminant's conversion is often used:

$$G_{50} = (0,5 c_0 V_s) / E_p f t_{50}, \text{ [mol/J]} \quad (3.8)$$

where:

t_{50} - time required for 50% pollutant's conversion, [min].

In the yield calculations, the fact, that power input is a global parameter that includes the energy lost due to the heat dissipation in liquid, evaporation of the liquid to create the plasma gas cavity, formation of the plasma itself, and at last the energy really spent for the particle acceleration and dissociation used for the chemical reactions must be taken into account (Ceccato, 2009).

3.1. Selected examples of plasma treatment techniques employing liquids

3.1.1. Removal of phenol

Phenols are very soluble in hydrocarbons such as benzene, in ethyl alcohol, in ether, and in several polar solvents. In water they behave as week acids and have a limited solubility. Phenols are used as disinfectants and sterilizers, as raw materials for synthetic pharmaceuticals, perfumes, resin, dyes, pesticides, tanning agents, solvents or lubricating oils (Calabrese and Kenyon, 1991; Zhang et al., 2009). They are often present in natural products such as wine, smoked food, tea. Long-term exposure to phenol influences human central nervous system, damages kidneys and lungs, may have teratogenic and carcinogenic effect (U.S. Department of Health and Human Services. RTECS, 1993).

Tab. 3.2. Basic reactions induced by corona discharge directly involved in phenol decomposition (Dors et al., 2005)

Chemical reaction	Reaction constant [M ⁻¹ s ⁻¹]
Phenol+•OH=o-C ₆ H ₅ (OH) ₂	8.0x10 ⁹
Phenol+•OH=m-C ₆ H ₅ (OH) ₂	1.0x10 ⁹
Phenol+•OH=p-C ₆ H ₅ (OH) ₂	6.5x10 ⁹
CO ₃ ²⁻ +•OH=CO ₃ ⁻ +OH ⁻	4.0x10 ⁸
2o-C ₆ H ₅ (OH) ₂ =Catechol+H ₂ O+Phenol	2.1x10 ⁸
2m-C ₆ H ₅ (OH) ₂ =Resorcinol+H ₂ O+Phenol	2.0x10 ⁸
2p-C ₆ H ₅ (OH) ₂ =Hydroquinone+H ₂ O+Phenol	1.0x10 ⁹
Phenol+H•=Products	1.7x10 ⁹
Phenol+e _{aq} =Products	3.0x10 ⁷
Catechol+•OH=Products	1.1x10 ¹⁰
Resorcinol+•OH=Products	1.2x10 ¹⁰
Hydroquinone+•OH=Products	5.2x10 ⁹

Plasma assisted removal of phenolic compounds, which belong to the most abundant pollutants in the industrial wastewaters, (thus, are often chosen as model pollutants), was deeply investigated over the last decade.

Extensive study on the kinetics of phenol decomposition in electrical discharge in liquids was done by many research groups (Brisset, 1997; Chrostowski et al., 1983; Dors et al., 2005; 2006; 2007; Hayashi et al., 2000; Hoeben et al., 1999; 2000; Lukes et al., 2003; 2005; Lukes and Locke, 2005; Sharma et al., 2000).

Pulse corona led to the formation of hydrogen peroxide, hydroxyl radicals, aqueous electrons, and other factors, appearing during radiation process, which further induced secondary chemical reactions leading to the phenol decomposition. Chemical reactions related to the oxidants' formation are summarized in Tab. 3.2.

Kinetic cycle of phenol molecule destruction was depicted in the work of (Zhang et al., 2009) and is presented in Fig. 3.1. It is commonly believed that phenol degradation with pulsed high-voltage discharge in aqueous solution shows a first-order kinetics (Chen et al., 2005; Kunitomo and Sun, 2001; Suarasan and Ghizdav, 2002; Wang et al., 2007; Zhang et al., 2009).

DC positive corona discharge generated in air with 1.5% CO₂ gaseous mixture above the water surface was producing ozone for phenol removal (Dors et al., 2006), (Fig. 2.16). Such an option allowed to avoid nitrogen oxides (appearing in atmospheric pressure glow discharge), which further, in reactions in liquid result in undesirable nitrates and nitrites.

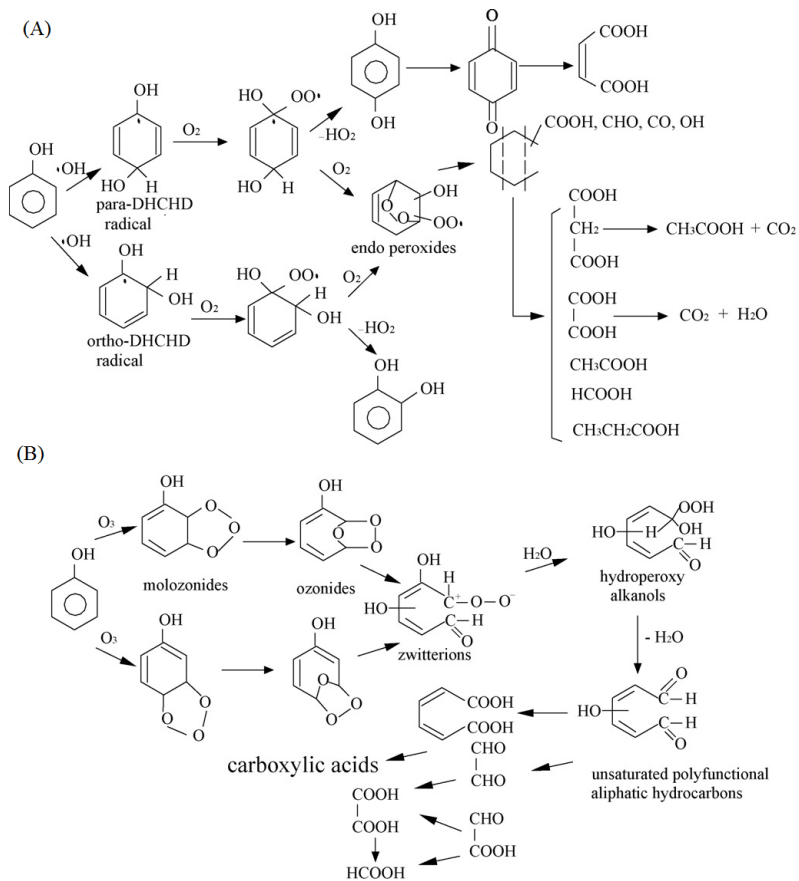


Fig. 3.1. Degradation pathways of phenol by pulsed electrical discharges under conditions of oxygen-containing ozone gas bubbling. $V=25\text{kV}$, $f=60\text{Hz}$, discharge gap 30mm, $[\text{Phenol}]_0=50\text{mg/l}$. (A) Attack of oxygen on phenol; (B) ozone addition to phenol (Joshi et al., 1995; Shen et al., 2008; Zhang et al., 2009)

It was found that ozone, which was produced by corona discharge in the gas phase above the water surface, further dissolved in water. Another phenol oxidant, hydrogen peroxide, was produced by corona discharge in the aqueous phase. Increasing corona discharge duration resulted in increased phenol degradation rate. Phenol was oxidized to dihydroxyphenols and aliphatic organic acids, which, led to the slight increase of water conductivity and acidity. These factors increased further with processing time mainly due to the presence of CO_2 in the gas phase (formation of CO_2^- and CO_3^- ions, which are precursors of carbonic acid). Oxidants generated by DC positive corona discharge oxidized

91% of phenol in 90min (Fig. 3.2). The energy efficiency of the phenol oxidation was about 3.5×10^{-10} mol/J (118mg/kWh) and was comparable to the results obtained in the pulsed corona discharge systems.

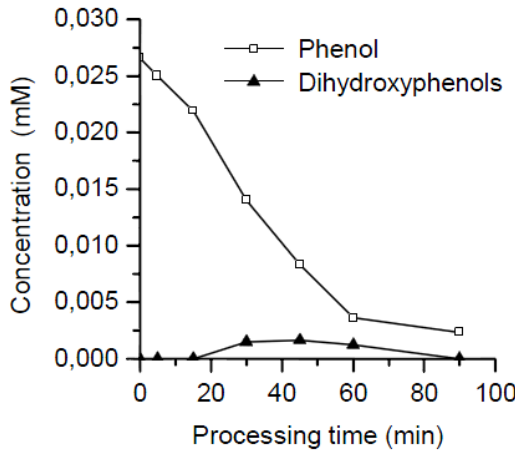


Fig. 3.2. Concentrations of phenol and dihydroxyphenols in the aqueous phase during DC positive corona discharge processing. Discharge current $75 \mu\text{A}$. Gas flow rate 1l/min. Initial phenol concentration 0.027mM (Dors et al., 2006)

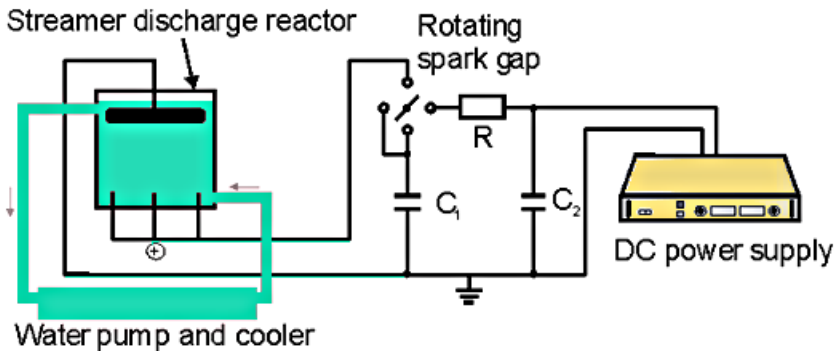
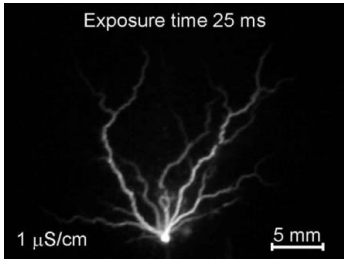
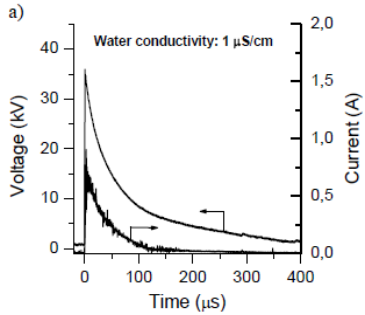
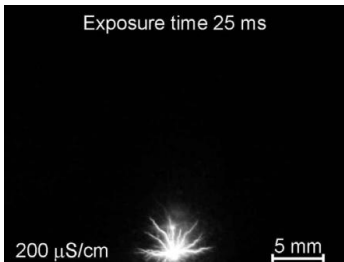
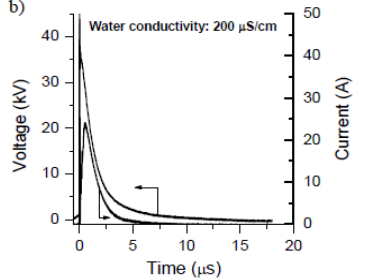
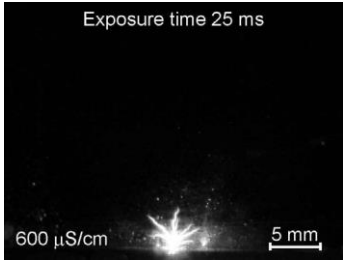
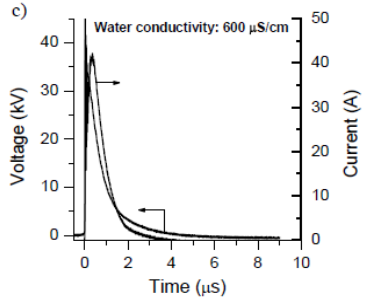


Fig. 3.3. Positive pulse streamer corona reactor for phenol treatment (Dors, 2007)

Group of (Grabowski et al., 2006) was able to remove 45% of phenol in 100ml 1mM batch in 5min of the pulsed corona discharges above thin layer of water, where ozone was generated in high concentration. Team of (Sun et al., 2000) proved that spark discharge over the water allowed faster removal of phenol but was more energy-consuming.

Tab. 3.3. Typical images, voltage and current pulses of pulsed positive streamer discharge in phenol-polluted water of different conductivities: (A) $1\mu\text{S/cm}$, (B) $200\mu\text{S/cm}$, (C) $600\mu\text{S/cm}$. Initial phenol concentration 0.62mM . Pulse energy 0.7J (Dors et al., 2007)

	Discharge photo	Voltage and current pulses
A $1\mu\text{S/cm}$		
B $200\mu\text{S/cm}$		
C $600\mu\text{S/cm}$		

Dors reported results of phenol degradation supported with Fenton reaction in tap water induced by positive pulsed streamer corona discharge generated between a stressed needle and a cylinder, both immersed in water contaminated with phenol (0.62mM) (Dors et al. 2007). The experimental set up is presented in Fig. 3.3. Typical images, voltage and current pulses of pulsed positive streamer discharge in phenol-polluted water of different conductivities are shown in Tab. 3.3. Streamer production and propagation were affected by the initial conductivity. Streamer length decreased evidently along with the increase of the conductivity, which also coincided with conclusion of other research

groups (Clements et al., 1987; Yang et al., 2004). An increase of medium's conductivity is clearly connected with a higher concentration of dissociated ions. An increase of the positive ion concentration causes a decrease in a number of free electrons, and that is why the number of the breakdown microchannels decrease and an influence of a space charge on the electric field distribution is lowered (Lubicki et al., 1996).

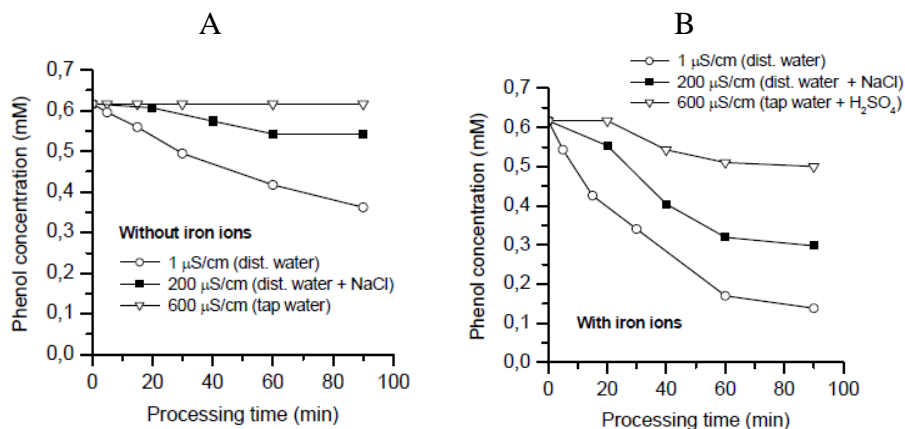


Fig. 3.4. Concentrations of phenol in phenol-polluted water of different conductivities: 1 $\mu\text{S/cm}$, 200 $\mu\text{S/cm}$, 600 $\mu\text{S/cm}$. Initial phenol concentration 0.62mM, without addition of iron salts (A) and with initial concentration of Fe_2SO_4 0.08mM (B). Water amount 500 cm^3 . Pulse energy 0.7J (Dors et al., 2007)

Phenol oxidation efficiency decreased when water conductivity increased (Fig. 3.4), lowering production of OH radicals, what was in a good accordance with other literature data (Locke et al., 2006; Sun et al., 1999; Sunka et al., 1999). Iron ions in the form of FeSO_4 (0.08mM) were added to water. They were supposed to enhance phenol degradation through Fenton reaction. It was found that Fenton reaction enhanced significantly phenol degradation rate only in distilled water of low conductivity (1 $\mu\text{S/cm}$). In tap water, which has relatively high conductivity (600 $\mu\text{S/cm}$), Fenton reaction was weak and had to be initiated by lowering the initial pH from alkaline (7.6) to acidic (4.1). During the phenol degradation, water acidity increased due to organic acids, which were the secondary products of phenol degradation. The primary products of degradation process were dihydroxyphenols.

Removal of phenol using rotating disc electrode was proposed by (He et al., 2005). Authors also confirmed the main role of OH radicals and proposed further improvement of removal rate by the addition of basic media. Bubbling of oxygen, argon and nitrogen via phenolic solutions led to increased decomposition rate of this compound (Busca et al., 2008; Shen et al., 2008).

Group of (Liu and Jiang., 2005) proposed the diaphragm glow discharge reactor for wastewaters containing salts. Complete phenol removal was achieved in 40min at pH 4,2 and 900V, 110mA discharge.

Application of three different types of corona reactors (Fig. 2.26): reference, hybrid gas/liquid parallel and hybrid gas/liquid series reactors for degradation of phenol in the presence and absence of synthetic zeolites (NH₄ZSM-5, FeZSM-5 and HY) have been investigated. 550ml of model solution (phenol concentration 0.1g/l) was constantly recirculated through reactors by a peristaltic pump at a flow rate of 0.4l/min. The inlet gas, carefully chosen for ozone generation and discharge stability (Kirkpatrick and Locke, 2005) consisted of a mixture of argon and oxygen with an argon flow rate of 0.2l/min and an oxygen flow rate of 0.15l/min. The duration of each experiment was 60min, (Kusic et al., 2005).

In order to determine major mechanisms responsible for phenol degradation in each reactor, 0.09 and 0.18M of methanol (significantly higher than 0.001M of phenol in the bulk to compensate slower reaction of OH with methanol, reactions presented below) were used as OH radical scavenger added prior to electrical discharge:

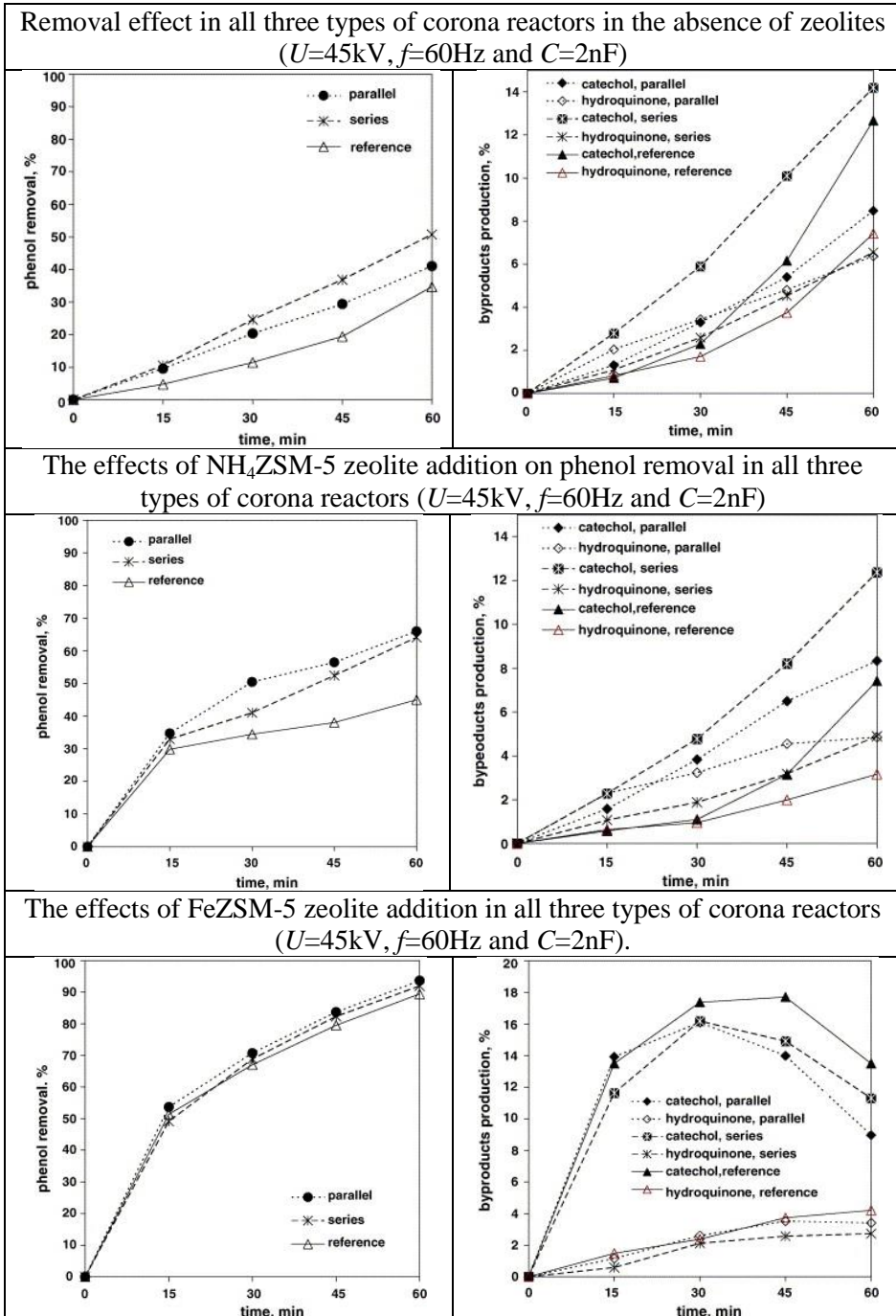


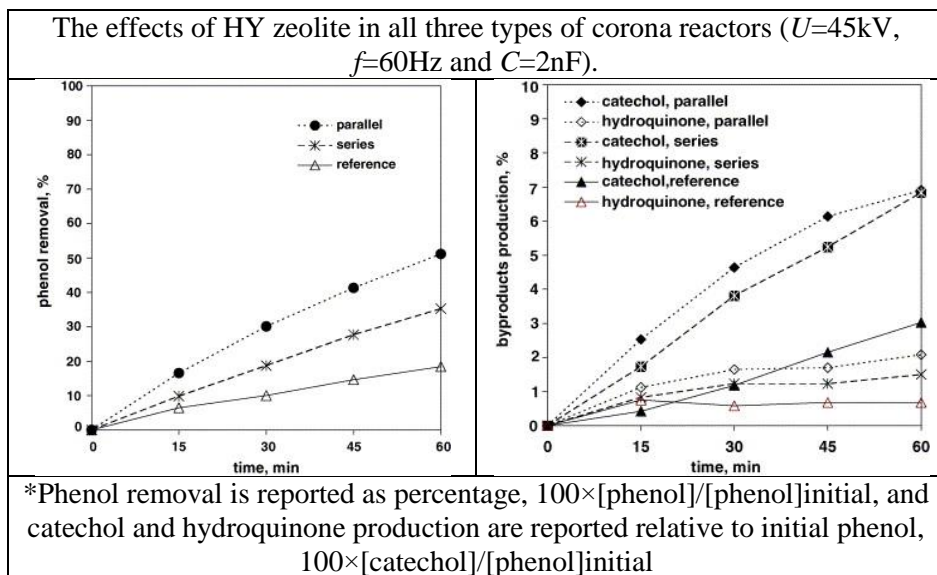
From the reactor type point of view, the hybrid-series corona reactor showed the highest rate of phenol degradation - 50.7% of removed phenol. It was primarily due to the higher OH radical generation than in the other two types of corona reactors, but also due to the ozone production in the gas phase of the reactor. A significant drop in degradation efficiency of phenol in the reference reactor was observed with methanol addition, where only 7.3% removal was found in the case with methanol addition compared to 34.7% in the case without methanol addition. Moreover, sharp decrease of catechol and hydroquinone production rate was noticed (Buxton et al., 1988; Kirkpatrick, 2004; Kusic et al., 2005).

Phenol removal using only zeolites ranged 7%, 30.4% and 33.2% for HY, NH₄ZSM-5 and FeZSM-5, respectively. The results were a bit contradictory in relation to the pore structures of zeolite and 0.68nm of diameter of phenol molecules' aromatic ring (pentastyl structure of ZSM-5 with pore sizes of 0.51 - 0.56nm vs. cubic structure of Y with pore sizes of 0.74nm) but explained by researchers as an effect of elasticity of molecule, thermal motion of pore opening and length of experiment.

The results of phenol removal employing the electrical discharge in various reactor's configurations and in combination with zeolites are summarized in Tab. 3.4.

Tab. 3.4. Treatment of phenol solution in corona reactors (Kusic et al., 2005)





Addition of zeolite enhanced phenol removal in all cases but the best phenol removal results were achieved in all three types of corona discharge reactors with the addition of Fe-exchanged zeolite, FeZSM-5, where between 89.4% and 93.6% phenol removal was due to the additional generation of OH radicals by the Fenton reaction between Fe^{2+} ions doped in the zeolites and H_2O_2 produced by corona discharge (Buxton et al., 1988; Grymonpre et al., 2003; Kirkpatrick, 2004).

Group of (Shang et al., 2010) reported that degradation of phenol by streamer corona plasma in aqueous solution was 10% higher when the TiO_2 suspension was present in the liquid. It further increased with the additional amount of TiO_2 in the range of 0 - $0.4\text{g}/\text{dm}^3$. The highest degradation rate of phenol was obtained when Degussa P25 (75% anatase and 25% rutile) was used rather than A30 and A50 (anatase); 95% of phenol could be degraded in 60min, and the corresponding removal rate of TOC reached 38.6%.

Addition of active carbon to the bulk liquid was investigated as a method for enhancement of inter-phase corona reactions and surface catalytic reactions on sorbent leading also to the partial regeneration of active carbon (Grymonpre et al., 1999; 2003; Lukes et al., 2005).

Degradation of 50 ppm of 4-chlorophenol, mineralization of TOC and energy efficiency in HDAW (one electrode submerged), HDBW (both electrodes submerged), and GD reactor (electrodes above water) at the same energy input and operation conditions (Fig. 2.24) was investigated by (Zhang et al., 2007; 2007a).

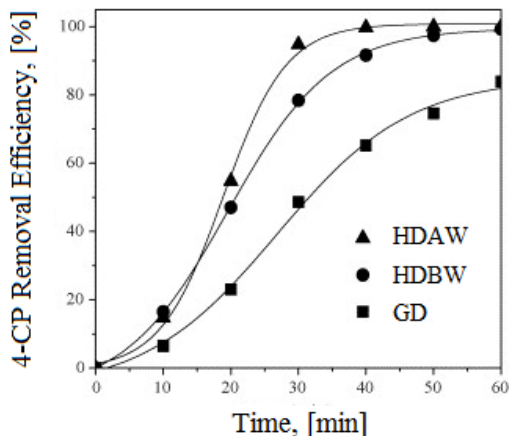


Fig. 3.5. Comparison of 4-CP removal in each electrical reactor, input voltage 16kV, pulsed repetition rate 100Hz, electrode distance 20mm, oxygen flow rate 0.2m³/h, initial pH 5.4, initial conductivity at 1.5 μ S/cm (Zhang et al., 2007a)

HDAW reactor combining discharge in gas phase and liquid phase enhanced the formation of ozone and hydrogen peroxide, thus, offered the best conditions for 4-CP degradation process, which is depicted in Fig. 3.5.

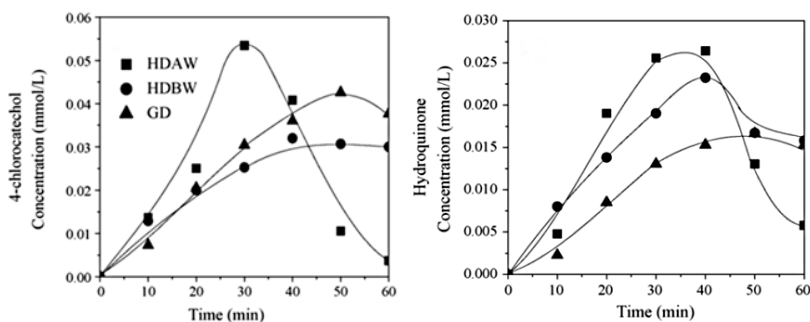


Fig. 3.6. Formation of byproducts in each electrical reactor: 4-chlorocatechol and hydroquinone (Zhang et al., 2007a)

After 40min, 99.7% of 4-CP was removed, 62.6% of TOC was mineralized after 60min, and 1.18×10^{-9} mol/J of energy efficiency was utilized (91.6% and 1.06×10^{-9} mol/J in HDBW reactor; 65.2% and 0.718×10^{-9} mol/J in GD reactor, respectively). Radical oxidation was proven to be the main degradation mechanism in these three reactors by adding *tert*-butyl alcohol as OH radicals' scavenger.

Degradation of 4-CP, mainly due to OH radicals, led to the formation of dihydroxycyclohexadienyl radical $\text{C}_6\text{H}_5(\text{OH})_2$ (DHCHD). Under the circumstance of oxygen, oxygen attacks these radicals to produce dihydroxycyclohexadienyl-peroxyl (DHCHDP) radicals. The DHCHDP radical may decay in a first-order process to form catechol by elimination of hydroperoxyl radical. Sometimes decomposition is described as an attack on the ortho position of OH^- to form 4-chlorocatechol or the Cl^- position to form hydroquinone (Fig. 3.6). The electrophilic attack of ozone molecule caused formation of various aromatic substances including primary and secondary intermediates as 4-chlorocatechol; hydroquinone; 1,4-benzoquinone; 2,4-dichlorophenol; 5-chloro-3-nitro-pyrocatechol; and 4-chloro-2-nitrophenol; formic, acetic, oxalic, propanoic and maleic acids, etc. Ozone also reacted through a 1,3-dipolar cycloaddition mechanism, which caused direct cleavage of the aromatic ring. Finally, the intermediates were mineralized to H_2O , CO_2 , including inorganic ions Cl^- (Bian et al, 2009; Lukes and Locke, 2005; NIST database; Zhang et al., 2007; 2007a).

Group of (Bian et al., 2009) reported 97% 4-CP removal in 36min discharge in HV pulsed discharge reactor consisting of two sets of electrodes. Gas was bubbled from the bottom via needle electrodes to air chamber filled with pure oxygen and further it was dosed through capillaries to liquid chamber, where the second pair of electrodes was placed. 4-hydroxybenzoate (HDB) was chosen for OH radical scavenger in indirect measurement of their concentration because 3,4-dihydroxybenzoic acid (DHDB) is the only isomer produced in quantitative reaction between HDB and $\bullet\text{OH}$ (Bian et al., 2007; Line et al., 1996).

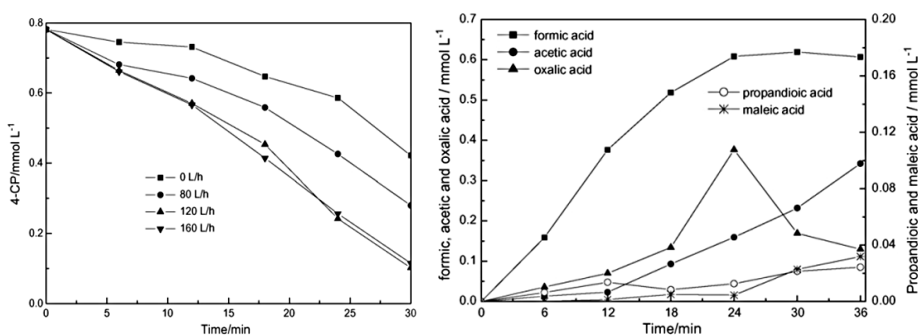


Fig. 3.7. Effect of bubbling gas on 4-CP degradation and yields of formic, acetic, oxalic, propanoic and maleic acid (Bian et al., 2009)

Fig. 3.7 shows the effect of bubbling gas on 4-CP degradation and variation in the concentrations of formic, oxalic and propanoic acids during 36min discharge. There is no maleic acid generated in the first 6min of the discharge duration. Concentration of maleic acid increased slowly from 12 to 24min, but then it increased quickly at 30min.

3.1.2. Removal of dyes and pollutants from textile industry

Textile, toys and printing industries generate large quantities of wastewater polluted with the non-biodegradable and hardly decomposable large molecule organic dyes. It causes variety of environmental problems as conventionally used chemical treatment methods are often based on the addition of chemical compounds thus may result in the secondary pollution and dyes are usually recalcitrant to the microbiological attack. Some of directly discharged dyes have carcinogenic or teratogenic health effects (Birhanli and Ozmen, 2005; DEPA, ISBN 87-7909-048-6, 1998; McLean et al., 1964; Metcalf, 1962). Positive influence of Advanced Oxidation Techniques on the textile wastewaters' decomposition yield was reported by many research groups (Aleboye et al., 2003; Chen, 2000; Choi et al., 2001; Choi and Wiesmann, 2004; Zhang et al., 2009a).

Azo-dyes are often chosen as model pollutants due to the fact that they are major colorants in the textile industry; they provide colors with outstanding colorfastness and wide spectrum. At the same time, azo-dyes are the most toxic, mutagenic and carcinogenic commercial dyes (Dojcinovic, et al., 2011; Zhou et al., 2009).

Decolourisation process using plasma discharges in water is complex and depending on the type of reactor it may include several mechanisms (Stara et al., 2009):

- reactions of dye with hydroxyl radicals and other active species produced by discharge,
- electrochemical reactions stimulated by electrolysis,
- photodecomposition of dye by UV radiation produced by discharge plasma.

Group of Brisset in many references (described below) again brought to the light the importance of pH and conductivity of the solution. Moreover, they emphasized the role of NO radicals in decolourisation of dyes.

Gliding arc discharge (Fig. 2.11) was able to rapidly fragmentize Yellow Supranol 4 GL (YS) and Scarlet Red Nylosan F3 GL (SRN) molecules, with efficiency and estimated rate constants of 92.5% and $3 \times 10^{-4} \text{s}^{-1}$ for YS, 90% and $4 \times 10^{-4} \text{s}^{-1}$ for dilute SRN, respectively (Abdelmalek et al., 2004). General evolution of spectra showed the occurrence of two isobestic points around 293 and 236nm for shortly treated solutions (up to 45min). This feature may be related to the first reaction step involving electron exchange equilibrium; the second reaction step would be then relevant to non-reversible oxidation. 60min treatment of YS was sufficient to abate COD (Chemical Oxygen Demand) from 480 to $36 \text{mg/dm}^3 \text{O}_2$.

The overall pollutant concentration was halved within less than 20min but COD evolution with t was complex:

- slow decreasing phase for first 10min,
- sharp decrease from 440 to 100mg/dm³O₂ for 10> t (min)>30, which corresponded to the degradation of dye, involving diffusion of plasma reactive species in liquid target as the key kinetic mechanism.

An overall first-order kinetic law was already observed for the corona degradation. Such a mechanism is consequent with the diffusion of the solute molecules at the liquid surface where they can react with the impinging plasma species, which are in larger quantities than the solute molecules for dilute solutions.

Degradation mechanism proposed by the group of Brisset involves the previous addition of OH or NO radicals on unsaturated bonds. Benzene rings are thus especially sensitive to these radicals and their degradation involves a ring opening step with the formation of ω -diacids (e.g., muconic acid in the case of phenol). Studies on the degradation of hydrocarbons by the OH radicals generated in a glidarc device showed more difficult breaking of C-C bonds and formation of polar functions, such as aldehydes, ketones and acid groups (which induced lowering of pH). General mechanism path also entails several radical steps, including formation of hydrocarbon radicals by abstraction of H, subsequent fixation of molecular oxygen to form unstable peroxy radical, later oxidized by NO radical and decarboxylation.

NO is engaged in the pH lowering effect and in the oxidizing action toward solutes of the plasma treatment. NO radical is oxidized to measurable compounds: HNO₂, and later to HNO₃ (Abdelmalek, 2003; Abdelmalek et al., 2004).

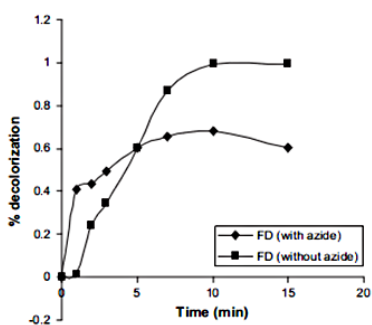


Fig. 3.8. Decolourisation rate (in %) of BTB with the treatment time (with and without added azide) (Doubla et al., 2008)

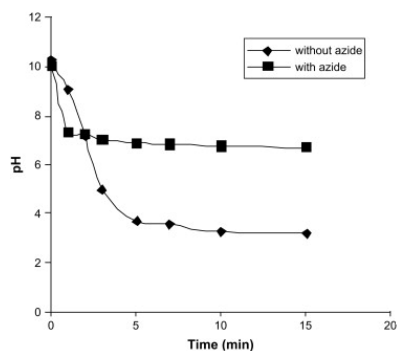


Fig. 3.9. pH evolution of the plasma treated BTB solutions against the treatment time (with and without added azide) (Doubla et al., 2008)

(Doubla et al., 2008) treated aqueous solutions of 3,30-dibromothymolsulfo-nephtalein (Bromothymol Blue) in gliding electric discharge. The addition of NaN_3 reduced decolourisation rate from 99.1% without NaN_3 to 68.2% and lowered the pH to 6.7. In contrast, H_2O_2 increased the extent of decolourisation from 60.6% to 94.0% after 5min treatment. The post-discharge phenomena increased decolourisation by 10% in the absence of discharge.

At high pH, proton concentration obeyed a mono-logarithmic variation with treatment time, which is similar to the titration plot of a strong base with a strong acid, and which is characterized by an equivalent point t_{eq} (Benstaali et al., 1998; 1999; 2002; Moussa et al., 2005). The pH fall resulted from the formation of H_3O^+ . The matching anions were identified to be NO_2^- and NO_3^- , which resulted from the occurrence of NO in the gas phase. NO readily reacts in air to yield NO_2 , which gives rise to the acidic species, HNO_2 and HNO_3 at the liquid/gas interface. The conductivity of the solution consequently increased with treatment time (Burlica et al., 2004). The bleaching properties of plasma treatment were thus presumed as directly related to its acidic nature. Another phenomena, e.g. the oxidative degradation of dye, was also related to acidity what was proven by (Moussa et al., 2005), who measured the acidity dependence on the solution oxidation potential, which changed by presence of OH and NO radicals. Summarizing, two matching phenomena described above accounted for the observed decolourisation and degradation processes (Figs.3.8 and 3.9).

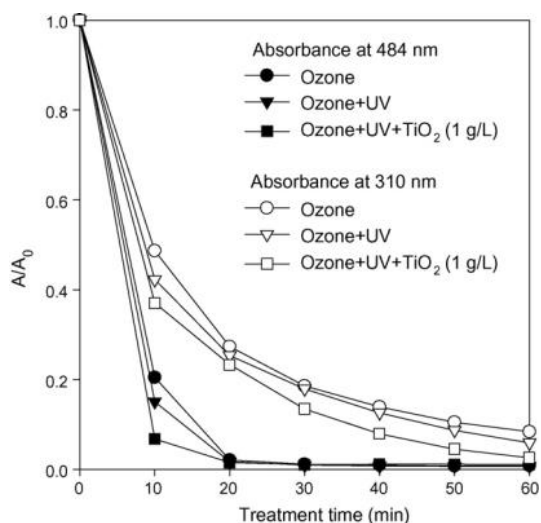


Fig. 3.10. Temporal variations of the absorbance at 484 (chromaticity) and 310nm (vibration of naphthalene rings in the dye molecules) for three degradation conditions (Mok et al., 2008)

Concentrated NaN_3 solutions have ability to limit the acidification of the medium in corona discharge (basic and strongly reducing character of N_3^-) thus prevent the formation of nitrous and nitric acids or even that of NO , and thereby, limit the decolourisation process, (Doubla et al., 2008). Dry substrate gases induce only limited change in acidity.

According to (Mok et al., 2008) a dielectric barrier discharge (DBD) system employing wastewater as one of the electrodes (as in Fig. 2.20), effectively fragmented benzene and naphthalene rings in azo dye (Orange II) molecule. UV emission from the DBD reactor could enhance the degradation of dye, particularly in the presence of titanium oxide photocatalyst, what could be seen in Fig. 3.10.

Group of (Zhao et al., 2004) suggested that the main byproducts formed by ozonation of azo dye are organic acids, aldehydes, ketones, and carbon dioxide. Researchers (Demirev and Nenov, 2005) proposed acetic, formic and oxalic acids as products of ozonation but according to (Mok et al., 2008) products resulting from the destruction of ring structures are highly recalcitrant against further oxidation to oxalic, acetic and formic acids and other small size molecules. Concentration of total organic carbon in the tests for gaseous byproducts in Mok's investigation indicated that only small amount of volatile organic byproducts were formed from the dye. Reduction in the concentration of total organic carbon was much more efficient with oxygen than with air.

Groups of (Stara et al., 2009) and (Kozakova et al., 2010) worked on decolourisation of several organic dyes with some inorganic additives in DC diaphragm discharge (Fig. 2.22). Tested electrolytes were NaCl , KCl , NaBr , KBr , Na_2SO_4 , NaNO_3 , $\text{Na}_2\text{HPO}_4 \cdot 12\text{H}_2\text{O}$.

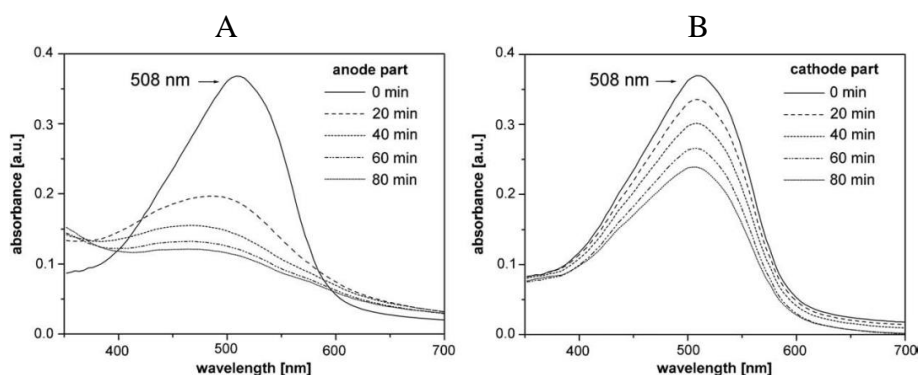


Fig. 3.11. Absorption spectra of dye solution (Direct Red 79, initial concentration 12 mg/dm^3) recorded during the diaphragm discharge treatment in the anode (A) and cathode part (B) of the reactor (input power of 160W) (Kozakova et al., 2010)

Concentration of treated dye decreased almost exponentially to the constant residual value but the substantial difference in the efficiency of dye decomposition was observed for both discharge polarities as stated in Tab. 3.5 and Fig. 3.11.

Tab. 3.5. Decolourisation in diaphragm discharge (Kozakova et al., 2010; Kuzhekin, 1995; Stara et al., 2009).

Negative polarity treatment (in the part with the anode)	Positive polarity treatment (in the part with the cathode)
Development of acidic conditions (up to 3)	Development of alkaline conditions (up to 10)
Electron velocity: 10^5 cm s^{-1}	Electron velocity: 10^6 cm s^{-1}
Plenty of short streamers with a large volume were formed at the pin-hole	Only one long streamer spreaded toward the plane electrode with minimal branching
Slightly higher increase of conductivity	Slightly lower increase of conductivity
High volume of solution was in contact with plasma	Volume of the solution, which is in contact with plasma is small
High removal rate: dye concentration dropped to 20% of the initial concentration during 10min of treatment	Significantly smaller removal rate: 20% of the initial concentration was reached after 100min of the discharge

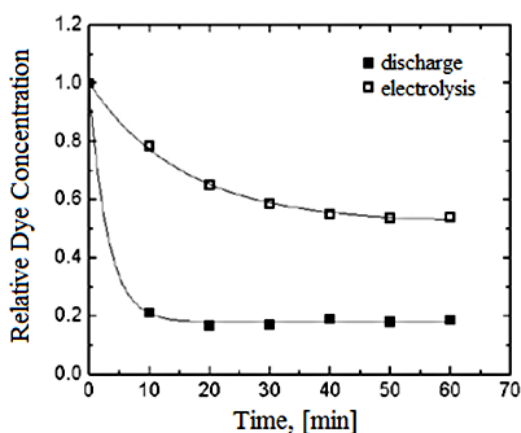


Fig. 3.12. Comparison of dye decomposition by diaphragm discharge and pure electrolysis in the 5M NaCl solution, (Direct Red 79, initial concentration of 12 mg/dm^3 , conductivity of $600 \mu\text{S/cm}$, discharge current of 100mA, electric power in discharge regime of 160W, electric power in electrolysis regime of 40W) (Stara et al., 2009)

Electrolysis (particularly, the electrochemical oxidation on the anode in the case of negative discharge) also contributed to the removal of dye as DC voltage was used for the discharge generation (Fig. 3.12).

However, the rate constant of decomposition in the presence of discharge ($k=0.33\text{min}^{-1}$) was remarkably higher than in the case when only electrolysis was active ($k=0.0064\text{min}^{-1}$). The residual concentration was evidently higher in the case of electrolysis only (Stara et al., 2009).

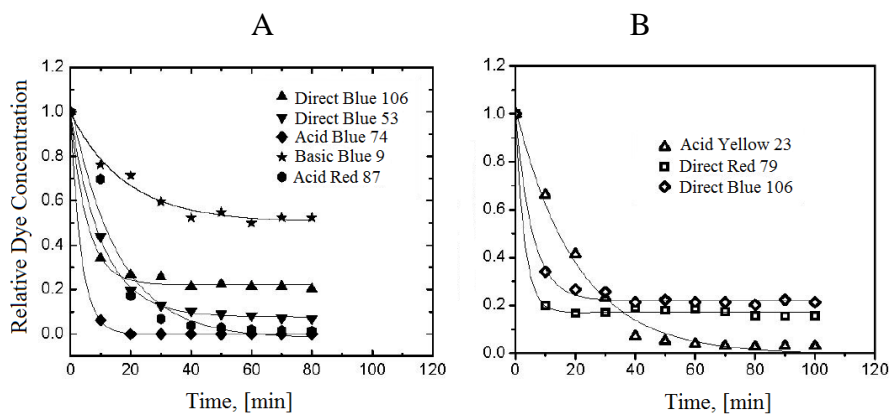


Fig. 3.13. Relative concentration decrease of organic dyes with various chemical structure: according to the dye class (A), and according to the dye colour (B) during the negative discharge treatment (initial dye concentration of approximately 12mg/dm^3 in a 4mM NaCl solution, input power of 160W) (Stara et al., 2009)

Dye decolourisation was affected by the dye structure: azo and diazo compounds were degraded significantly faster in comparison to thiazine compounds. However, in the case of tested azo-dyes of different colours (variably conjugated chains of double bonds and various chromophores, but with the same double bond between two nitrogen atoms) there was no dramatic dependence of degradation process on the dye structure as shown in Fig. 3.13. Degradation process required adjustment of the initial solution conductivity (the optimum was found around the value of $600\mu\text{S/cm}$) with NaCl and NaBr electrolytes. Halogen compounds were considered the best choice for this adjustment procedure as they did not strongly affect dye decolourisation (Stara et al., 2009).

Wang found that decolourisation of aqueous Polar Brilliant B (PBB) induced by contact glow discharge electrolysis (CGDE) also proceeded faster in chloride solution than in phosphate or sulfate solutions (Figs 2.13 and 3.14). Increasing of applied voltage from 450V to 550V did not enhance decolourisation when the applied current was kept constant (Wang, 2009).

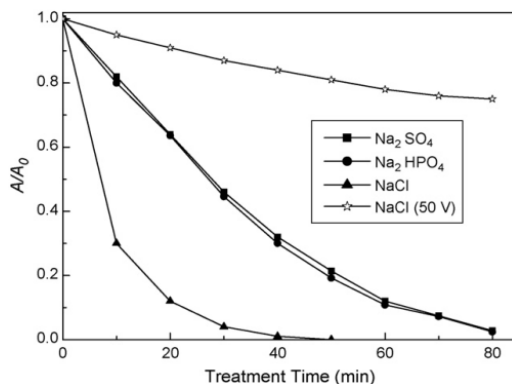
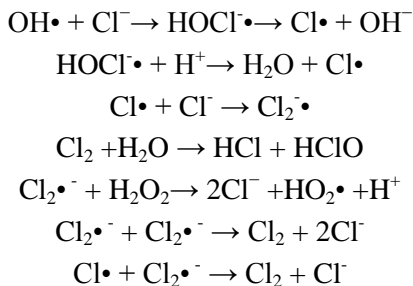


Fig. 3.14. PBB decolourisation in different electrolytic solutions (Wang, 2009)

During the treatment, TOC of the solution smoothly decreased whereas COD of the solution gradually increased due to the production of H₂O₂ in the liquid phase. Iron salts enhanced decolourisation significantly because of additional Fenton reaction. Higher initial PBB concentration resulted in lower color removal efficiency, indicating that PBB decolourisation by CGDE did not obey the first-order reaction kinetics in inert electrolytic solutions. Only in the case of very low initial concentration of pollutant decolourisation was first-order, as stated by other research teams (Tomizawa and Tezuka, 2007).

Generally, when CGDE occurs in the inert solution, hydroxyl radicals and hydrogen peroxide are produced, (Hickling, 1971). Hydroxyl radicals are the strongest non-selective oxidants and they induce decolourisation. When CGDE was performed in chloride solution, authors observed that chloride ions would be transformed to chlorine atom. Chlorine atoms react with each other to form molecular chlorine (Cl₂). Reactions with H₂O₂ (also formed in the solution) can give singlet oxygen (Aubry, 1985; Hochnadel, 1962; Lukes et al., 2002):



However, the reports concerning chloride influence mostly state it as H₂O₂ inhibitor, in the case of Wang it enhanced polar brilliant B decolourisation process and it was the most efficient in the presence of Cl ions (Figs 2.13 and 3.14).

Group of (Zhang et al, 2009) used pulsed discharge on the pinhole of an insulating plate which was inserted between two plate electrodes for Methyl Orange decolourisation. As expected, the decolourisation rate of MO solution was increased with increasing of the peak voltage, pulsed frequency, and decreasing of initial solution conductivity. When MO solution was treated with different gases bubbling, the different decolourisation rate was obtained and the order of decolourisation rate was: oxygen > air > nitrogen.

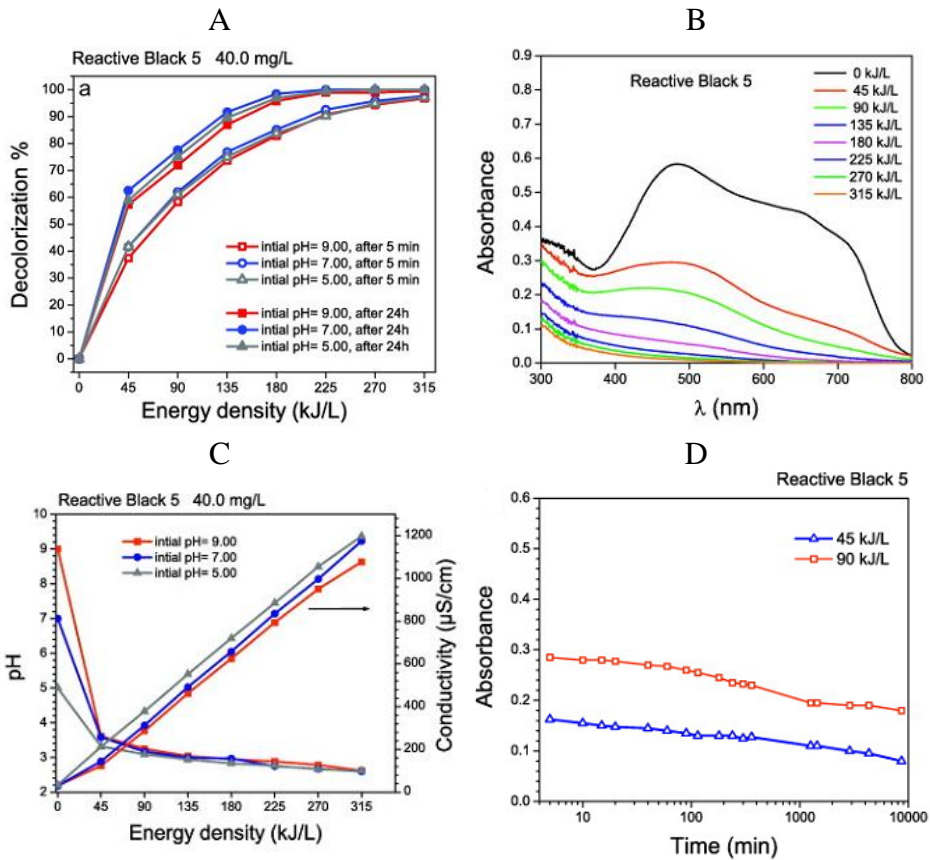


Fig. 3.15. Reactive Black: effect of initial pH value on the decolourisation efficiency (A), visible absorption spectra (initial dye concentration $40.0 \text{ mg}/\text{dm}^3$, initial pH 9.00, after 24h of treatment time) (B), change in the solution pH and conductivity values during the reaction process for different initial pH (after 5min of treatment time) (C), effects of residence time on absorbance for λ_{max} after introduction the energy density in the solution of 45 and $90 \text{ kJ}/\text{dm}^3$ (absorbance of initial solution, before the plasma treatment 0.475 , $c_0=40.0 \text{ mg}/\text{dm}^3$, initial pH 9.00) (D) (Dojcinovic et al., 2011)

Water falling film dielectric barrier discharge (Fig. 2.21B) was extensively tested for the abatement of Reactive Black 5, Reactive Blue 52, Reactive Yellow 125 and Reactive Green 15 (Dojcinovic et al., 2011). The effects of different initial pH of dye solutions, and addition of homogeneous catalysts (H_2O_2 , Fe^{2+} and Cu^{2+}) on the decolourisation during subsequent recirculation of dye solution through the DBD reactor, i.e. applied energy density ($45\text{--}315\text{kJ/dm}^3$) were studied. Influence of residence time was investigated over a period of 24h.

Results on the example of Reactive Black 5 are presented in Fig. 3.15. It was found that the initial pH of dye solutions and pH adjustments of dye solution after each recirculation did not influence decolourisation. In all cases decolourisation after the first treatment (i.e. 45kJ/dm^3) measured 5min after passing through the DBD reactor was 40 - 60% while 24h after plasma treatment, decolourisation increased to 70 - 97%, depending on the dye. For the dye Reactive Black 5, decolourisation value measured 24h after one pass through DBD reactor reached the same value as decolourisation obtained in two passes (i.e. 90kJ/L) and measured after 5min, for other dyes it was necessary to add more passes to attain the same decolourisation as in 24h. This indicates that the effect of plasma treatment can be intensified in aqueous solutions by the primary products formed during water treatment (Dojcinovic et al., 2011; Magureanu et al., 2008).

Besides very short lifetime species, which can only react with the dye molecules while the solution flows through the plasma reactor; oxidants such as ozone and hydrogen peroxide, stable enough to react with the dye molecules in long time span are produced. According to (Dojcinovic et al., 2011; Ozmen et al., 2009; Rauf and Ashraf, 2009) some prolonged influence is also caused by the reactions, which occur through the formation of alkyl, alkyl peroxide radicals, and hydroperoxides, with the third of these being responsible for the autocatalytic decomposition of organic compounds.

Ceccato stated that underwater plasmas are efficient for liquid treatment with a yield similar to the yield per molecule obtained in gas phase plasma treatment. Best energy efficiency is obtained using plasma over water- and this acts only on small fraction of the liquid so the problem of the treatment of pollutant in large volume still remains. Moreover, this energy efficiency is still in the kWh/g of pollutant range and must be associated to another complementary process for commercial use (Ceccato, 2009). Typically, for liquid treatment a first plasma stage followed by the biodegradation stage seems to be a better solution.

3.2. Foaming system for abatement of organic compounds

Group of Pawłat made extensive study on removal of colour causing organic compounds and surfactants using electrical discharge in foam (Pawłat 2004; 2005; 2009; Pawłat et al., 2003; 2003a-h; 2004; 2004a-h; 2005; 2005a,b; 2006;

2006a-c; 2007; 2007a; 2008; 2008a-c; 2009). Investigated dyes were Ethyl Violet (EV) Methylene Blue (MB), Indigo Blue (IB) and Methyl Orange (MO).

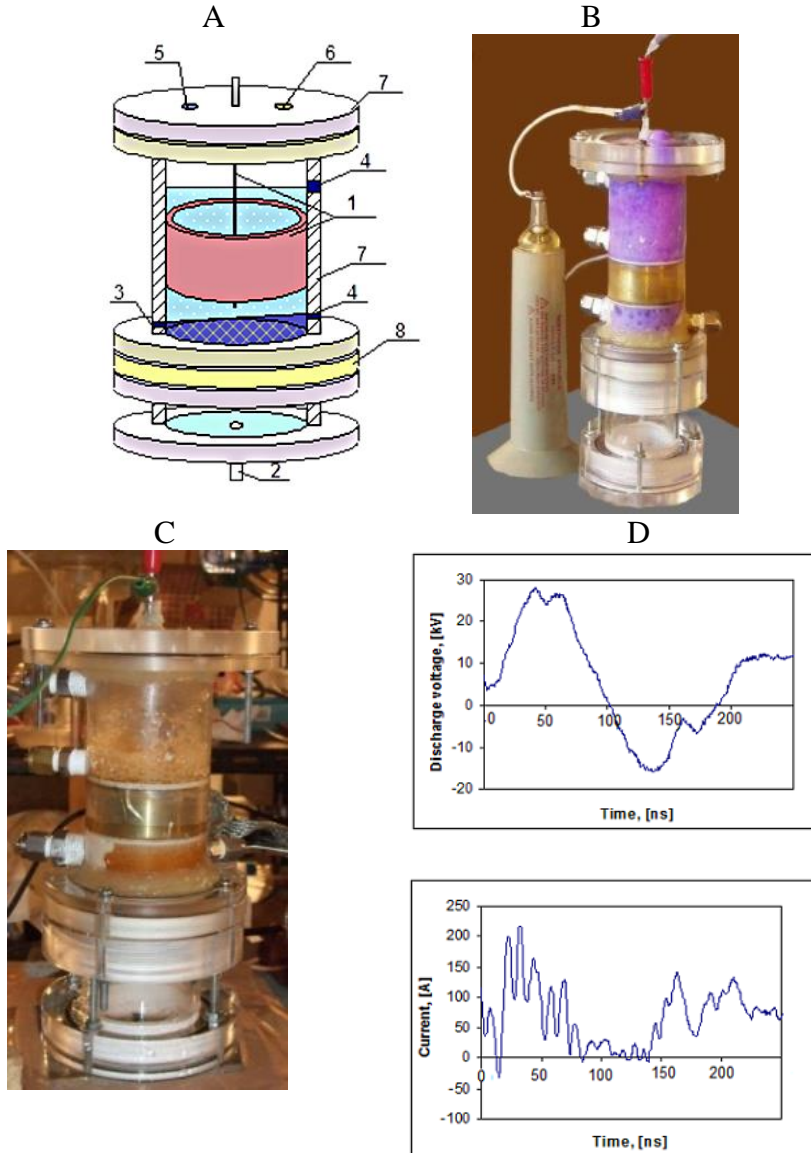


Fig. 3.16. Cylindrical foaming column: 1 - electrodes, 2 - gas inlet, 3 - water inlet, 4 - overflow, 5 - gas outlet, 6 - sampling point, 7 - polyacrylate housing, 8 - ceramic diffuser (A), the photograph of foaming reactor (EV foam) (B) and MO foam (C), oscillograms of the discharge in EV foam (substrate gas: oxygen) (D)

Foam reach in hydrogen peroxide, dissolved ozone, OH radicals and small amount of gaseous ozone was formed without the addition of surface-active compounds. Cylindrical reactor of the foaming system is depicted in Figs. 2.31, 2.32 and 3.16. The photo of apparatus filled with EV foam is presented in Fig. 3.16B, followed by the oscillograms of the discharge in EV foam. The average energy per pulse ranged from 2 to 4mJ, average discharge power (30Hz) was 0.05 - 0.12W. Temperature of surrounding water rose with extending of the treatment time (about 10°C in 25min). However, the color removal rate was rather constant for all investigated pollutants so we consider that this temperature rise was not high enough to seriously influence the reaction kinetics.

Foaming column was proved being useful during the treatment of various organic compounds. Ethyl Violet (Basic Violet 4, $C_{31}H_{42}N_3Cl$), which molecular structure is presented in Fig. 3.17A, has been recommended for inclusion in mixed dye solutions of the iron resorcin fuchsin type for demonstrating elastic fibers (Adam et al., 1988). It is also used as an indicator in chemical and medical industry added to many carbon dioxide absorbents.

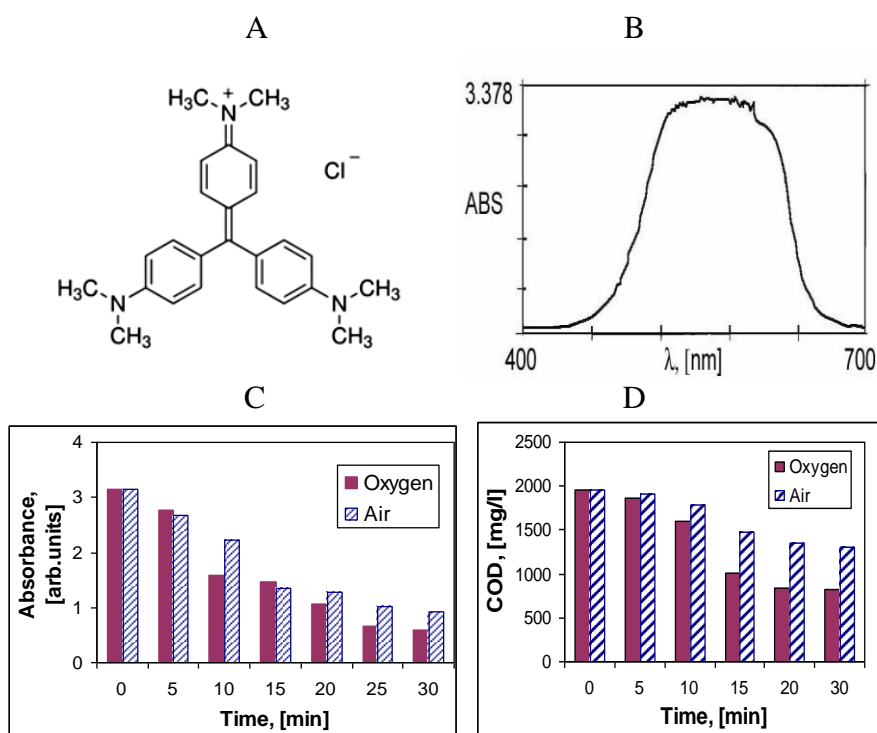


Fig. 3.17. Ethyl Violet: molecular structure (A), absorbance peak (B), purification of EV solution (C), removal of COD (dodecyl solution and Ethyl Violet, substrate gas- oxygen) (D)

EV is a green crystalline powder, which colors water solutions in persistent, very deep purple. In the performed investigations pure water was mixed with EV to obtain 34mg/l solution. 17ml of this highly foamable substrate liquid was dosed to the reactor. The flow rate of substrate gases: oxygen and air ranged 0.3l/min.

Measurements of the ultraviolet (UV) absorbance to confirm EV removal were performed using HACH spectrometer. COD was measured using HACH spectrometer and COD 2720 method at 620nm wavelength.

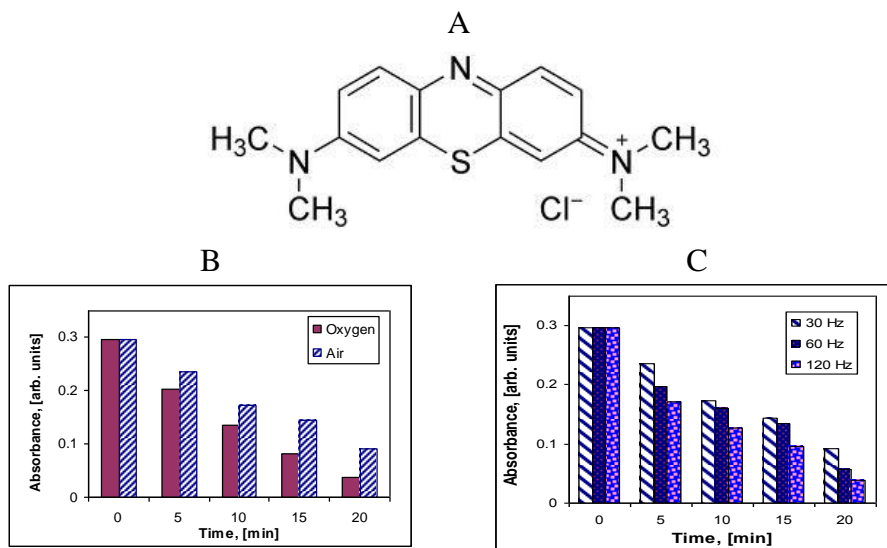


Fig. 3.18. Methylene Blue: molecular structure (A), the decomposition of MB in dependence on supplied gas (30 Hz) (B) and frequency (air) (C)

Typical absorbance curve of $C_{31}H_{42}N_3Cl$ is shown in Fig. 3.17B. The highest light absorption peak of EV at the wavelength of 596nm was analyzed for various treatment times. The EV decomposition during the application of electrical discharge within foam was observed also visually. For 30min treatment, Ethyl Violet removal rate ranged 81% and 71% in oxygen and air, respectively (Fig. 3.17C). 58% reduction of COD was observed after 30min treatment of dodecyl surfactant and EV residues (Fig. 3.17D) in oxygen. EV is highly pH-sensitive dye, which reacts mostly via OH reaction route. Alkalinization of solution could bring to dramatic improvement of decomposition efficiency (Barth et al., 2005).

Process of decomposition of Methylene Blue, toxic halogenated aromatic hydrocarbon was studied by group of Pawłat. MB ($C_{16}H_{18}N_3ClS$) is an odorless, green crystalline powder, soluble in water. This member of the thiazine dye group is often applied as a test model pollutant in semiconductor photocatalysis (Lee and Mills, 2003).

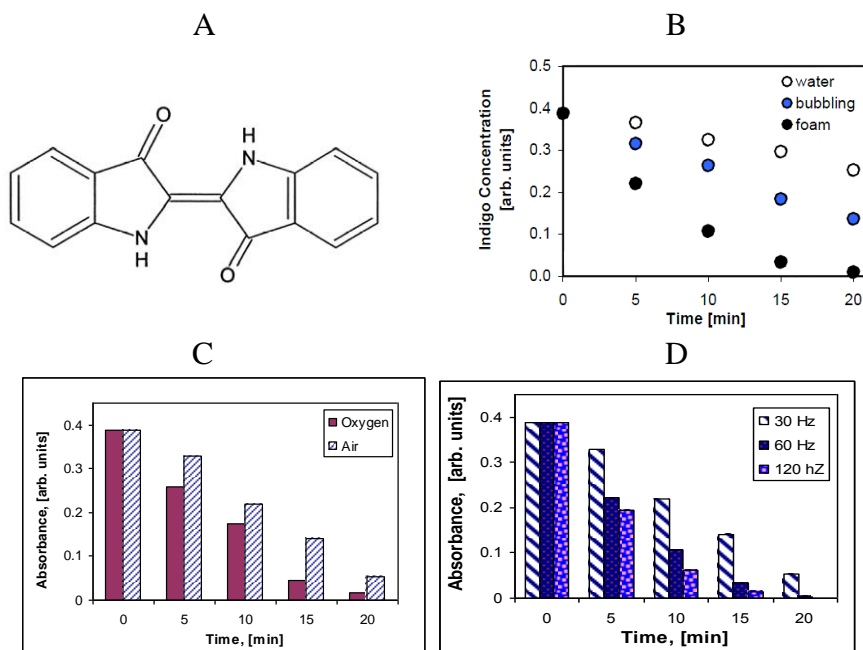


Fig. 3.19. Indigo Blue: molecular structure (A), decomposition of IB in water, bubbling and foaming systems at 60 Hz (B). Foam: decomposition of IB in dependence on supplied gas (30Hz) (C) and frequency (air) (D)

It participates in the transport of oxygen in blood and it is also used as a dye to stain certain parts of the body before or during surgery. Main oxidation path of the dyes decomposition is claimed to be by direct ozone attack and the conversion products are strong acids (Benitez et al., 1993; Grabowski et al., 2007). However, the catalyst-supported oxidization of the MB was found difficult, if only ozone was used (Randorn et al., 2004), what may suggest the radical way. The molecule of Methylene Blue is depicted in Fig. 3.18A. 60ml of 35mg/l solution was used as a substrate liquid in experiments performed by group of Pawłat for various pulse frequencies and substrate gases. Gas flow rate was 4.5l/min.

The concentration was measured after each 5min of the discharge treatment. Analyzed UV absorption (550 - 665nm) decreased constantly with time as it is presented in Fig. 3.18B. After 20min treatment, 88% removal efficiency was achieved in oxygen and 69% in air. The color removal process took less time when the higher discharge frequencies were applied (Fig. 3.18C). Indigo molecule, presented in Fig. 3.19A has two groups of electron donors and two groups of electron acceptors. The color of the solution is determined by the fact if the terminal O and H atoms are engaged in hydrogen bonding with atoms of a solvent or they form hydrogen bond with one another. Color disappears after the indigo molecule is decomposed onto the isatin and further onto more simple by-products (Zollinger, 1987). The absorption band of Indigo Blue at 612nm was used for the analysis by group of Pawłat. Initial concentration was 20mg/l. The results of decomposition of Indigo Blue by pulsed discharge are presented in Fig. 3.19B-D. Using the same reactor's geometry, the best results were achieved in foaming system comparing bubbling and the discharge in liquid phase.

Visually, full removal of color was achieved quickly and IB was relatively easy to decompose in foam mainly via reaction with dissolved (but also gaseous) ozone and generated radicals (Ince and Gonenc, 1997; Mills and Wang, 1999).

Methyl Orange (4-dimethylaminoazobenzene-4'-sulfonic acid sodium salt, $C_{14}H_{14}N_3NaO_3S$), of structure presented in Fig. 3.20A widely used as a pH indicator, dissolves in water forming bright orange solution. 70ml of 30mg/l solution was dosed by group of Pawłat to the foaming reactor. Gas flow, necessary to form the foaming conditions was 3l/min. Change in the absorbance at 403nm wavelength during the application of electrical discharge is presented in Fig. 3.20B.

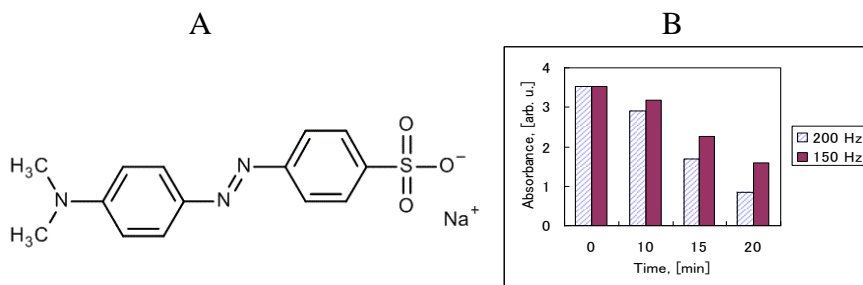


Fig. 3.20. Molecular structure of MO (A) and removal of color caused by MO in dependence on electrical discharge frequency in foam

After 20min of treatment in oxygen, 76% decrease in absorbance and total decolourisation was visually observed. Chemistry of azo-dyes decomposition is highly pH dependent. OH radicals and superoxide reactions are considered the most probable decomposition pathways (Destaillets et al., 2002).

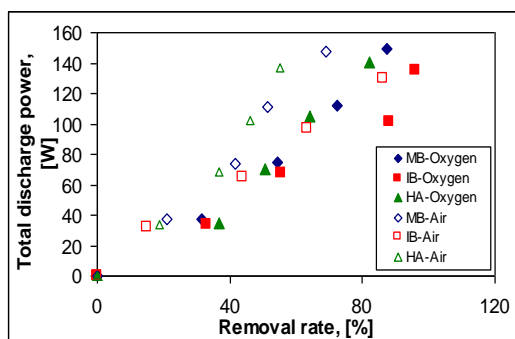


Fig. 3.21. Removal rate of MB, IB and HA versus total discharge power, frequency 30Hz

After 30min treatment in oxygen, 81% EV removal efficiency and 58% COD removal were achieved. 76%, 88%, and 96% removal efficiency were achieved for 20 min treatment in oxygen for MO, MB, and IB, respectively. In all above cases decomposition was slightly better using oxygen as a substrate gas.

Removal rate of MB, IB and humic acids (HA) versus total average discharge power consumed during treatment time is depicted in Fig. 3.21 for 30Hz frequency. In all analyzed cases decomposition was only slightly better using pure oxygen than air. It may indicate that decomposition route of tested dyes went more probably via less-selective but quick reactions with free radicals than throughout slower, direct oxidation. In aqueous foam OH[•] reactions path seemed to be the most favorable scenario for the dye decomposition. Because of small volumes of treated liquids, total achieved energetic efficiencies were very low: 21mg/kWh, 8mg/kWh, 35mg/kWh and 13mg/kWh for EV, IB, HA and MB, respectively. Those values were much lower than in the case of other treatment methods such as for instance pulsed corona above the water (Grabowski et al., 2007; Malik, 2003; Malik et al., 2002) but comparable to those obtained by the group of Itoh, who investigated pulsed discharge generated by Blumlein type power supply in helium and nitrogen bubbles in humate solutions and reported discoloration after 45min treatment (Fukawa et al., 2011; 2012; Rokkaku et al., 2012).

Many kinds of surface-active foaming materials can be distinguished like particles of dust, liquid crystals, polymers or specific cations or anions from inorganic salts. Some of water contaminants from textile industry show

the surface-active character. They can change and extremely enhance the foaming properties of the purified solution, causing foaming in very low concentrations, even 10^{-9} M (Pugh, 1996).

Large-molecule, nonionic surfactants do not dissociate into ions in aqueous solutions. They have plenty domestic, medical and industrial applications as mild and non-denaturing detergents. Showing excellent chemical stability, they are good solvents of moderate foaming properties but they also have a tendency to bioaccumulation.

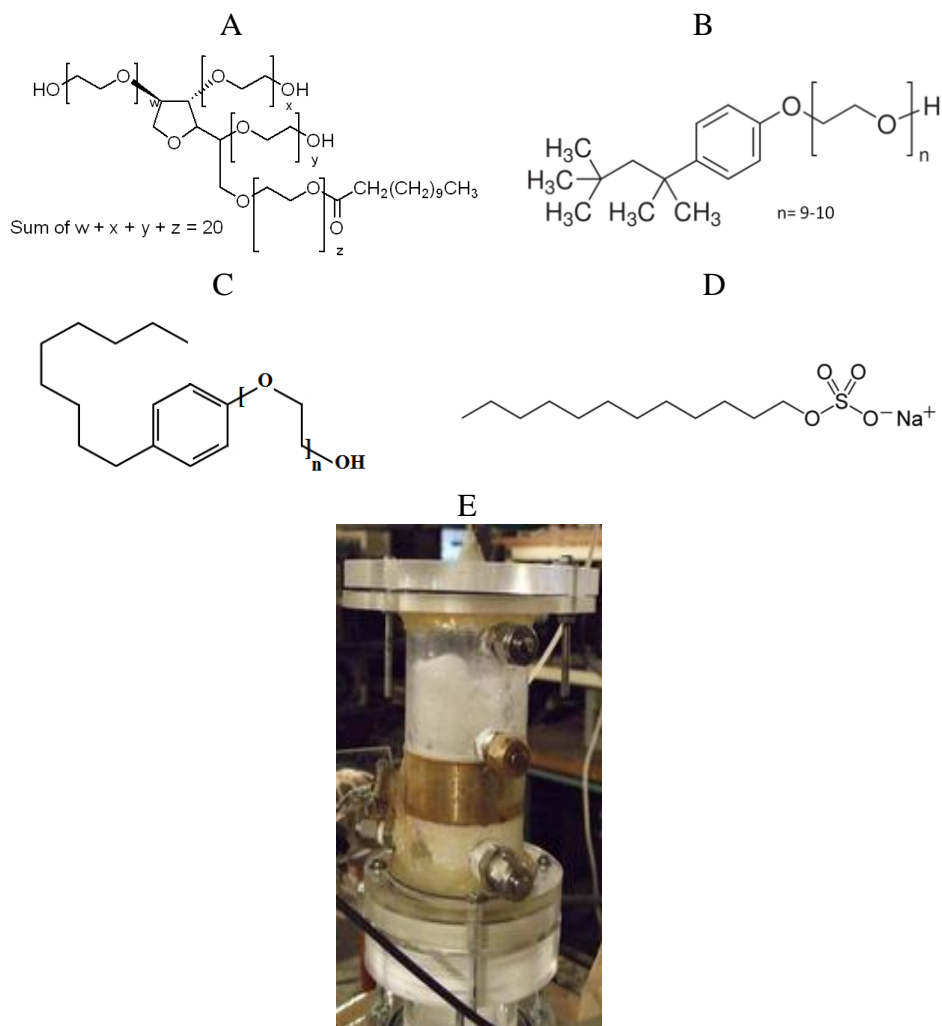


Fig. 3.22. Chemical structure of TWEEN-20 (A), TRITON-100 (B), polyoxyethylene nonylphenyl ether (C), dodecyl sodium sulfate (D). Photograph of the foaming process in P5NPE solution (E) (<http://chemicalland21.com>; www.sigmaaldrich.com; www.mpbio.com)

Tween® 20 (polyoxyethylene sorbitan monolaurate), Triton X-100 (polyoxyethylene octyl phenyl ether) and polyoxyethylene (5) nonyl phenyl ether (P5NPE, NE) were chosen as the model pollutants, (Fig. 3.22A-C).

Polyoxyethylene sorbitan monolaurate is yellow, viscous liquid miscible with water and used in the biotechnology, textile production and food industry.

Polyoxyethylene octyl phenyl ether is very stable non-ionic detergent soluble in water, benzene, toluene, xylene, trichloroethylene, ethylene glycol, ethyl ether, ethanol, isopropanol, and ethylene dichloride. At 10% (v/v) in water, it gives a clear to slightly hazy and yellow solution (sigmaaldrich.com). It absorbs in UV region at 280nm. Triton X-100 is relatively non-toxic and widely used in biochemical procedures.

Polyoxyethylene (5) nonyl phenyl ether is large molecule nonionic surfactant playing important role in nanotechnology and biochemistry, but it also occurs to be a skin sensitizer, sometimes causing allergies (Kabasawa and Kanzaki, 1989; <http://chemicalland21.com>).

0.025% water solutions of Tween® 20, P5NPE, and Triton X-100 were prepared by group of Pawłat. 50ml of above solutions were dosed to the foaming apparatus. Oxygen flow rate was fixed at 1l/min. Change of COD during treatment by the discharge in foam was tested for each pollutant. After chemical processing and heating period, COD was measured using same method as in page 84.

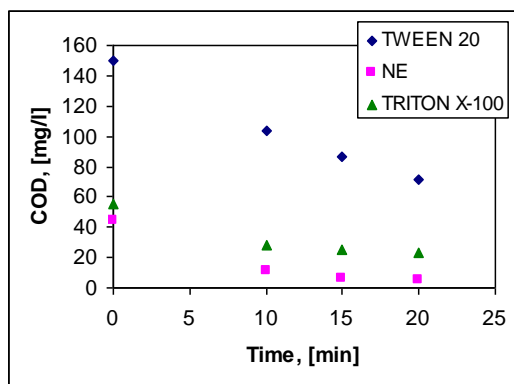


Fig. 3.23. Change of COD in dependence on the treatment time

After 20min treatment at 30Hz and 17kV discharge voltage, 53%, 87%, 58% COD removal efficiency was achieved for Tween® 20, P5NPE, and Triton X-100; respectively. Obtained data are summarized in Fig. 3.23.

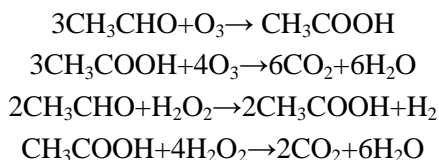
Acetaldehyde is used in various branches of industry as a chemical intermediate and basic substance for the production of acetic acid, pyridine and pyridine bases, peracetic acid, butylene glycol, esters, flavor and fragrance

acetals, paraldehyde, metaldehyde, phenolic and urea resins, antioxidants, polymers, and various halogenated derivatives. It is also a common compound in manufacturing of aniline dyes, synthetic rubber, silver mirrors, fuel compositions, disinfectants, drugs, perfumes, explosives, pesticides, and room air deodorizers. Acetaldehyde is used as a fungicide, substrate of food flavorings, preservatives, lacquers and varnishes, photographic chemicals as well. It oxidizes readily to form corrosive acetic acid. Acetaldehyde is also considered a mutagen and possible human carcinogen. Exposure by inhalation is irritating to the respiratory tract and mucous membranes; this substance is a narcotic and the chronic exposure can produce symptoms similar to alcoholism. Ingestion of acetaldehyde may cause severe irritation of the digestive tract. Ethanal causes irritation upon skin contact and eye burns (IARC, 1985; 1987; 1999).

Above premises gave additional propulsion for research centers to study on the removal of acetaldehyde from exhaust gases and wastewaters. Acetaldehyde decomposes above 400°C to form mainly methane and carbon monoxide; however, thermal methods with large volumes seemed to be quite costly. Various attempts of immobilization and treatment of acetaldehyde have been done. The amorphous silica (Natal-Santiago et al., 1999), activated carbon with about 13% adsorption efficiency (El-Sayed and Bandosz, 2001) and the polymer filters (Shiratori et al., 2001) were used to limit the concentration of acetaldehyde in the outlet fluid. Interesting solution based on biodegradation of ethanal in packed column with immobilized activated sludge gel was presented by (Ibrahim et al., 2001).

Other direction was the photodecomposition using surfactants and organic solvents, which amplified the overall decay rate (Chu and Kwan, 2002). The photon dissociation of acetaldehyde was described by (Shin et al., 2001; Wirtz, 1999), with indicating formaldehyde, metylhydroperoxide, CO as the products generated mainly via free radical channel. Those results were partly confirmed by the report based on acetaldehyde reactions with hydroxyl radicals (Vandenberk and Peeters, 2003).

The ideal treatment process of acetaldehyde using generated oxidants could be described by the equations:



In performed investigations pure water or pure water with addition of common surfactant (1ml/500ml H₂O) and Tritron X-100 (1ml/300ml H₂O) was used. Substrate gas was acetaldehyde with nitrogen as a carrying gas.

The process of absorption of acetaldehyde within foam without and with addition of Tritron X-100 was studied. The example of one absorption cycle with 5ml of surfactant's solution in pure water is presented in Fig. 3.24. In that case acetaldehyde in nitrogen gas flow rate was 1.2l/min and initial concentration of ethanal was 250ppm. After 80min of saturation time, the electrical discharge was applied. Proceeding of electrical discharge caused releasing of acetaldehyde absorbed before and decomposition of the surfactant, then gradually concentration of CH₃CHO decreased achieving removal rate of 62 – 76% depending on the discharge condition. However, by-products were not analyzed. The absorption process in presence of Tritron was much more efficient than in the case of pure water only because of hydrophobic nature of acetaldehyde molecule.

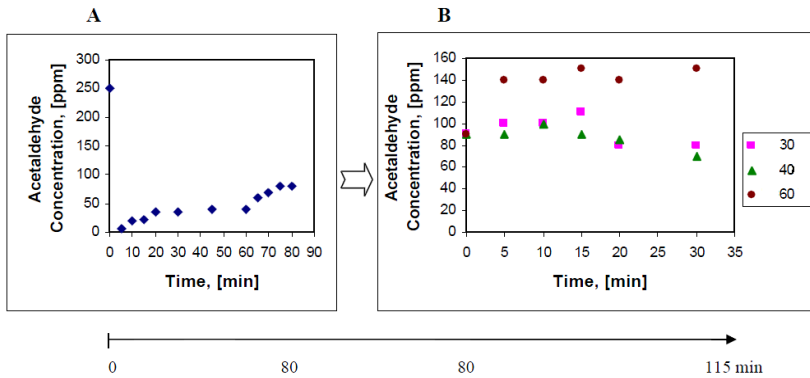


Fig. 3.24. Absorption of acetaldehyde within foam with addition of Tritron X-100 versus time (A) and change in acetaldehyde concentration after application of electrical discharge to the saturated solution (power with losses included, [W]) (B)

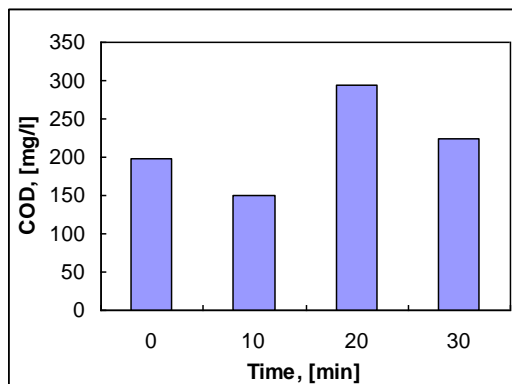


Fig. 3.25. COD in dependence on the treatment time at the lower pulse energy (P5NPE)

Dodecyl sodium sulfate (SDS, lauryl sulfate sodium salt, Fig. 3.22D) is a white powder soluble in water giving colorless liquid. This anionic detergent is widely used in molecular biology, drug and food industry, ceramics, and in methane hydrate formation (Dutta et al., 2003; Vladimirova and Morgunova, 1995; Watanabe et al., 2005).

58% reduction of COD was observed after 30min treatment of 15ml SDS surfactant solution ($0.05\text{g}/\text{dm}^3$) and residues of cationic dye: Ethyl Violet at $0.3\text{l}/\text{min}$ oxygen flow.

For the lower pulse energies after COD reduction in the first 10min, rapid increase of COD, sometimes exceeding the primary untreated value was observed. For instance, in the case of P5NPE solution, 30min treatment time led to 13% increase in COD comparing the initial value (Fig. 3.25). After initial decrease in COD, what may suggest breaking the large molecule compound, further application of the electrical discharge promoted the unwanted reaction paths and formation of some other large-molecule species. In such a condition, attempt of SDS and EV residues solution treatment due to the complicated chemical structure of both compounds caused rapid increase of COD even by 30 times during the first 10min and then slow decrease of this value, which after 30min was still 15 times higher than untreated one.

In all observed cases, there was a visible decrease in the foamability of treated solutions and in the last 5min of treatment, bubbling prevailed over the foaming phenomena. The most efficient generation of oxidants, thus the highest treatment efficiency was observed for higher frequencies and gas flow stabilized at the level, which was the most fruitful from the foam formation point of view.

Humid environments, including those formed in the foaming column, are an interesting alternative for conventional methods of oxidant's generation often allowing for reduction of the chemical additives' amount. These types of set-ups may lead to simplification of the technological process as various oxidative species are generated and used in one reaction vessel (even in polluted media). Moreover, unique properties of foam allow extending the phase-to-phase contact area what leads to the intensification of oxidation process. Electrical discharges in foam, their practical employment for the generation of oxidants and abatement of pollutants were not investigated by other research groups so far. The energetic yields for the abatement of pollutants from liquids in state of foam are lower in comparison to the reactors based on pulsed corona. Many hybrid reactors are plug-flow type and their purpose is the treatment of pollutant in liquid phase only. However, in the specific foaming system, where large volumes of gas and only small volume of liquids are used, humid gas and aerosol treatment may be more energetically reasonable option than in the case of liquid-phase purification. There is a perspective for application of plasmas in foams for the exhaust gas treatment, even possibly to three-phase media. Nature of foaming reactor with high gas flow rates, may allow for treatment of large volumes of industrial gases and aerosols in relatively short time.

4. Selected applications of plasmas and oxidative species for multi-phase environments

Plasma plays an important role in variety of industrial applications and non-thermal plasmas for single phase environments are well established in the market. Plasma displays are only one example. Plasmas are used in material processing, semiconductor manufacturing, light sources, propulsion, analytical spectrochemistry, laser technology; they can be source of particles, and many more.

Technologies based on ozone produced as a result of electrical discharges are successfully used for purification of water, for waste-water and exhaust gas treatment. Plasma discharges in liquids are applicable for biological, environmental, and medical technologies, where electrical breakdown is proposed as a non-chemical, alternative treatment method. Some miscellaneous applications of plasmas, especially for multi-phase environments are briefly introduced in this chapter.

4.1. Plasma application for biomedical purposes

With increasing of pathogens' drug resistance it is necessary to develop sterilization and decontamination methods based on alternative approach: cost-effective sterilization tool, which combines physical and chemical treatment and could be safely and flexibly applied to various surfaces and materials including multi-phase items and sometimes living tissues.

According to (Favero, 1998; 2001) any item, device, or solution is considered to be sterile when it is completely free of all living microorganisms and viruses, including bacterial endospores. From the practical point of view sterility assurance level defined as probability of a microorganism surviving on an item subjected to treatment of less than one in one million (10^{-6}) was introduced.

There is number of factors, which influence sterilization process including the type of pathogen, type and condition of surface undergoing sterilization, environmental conditions (e.g. temperature, pressure), amount of other contaminants, etc., (Guideline for Disinfection and Sterilization in Healthcare Facilities, 2008; Spaulding, 1968; 1972).

Pathogens can be present in variety of forms deposited on inert and living surfaces like walls of equipment, wound dressing, living tissues, medical prosthetics, food containers and food itself. National Institute of Health have reported that 80% of all known infections are caused by biofilms (Wolcott and Ehrlich, 2008), which are complex communities of microorganisms (bacteria, fungi, protozoa, etc.) embedded in self-secreted matrix of strongly adhesive hydrated polymers. Some studies have shown that bacteria in biofilms can be 1000-fold more resistant to antimicrobials than are planktonic cells (Mah et al., 2003).

4.1.1. Methods of decontamination

The idea of plasma sterilization was already proposed in 60-ties (Menashi, 1968) as a good, low toxicity method for patients and operating staff. In spite of the fact that the number of research papers and devices related to this topic is constantly increasing, most of solutions were not fully implemented, mainly because of lack of system's optimization, lack of comparability between the proposed reactors and methods, lack of matching between plasma properties and sterilized material, and because of the incomplete sterilization in the case of multi-microorganisms biofilms. Therefore, industrial plasma-based decontamination is still a great challenge.

For medical sterilization several techniques have been implemented so far:

- the most popular thermal sterilization: dry and moist heat. Temperature in the autoclave is about 121°C, which cannot be applied to the heat-sensitive materials;
 - membrane filters for liquid heat-sensitive components (problem with filter recycling);
 - commercially used ethylene oxide sterilizers (EtO), method with many questions concerning the carcinogenic properties of the EtO residues adsorbed on the materials after processing (Steelman and Aorn, 1992) and worries about the safety of operators when opening the sterilizer before the end of the very long vent time. Because of high toxicity one cycle of EtO operating ranges from 12 to 48h (sterilization itself - about 60min);
 - liquid formaldehyde and glutaraldehyde, not applicable to the tissues, not environmental-friendly;
 - costly gamma irradiation process, with many questions about the location of the operation site and damaging of the disinfected materials' surface (Henn et al., 1996). Method is sometimes used for sterilizing selected kinds of foods;
- Pulsed electric field processing (15 - 50kV cm⁻¹, pulse frequency of 200 - 400Hz) and high pressure method for food sterilization (300 - 700MPa) (Wan et al., 2009) are currently gaining attention. However, the last one alone seems to be ineffective towards endospores. Sterilizing efficiency of ultrasonic devices is very low.

All above methods cannot be applied to the living tissues and in most of the cases, they require closed systems. Except the thermal one, the traditional medical sterilizers involve harmful compounds. Thus, application of plasmas seems to be reasonable solution for biological decontamination. Pathogens such as Gram-negative and Gram-positive bacteria, microbial spores, molds, fungi, and viruses can be inactivated by plasma.

Presently, low-pressure plasma sterilizers are commercially offered in the market (www.sterrad.com). However, low-pressure plasma besides the costly vacuum system shares some of the traditional sterilizers' disadvantages - it requires closed reactor and cannot be applied to the living tissues.

Many research groups concentrate on the efforts of designing plasma sterilizing device working in the ambient conditions (Banerjee et al., 2010; Kamgang -Youbi et al., 2010; Kim et al., 2011; Laroussi, 1999; Laroussi and Leipold, 2004; Liu et al., 2008; Machala et al., 2006; Moisan et al., 2001; 2001a; 2002; Montie et al., 2000; Ohkawa et al., 2006; Pawłat, 2012, 2013; Pawłat et al., 2012; Pongráč and Machala 2011; Vleugels et al., 2005; Yu et al., 2006; <http://www.cerionx.com>; <http://www.neoplas.eu>) using variety of methods such as barrier discharge, pulsed corona reactors, or plasma jets.

To maintain the uniform discharge under atmospheric pressure mainly quite expensive gases as helium and argon are used in high concentrations. Plasma disinfection time given in the literature varies from several minutes to even hours.

Recently, many investigations concern atmospheric-pressure plasma jet (APPJ) as the compact, portable, low-temperature gas discharge plasma device for cold sterilization of various heat-sensitive surfaces and materials.

The pathogens are going to be inactivated due to:

- direct destruction, volatilization and etching of the cells, decreasing of biofilm's adhesivity by the decomposition of polymer matrix,
- oxidative stress (due to the fact of active agents' formation (ozone, OH and O radicals, hydrogen peroxide, etc. during the electrical discharge),
- nitrogen stress (recent research results suggest cells' damage from reactive nitrogen intermediates as nitric oxide, peroxyxynitrite, nitrous acid, nitrogen trioxide, etc. (Barraud et al., 2006)).

4.1.2. Atmospheric pressure plasma jet

APPJ for decontamination purposes proposed by group of Pawłat consisted of:

- gas and liquid dosing sub-system,
- electrical discharge generating sub-system,
- chemical and biological analyzing sub-system.

The main part of device was powered changeable needle electrode encapsulated in a tubular metal case. Surface of the needle electrode was turtle-shell shaped to assure uniformity of the discharge. Discharge gap between the electrodes was 2mm. Device was powered by a regulated RF supply through an impedance matching network. For the best operation on heat non-resistant materials, temperature of plasma should not exceed 70°C. For the treatment of living surfaces (wounds, skin) temperature of APPJ outlet post glow gas below 40°C is recommended. Such a device was developed in LUT assuring safe operation with 35°C measured at the outlet of the nozzle (Fig. 4.1) (Pawłat, 2012; 2013; Pawłat et al., 2012; Samoń and Pawłat, 2011).

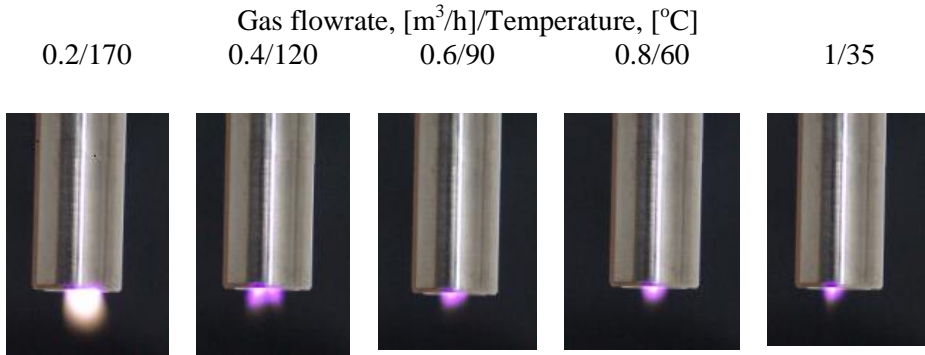


Fig. 4.1. Photographs of the plasma jet generated in RF powered device with different flow of air. P=80W, 12.98MHz frequency

Implementing APPJ can ensure the sterile conditions for production, handling and preservation of variety of materials. APPJ device could be applied on the different stages of medical and biochemical procedures, in food factories and restaurants, for a broad range of curvatures and surfaces.

4.2. Application of oxidative species for treatment of soil

Soil remediation is especially difficult procedure because it must be performed on site and cover relatively large surface area with various geological settings while keeping also penetration deepness. The organic matter has the greatest influence on the sorptive capacity of the soils. Besides organic matter, grain-size distribution is an important factor influencing the sorptive capacity of soils, especially the content of very fine and colloidal particles, i.e. the kind of soil. Distribution of cations in the sorptive complex depends on pedogenesis (soil forming process), that is on their typology. Total exchange of cations in the sorptive complex and the base saturation depend on kind of the parent rock, (for instance, the presence of carbonates) (Melke et al., 2003).

The processing of soil for its remediation is correlated with several factors including:

- type of soil (content of water, organic compounds, consistence, structure),
- type of pollutant,
- treatment technique,
- geological and atmospheric circumstances.

Pollutants might be distributed in soil in several ways:

- in soil matrix,
- in vapor phase,
- in non-aqueous phase,
- in groundwater.

Chemical methods of soil sterilization are based on chlorine, methyl and ethyl derivatives such as trichloromethane, ethylene oxide, or methyl bromide. The last one, quite commonly applied for fungal and bactericidal decontamination (fumigation, disinfection and sterilization) was considered environmentally harmful for ozone layer and according to Montreal Protocol (1993) was banned from practical uses (in developed countries since 2005; in other countries including Poland since 2015). Many techniques of soil remediation such as heating, flushing with chemical additives (surfactants), irradiation, irradiation with catalyst, soil vapor extraction, landfilling, incineration, aeration, oxidation and bioremediation were tested alone or in combinations.

4.2.1. Ozone and soil properties

Oxidation techniques of soil may involve ozone, hydrogen peroxide, chlorine dioxide, and potassium permanganate. Because of its relatively good solubility in aqueous phase, ozone generated during electrical discharges seems to be especially potential for the soil treatment because it can be applied in both: gaseous and aqueous phase.

There are numerous works covering application of Fenton's reagent to the soil treatment. Higher H_2O_2 concentration provided faster reaction times but less efficient oxidants' use (Jans and Hoigné, 2000; Watts, 1990; Watts et al., 1992; www.h2o2.com). Watts reported using H_2O_2 for cleaning soils mentioning following main factors influencing efficiency:

- availability of iron (crystalline soils are easier to treat than amorphous ones),
- buffering capacity (Fenton reactions perform best at pH 2 - 4 and carbonate ions are usually strong free radical scavengers (retarding reaction)),
- natural humus content (competitive oxidative reactions between background and contaminant).

Trials employing usage of ozone alone or combined with AOPs for the treatment of soil, which are presented in this chapter were mostly performed by cooperating research groups from Japan and Poland. Various aspects of ozone soil treatment and its further influence on plants' growth, pH, temperature, biological phenomena were analyzed by those groups and reported in following papers: (Ebihara, 2006; Ebihara et al., 2005; 2006; 2006a; 2008; 2008a; 2009; 2011; 2011a; 2013; Pawłat et al., 2009b; 2010; 2011a-g; Stryczewska, 2009; Stryczewska, et al., 2005; 2011; 2012; Takayama et al., 2006).

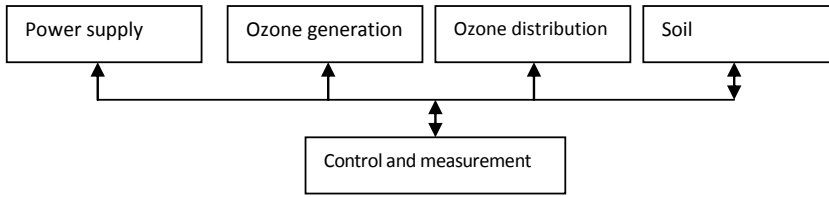


Fig. 4.2. Block diagram of integrated system for soil treatment

Integrated soil sterilization system using high concentration of ozone was proposed by above groups of researchers. It consisted of several modules (Fig. 4.2):

- contact columns,
- ozone generation module,
- gaseous ozone distribution system within soil,
- ozonized water distribution system (on and sub-surface),
- power supply system,
- monitoring system.

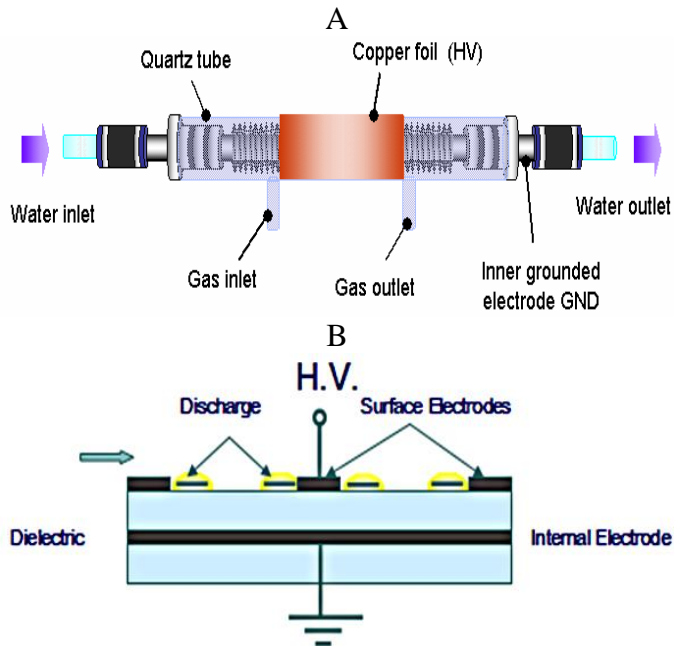


Fig. 4.3. Ozone generators used in the soil sterilization system: screw type ozonizer (A), OP-20W ozonizer (B)

Main parts of the set-up were ozonizers: barrier discharge screw type electrode ozonizer and TiO₂ based surface discharge commercial OP-20W Iwasaki ozone generator (presented in Fig. 4.3A and Fig 4.3B, respectively). 106g/m³ of ozone was generated at 0.5dm³O₂/min of substrate gas (oxygen) flow. Maximum energetic efficiency - 55gO₃/kWh was reached at concentration of 50 - 60 gO₃/m³.

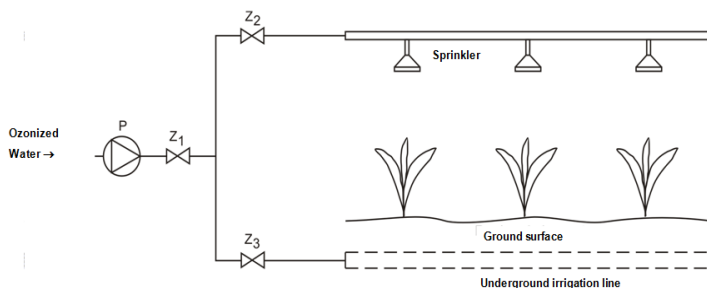


Fig. 4.4. Ozonized water distribution system

Module for on-field distribution of ozonized water is depicted in Fig. 4.4. Water from contact columns was pumped into sprinklers (every 33cm) and underground irrigation line IRRITEC Multibar. Both lines were made of inert and chemical resistant materials.

Water distribution system enabled precise and long-time irrigation what could be especially advantageous for large areas with surface levels difference. Ozonized water flow rate ranged 90dm³/h.

Sub-system for on-site ozone injection into soil is shown in Fig. 4.5. It consisted of 10 electrodes and the treatment container (Fig. 4.5C), which was developed for sterilizing and monitoring of agricultural soil in large volume. The pH value, electrical conductivity and temperature of the soil were observed to investigate the effect of ozone treatment on soil properties. Alternatively, porous ceramics was used for ozone distribution within soil in various concentrations. Ozone injection deepness ranged 70 - 150cm.

In-situ changes of the ozone penetration into soil after plasma treatment are difficult for observation; therefore, the indigo-colored silica gel was used to model the soil and to observe the ozone diffusion dynamics while it discolored indigo to colorless isatin. It was proven (Fig. 4.6) that ozone can disinfect about 200cm³ of soil volume during 60min of treatment at 1l/min of gas flow and ozone concentration of 1g/m³.

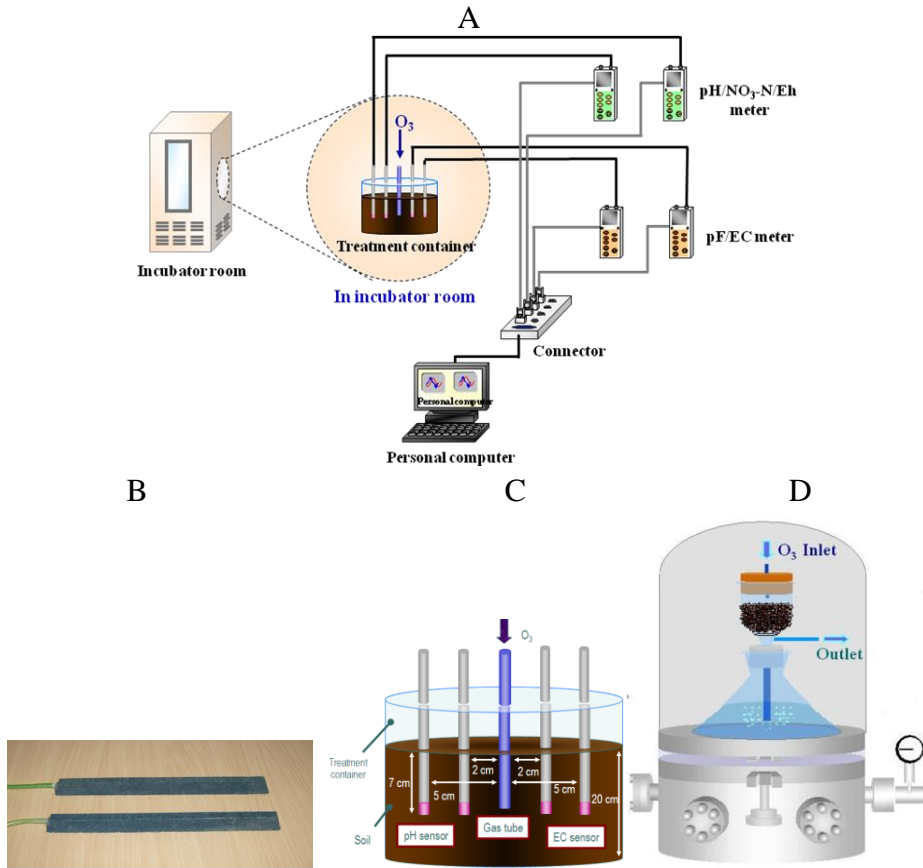


Fig. 4.5. Experimental set-up for general soil treatment (A), ceramic diffuser (B), multi-electrode injection system (C), set-up for sterilization of pathogens within soil (D)

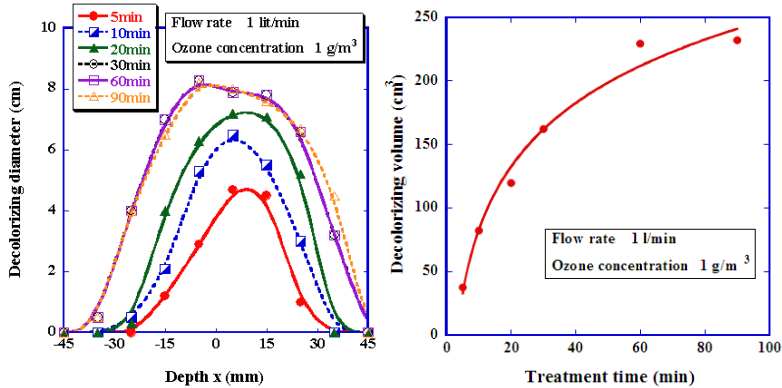


Fig. 4.6. Ozone diffusion into soil

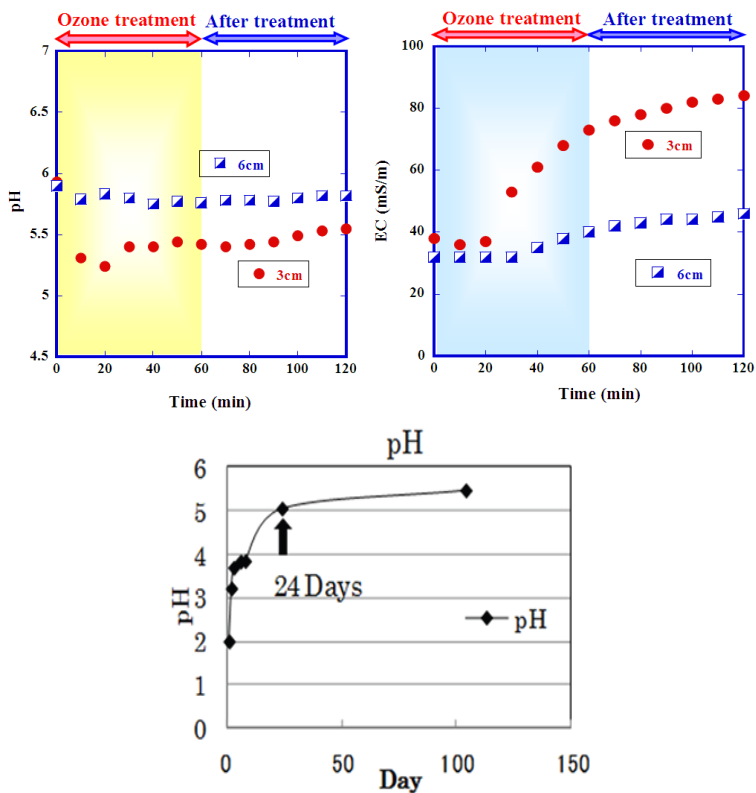


Fig. 4.7. Changes of pH and electrical conductivity during and after soil ozonation

The reaction of soil components with ozone caused remarkable change in physical and chemical properties of soil. Chemical exothermic reaction between the soil and the gas-phase resulted in rapid temperature increase up to 70°C. In-situ measurements showed the decrease of pH value and gradual increase of electrical conductivity due to the formation of carboxylic acids originating from the oxidation of organic matter. Changes of above parameters during the course of ozonation (gas flow rate 2l/min, 100gO₃/m³) and in post-ozonation phase are depicted in Fig. 4.7.

4.2.2. Oxidants in abatement of chemical pollutants in soil

Organic compounds from badly shielded landfills, leaky storage-tanks, old gasoline stands, refineries and accidental spills are considered a main source of soil pollution (Hutzler et al., 1991).

Eco-oxidative techniques can improve soil's aeration, thus will inhibit denitrification processes making them useful in, for instance, after-flood remediation. Application of AOP helps to preserve natural structure of soil, prevents its acidification, leaching and releasing metallic compounds.

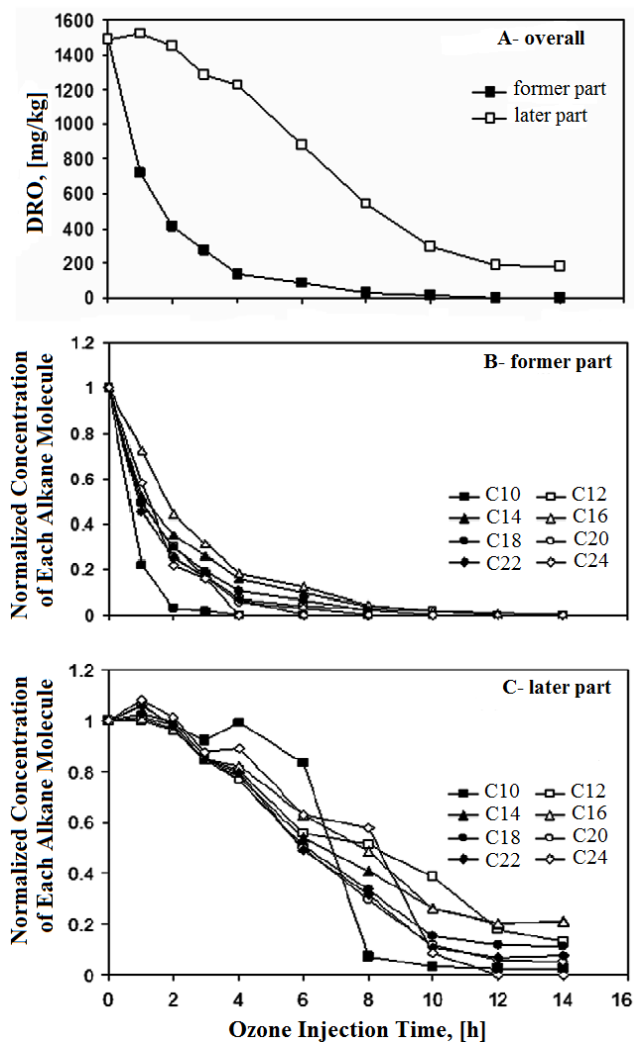


Fig. 4.8. Average DRO concentrations from the soil column as a function of ozone injection time and cumulative ozone mass (A). Relative concentrations of diesel range alkanes as a function of ozone injection time at the (B) former (near the gas inlet), and (C) later (near post-reaction gas outlet) part of the soil column (the initial concentrations of C₁₀, C₁₂, C₁₄, C₁₆, C₁₈, C₂₀, C₂₂, and C₂₄ were 228, 223, 273, 225, 189, 160, 110, and 78mg/kg soil, respectively) (Yu et al., 2007)

Contaminated soil may contain variety of organic pollutants including simple hydrocarbons, alkanes (making up to 80% of diesel fuel), volatile organic compounds, chlorinated organic compounds, PAHS (polycyclic aromatic hydrocarbons), BTEX (benzene, toluene, ethyl benzene, and xylenes) found in petroleum derivatives, pesticides and herbicides. In the case of soil, ozone remediation process can be divided onto 2 phases (Lim et al., 2002):

- instantaneous ozone demand phase, when the rapid interactions with soil organic matter and metal oxides occur and most of pollutants’ removal process takes place,
- relatively slow decay stage.

AOT results in ring cleavage of poorly soluble aromatic compounds, and insertion of oxygen, which increases their water solubility, thereby facilitating their degradation in the natural environment (www.h2o2.com).

Group of (Yu et al., 2007) reported 94% removal of diesel range organics (DRO, corresponding to the range of alkanes from C₁₀ to C₂₈ and a boiling point range of approximately 170°C - 430 °C) over 14h of continuous ozone injection.

Ozone oxidation demonstrated effective removal of non-volatile DRO in the range of C₁₂ - C₂₄. Each alkane compound displayed comparable degradation kinetics, as shown in Fig. 4.8. An estimated ozone demand was 32mg O₃/mg DRO. Ozone treatment supported acetic acid flushing reduced the remediation time more than 29% in the case of trichloroethylene (Alcantara-Garduño, 2008).

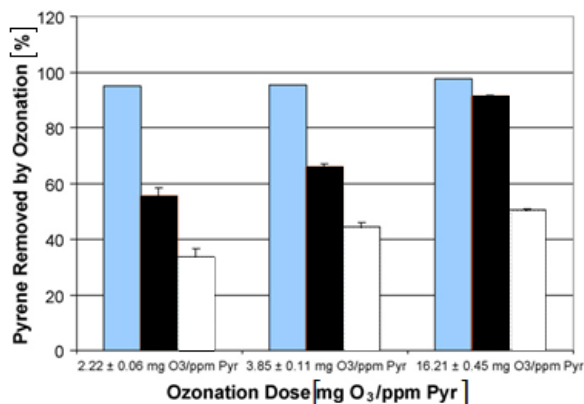


Fig. 4.9. Comparison of percent pyrene removal in pH 6 for dry soils (blue), 5% moisture (black), and 10% moisture (white) at various ozone doses (Luster-Teasley et al., 2009)

PAHs (polycyclic aromatic hydrocarbons) are the group of hydrophobic compounds that consists of two or more fused benzene rings. They are widely distributed in the environment, being present in coal tars, diesel fuel, oil

and gasoline, as by-products of incomplete combustion or pyrolysis. PAHs tend to be absorbed in organic fraction of solid (Tremblay et al., 2005) and are highly recalcitrant. Numbers of PAHs are catalogued as carcinogens by the international agencies (Li et al., 2005). The extensive studies of PAHs treatment with ozone were reported by many researchers concluding that ozone oxidation can be successfully applied to their degradation. The decomposition goes via direct reaction with molecular ozone. It was found that soil's pH and moisture content impacted the effectiveness of PAHs oxidation in unsaturated soils. In air-dried soils, as pH increased, removal increased, such that pyrene removal efficiencies at pH 6 and pH 8 reached 95 - 97% at a dose of 2.22mg O₃/mg pyrene (Luster-Teasley et al., 2009). Removal rate comparison for various moisture contents and pH of soil was depicted in Fig. 4.9.

Removal of pyrene was slower in moisturized soils, with the efficiency decreasing as the moisture content increased. Greater than 95% removal of phenanthrene was achieved with ozonation time of 2.3h at ozone flux of 250mg/h. More hydrophobic PAHs tended to react more slowly than would be expected on the basis of their reactivity with ozone, suggesting that partitioning of the contaminant into soil organic matter may reduce the reactivity of the compound (Masten and Davies, 1997). Group of (Rivas et al., 2009), reported 50, 70, 60 and 100% conversion for acenaphthene, phenanthrene, anthracene and fluoranthene, respectively. In this case, the influence of the gas flow rate on the efficiency was not noticed. The rate of reaction for ozone with the soil matrix was observed to be independent of the ozone gas pore velocity, indicating that the overall reaction rate is dominated by chemical reactions rather than by interfacial mass transfer (Hsu and Masten, 1997).

Using ozone for the removal of phenanthrene from several different soils was examined by (O'Mahony et al., 2006). The greater the water content of the soil the less effective is the ozone treatment, with air-dried soils showing the greatest removal of phenanthrene (85% removal in sandy soils after 6 h at 20 ppm ozone treatment).

In highly cultivated areas, the soil and groundwater contamination with herbicides and pesticides causes severe health problems (bioaccumulation) and decreases the amount of crops. Decomposition of trifluralin (carcinogen of herbicidal properties) and aniline (used in pesticides and agriculture industry) was studied by (Pierpoint et al., 2003). Rapid degradation of 77 - 98% of aniline exposed to 0.6% O₃ at 200ml/min after 4min in the moist conditions was observed. Initial ozonation products included nitrosobenzene and nitrobenzene, while further oxidation led to simple CO₂. Trifluralin removal rates were slower, requiring 30min to achieve removals of 70 - 97%.

Moreover, 80% effectiveness of new generation of peroxygen chemicals (calcium or magnesium peroxide and persulphate with or without addition of H₂O₂) for the chlorophenols contaminated soil remediation at natural soil pH was demonstrated by (Goi and Trapido, 2010).

Plasma effectiveness in abatement of selected chemical contaminants in soil was proven by the group of Kołaciński (Kołaciński et al., 2010; 2013; Raniszewski et al., 2012; 2012a).

4.2.3. Influence of ozone treatment on plants' growth and microorganisms in soil

Anti-microbial properties of plasmas in the case of decontamination of water, ambient air and surfaces were previously widely proven and discussed (Czernichowski, 1994; Kamgang-Youbi et al., 2007; 2007a; 2008; Machala et al., 2009; Miller et al., 2008; Moisan et al., 2001; 2001a; Moreau et al., 2005; Naitali et al., 2010; Pierpoint et al., 2003). Contamination of soils in the public grounds with various microorganisms including the parasite eggs coming from pets, wild animals and severs in both: developing and developed countries rises public concern. The contamination of samples with ascarid eggs can reach up to 92% and it is estimated that 1.4-billion people are infected worldwide (Crompton, 2001; Özkayhan, 2006; Rinaldi et al., 2006).

Group of (Mun et al., 2009) reported 0.13log inactivation of quite ozone-recalcitrant *Ascaris lumbricoides* eggs in 25g of soil with 5.8 ± 0.7 mg/l of dissolved ozone dose for 30min in a continuous diffusion reactor. Team of (Moisan et al., 2002) stated that at reduced pressure (10Torr) the UV photons dominated the inactivation process associated with DNA destruction of the spores. Choi showed the dielectric barrier discharges at atmospheric pressure sterilizing *Escherichia coli* with 99.99% efficiency and that ozone molecules were the dominant germicidal species (Choi et al., 2006).

Tomato fruit exposed to ozone concentrations between 0.005 (control) and $5.0 \mu\text{mol/mol}$ up to 13 days at 13°C, prior to, or following, inoculation by *Alternaria alternata* or *Colletotrichum coccodes* (causes of black spot and anthracnose, respectively) were tested by (Tzortzakis et al., 2008). Low-level atmospheric ozone-enrichment gave a modest, but statistically significant, reduction in fungal lesion development; higher concentrations of the gas resulted in greater effects. Fungal spore production was markedly reduced.

On the next stage of research Japanese and Polish groups investigated the biological effect of ozone treatment on living organisms. Laboratory-scale set-up presented in Fig. 4.10. was used for DNA treatment. $0.46 \mu\text{g}/\mu\text{l}$ of λ -*E. Coli* DNA (Nippon Gene) was diluted with 10 mM Tris-HCL (pH 7.9) and 1.0M EDTA. DNA solution was further diluted with 0.5ml of distilled water in a microcentrifuge tube. A stream of oxygen containing 5% wt. ozone was bubbled into the microcentrifuge tube containing the DNA solution. 0.2 - 1g of ozone was supplied to 0.5ml of DNA solution during 5 - 20min of treatment at 0.5l/min gas flow rate. In this case ozone was generated by the high-power TiO_2 based ozonizer (OP-20W, Iwasaki) during the surface discharges.

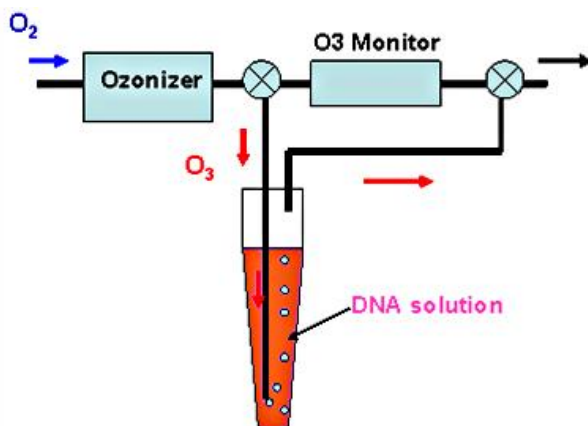


Fig. 4.10. Set up for ozone treatment of DNA solution

Before and after ozone treatment DNA samples were prepared on the mica substrates. The DNA solution of 10 μ l was dropped on the mica substrate and was dried in the chamber at reduced pressure and room temperature. Atomic Force Microscopy (AFM) was employed to data analysis (Shubo et al., 2003). Fig. 4.11. shows the image of DNA sample deposited on the mica substrate. It was found that there were many kinds of structures depending on the location and localized conditions (such as DNA condensation).

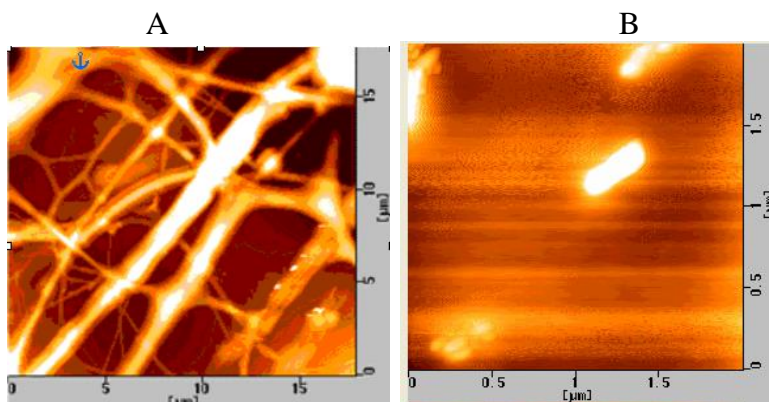


Fig. 4.11. AFM image of DNA sample prepared on mica substrate (A) before ozonation, (B) after ozonation

The fine threads were considered to be double strand DNA and the bundle structures of heavy threads were composed of multiple fine DNA threads with surface covered by diluted material remnant. The threads and the bundles

were connected together to form mesh type structures (Fig. 4.11A). Molecular structure of DNA collapsed completely when high concentration of ozone was introduced into the DNA solution. Ozonation broke the *E. coli* DNA and split it into many fragments of the typical length and width of 380 - 390nm and 15nm, respectively. These peculiar pieces have almost been not observed when the DNA samples were treated for 20min (Fig. 4.11B).

Several possible paths of cell inactivation by oxidative species were presented in literature data (Cheng et al., 2003; Choi et al., 2006; Daia et Upadhyaya, 2002; Dubeau and Chung, 1984; Doubla et al., 2007; Golota et al., 2004; Hamelin, 1985; Hamelin and Chung, 1981; Ishizaki et al., 1987; Ito et al., 2005; Komanapalli and Lau, 1996; Moisan et al., 2002; Morar et al., 1999; Mun et al., 2009; Van Der Zee et al., 1987).

Oxidation caused change in DNA structure (in all base and sugar moieties; resulting in strand breaks, DNA inter-strand cross-links and DNA-protein cross-links) as follows:

- change of dGMP, dCMP and dTMP bases, production of 8-oxoguanine, which leads to common gene mutations: G-A transversion (directly by ozone),
- DNA backbone cleavages, dAMP base and the deoxyribose ring destructions (indirectly, by secondary oxidants such as OH radicals or/and singlet oxygen).

Influence of ozone soil treatment on *Fusarium species*, which produce mycotoxins as secondary metabolites was also tested. Mycotoxins cause a toxic response, termed a mycotoxicosis, when ingested by higher vertebrates and other animals and can lead to deterioration of liver or kidney function. Damages caused by main mycotoxins produced by *Fusarium* are summarized in Tab. 4.1 (Ross et al., 1990; Segvic and Pepeljnjak, 2001; Swamy et al., 2004; Wing et al., 1993).

Tab. 4.1. *Fusarium* mycotoxins

Mycotoxins	Causes
Trichothecenes	Immunotoxic, cytotoxic to mammalian cells, increase sucebility to other microbial infections, potent inhibitors of protein synthesis known to cause alimentary toxic aleukia, fusariotoxicozes
Fumonisin	Hepatotoxic and hepatocarcinogenic in rats, inhibitors of sphingolipid biosynthesis, carcinogenic (associated with an increased risk of human esophageal cancer)

50g of soil sample has initially been inoculated by *F. oxysporum* fungus (Fig.4.5D). Conventional biological method of the CFU (colony forming unit) counting showed that *F. oxysporum* in the soil was almost eliminated by ozone treatment with the concentration over 20gO₃/m³ achieving decontamination rate up to 99.9%. Results of experiment are summarized in Tab. 4.2 and in Fig. 4.12.

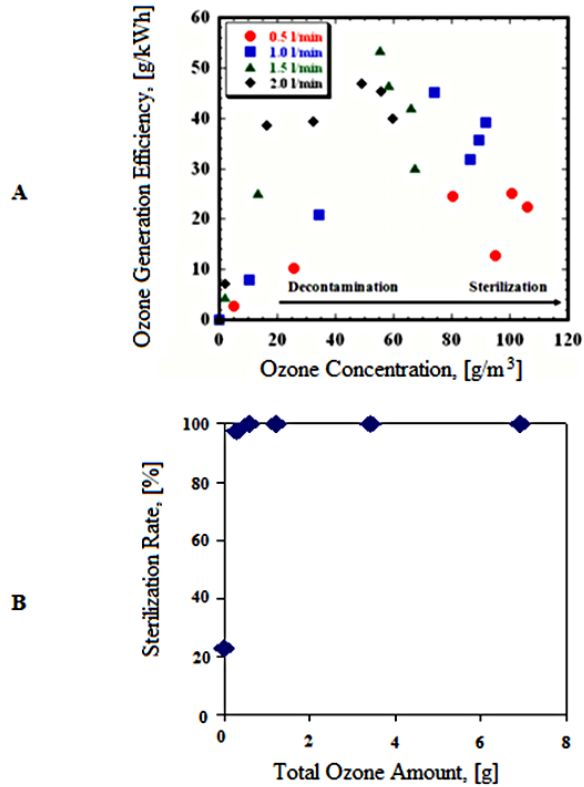


Fig. 4.12. Ozone concentration vs. efficiency for screw-type ozonizer, (10kHz, 15°C) (A), sterilization rate as a function of ozone amount (B)

Tab. 4.2. Soil sterilization by in-situ ozone treatment

<i>Fusarium Oxysporum</i>			
Untreated [CFU/cc]	1.8×10^5	5.7×10^6	
Gas flow rate [l/min]	1	3	
Concentration [g/m³]	20	10	20
Duration [min]	20	10	10
Ozone treated [CFU/cc]	2.7×10^4	1.4×10^5	1.7×10^2
Sterilization rate [%]	86	97.5	99.9

Influence of ozone in air and soil on seeds' and plants' development was broadly investigated by numerous researchers. Results highly depended on the kind of plant and were sometimes contradictory. Chronic exposure to ozone significantly reduced the rate of CO₂ assimilation in sugar maple (Bertrandet al., 1999). On the other hand, there was no treatment effect on the freezing tolerance of roots, even though roots in the high-O₃ treatment accumulated higher concentrations of the cryoprotective oligosaccharides raffinose and stachyose than control roots. Ozone (alone or in mixtures with CO₂ to maintain its concentration within soil) injected in previously oversaturated soil was reported to be beneficial for growth of tomatoes or some kinds fungi (such as *Trichoderma, spp.*), which are parasitic to detrimental fungi such as *Fusarium* (Pryor, US Patent 6173527).



Fig. 4.13. Influence of soil pre-ozonation on spinach

AOPs (ozone, hydrogen peroxide, electric field, UV radiation, etc.) were widely used for the treatment of seeds and bulbs causing 15 - 20% improvement of immunity of cotton plants to diseases and improvement of morphobiological and technological parameters of cotton fiber (Onishchenko et al., 2005);

12 - 15% higher grain yield with better quality of corn grain (Golota et al., 2004); over 60% improvement in bean seeds germination (Morar et al., 1999; Yvin and Coste, US Patent 5703009).

Seedlings and seeds of Chinese cabbage (*Brassica pekinensis*), Garland chrysanthemum (*Chrysanthemum coronarium*), muskmelon (*Cucumis melo*), tomato (*Solanum lycopersicum*) and spinach (*Spinacia oleracea*) were placed by our group in separated containers with pre-ozonized soil (after 23 days from ozonation, pH 5) and with non-ozonized soil, respectively. Soil ozonation influenced plants' growth in various ways. There was 24% of growth inhibition after 79 days in the case of cabbage due to the decreasing pH of soil and elimination of beneficial microorganisms.

Improvement of growth was observed in the case of melons, tomatoes and plants, for which environmental stress has a beneficial influence on growth and fruit formation. The positive influence of soil pre-ozonation on spinach was depicted in Fig. 4.13.

Application of ozone as an environmental-friendly plants' growth supporting factor should be carefully justified because influence of this oxidant strongly depends on the plant's type. The set up for agricultural microbial ozone sterilization purposes was developed. Gaseous ozone sterilization was proven to be satisfactory for the treatment of soil infected by *Fusarium oxysporum*; however, establishing potentially beneficial doses for certain species still requires further research work.

5. Conclusions

Uncontrolled release of pollutants due to the industrial development and wasteful exploitation can cause serious environmental hazard affecting not only local communities but bringing to climatic changes. International standards in the nature protection field, especially in Europe, are getting more rigorous to prevent against excessive contamination and to preserve clean air and water for the future generations. Many efforts are made to obey those requirements and to find new, clean technologies and more effective way of the gaseous, liquid and solid wastes' reprocessing.

With growing pollution, techniques of purification and environmental protection must be more efficient and complex. Biological and chemical treatment sometimes is not sufficient any more. Ozone can improve biodegradability and inactivate many specific and hazardous chemical compounds such as pesticides, detergents, large molecule organic compounds and inorganic compounds such as sulfides and cyanides. Application of ozone is considered a waste-free and environmental friendly.

However, in the case of some contaminants it is necessary to find out more sophisticated treatment solutions by combining many novel techniques of already proven efficiency. Application of ozone and other strong oxidants during advanced oxidation processes (AOP) become popular, and in many cases, necessary implement of the cleaning procedure. Very active species like hydroxyl and nitrogen radicals are involved in AOP beside ozone and hydrogen peroxide.

Plenty dry treatment technologies exist, but some technological processes require connection of flows of gaseous and liquid phases. Multi-phase environment can lead to the formation of new oxidants, which further contribute to improvement of the purification process and it has not been well investigated yet.

Traditionally, silent or surface discharges are used for ozone generation in larger amounts. Ozone gas is then dosed to the polluted medium. Simultaneously, hydrogen peroxide is introduced. System after ozone addition can be also irradiated to generate more OH radicals.

In the recent years, idea of generation of active species directly in liquid appeared. Many types of reactors were tested but so far they were not fully implemented because of complexity of the process, especially difficulties in obtaining electrical discharges' homogeneity in liquid; and quite low energetic efficiency. Scientific reports on the last one vary dramatically as the different power supply designs and different measurement approaches are used.

Extremely unique environment for pollutants' treatment: electrical discharge in foam was proposed by the author of this review. Foaming is well known phenomena; however, experiments presented in this work using the electrical discharge in foam can be considered a completely innovatory attempt. In most of the cases, foam was created without addition of foaming agents, using only the kinetic energy of gas flow, keeping the strict conditions of medium flow and using diffusers. Flat reactor with several types of electrodes and cylindrical reactor were tested.

Application of high voltage and oxidants' formation as its consequence makes the process comparable to the other AOP methods employing discharges in liquids. All oxidants' concentrations increased with applied voltage and depended strongly on the discharge and foam uniformity. They decreased when foaming conditions tended to bubbling and when the arc dominated over the other discharge types.

Extended mass transfer area can improve chemical yield. Foaming column allowed obtaining various species in one compact apparatus, even directly in polluted medium and it was successfully tested for decolourisation of dyes but the system itself has a great potential to be included in the treatment and remediation procedures. Its large capacity makes it useful for industrial purposes and allows reducing the number of sub-units in installation. A compact apparatus is easy to operate and control. The foaming system with its humid environment can be an interesting and relatively cheap alternative for conventional oxidants' generators.

New fields for application of plasmas in humid environments such as medicine, biotechnology, agriculture and food industry were introduced. However, to fully implement hybrid plasma reactors, investigation of electromagnetic interferences from devices' power sources and their standardization is necessary. Also, study on the influence of variety of factors such as gas temperature, radiation, electromagnetic fields, generation of highly oxidative species and toxic by-products, power transfer from plasma is necessary to optimize plasma generators and to evaluate the long-term biological effect of plasma treatment.

6. References

- Abdelmalek F., Gharbi S., Benstaali B., Addou A., Brisset J. L., *Wat. Res.* 38, 2004, 2339-2347
- Abdelmalek F., *Plasmachimie des solutions aqueuses. Application à la dégradation de composés toxiques*, Université de Mostaganem, Algeria, 2003
- Abdelmalek F., Torres R., Combet E., Petrier C., Pulgarin C., Addou A., *Separation and Purification Technology*, 63(1), 2008, 30-37
- Adam A., Gorenc B., Gorenc D., *Acta Chimica Slovenica*, 35, 1988, 339-350.
- Agiral A., Nozaki T., Nakase M., Yuzawa S., Okazaki K., Gardeniers J., *Chem. Eng. J. I*, 167(2-3), 2011, 560-566
- Alcantara-Garduno M., Okuda T., Tsai T., Nishijima W., Okada M., *Separation and Purification Technology*, 60(3), 2008, 299-307
- Aleboyeh A., Aleboyeh H., Moussa Y., *Dyes and Pigments*, 57, 2003, 67-75
- Anotai J., Su C., Tsai Y., Lu M., *J. Hazard. Mat.*, 183(1-3), 2010, 888-893
- Anpilov A., Barkhudarov E., Christofi N., Kopev V., Kossyi I., Taktakishvili M., Zadiraka Y., *Let. Appl. Microb.*, 35, 2002, 90-94
- Antelman M., *The encyclopedia of chemical electrodes potentials*, Plenum Press, London, 1982
- Atrazhev V., Dmitriev E., Iakubov T., *IEEE Trans. on Electrical Insulation* 26(4), 1991, 586-591
- Atrazhev V., Timoshkin I., *IEEE Trans. on Dielectrics and Electrical Insulation*, 5(3), 1998, 450-457
- Aubry J., *J. Am. Chem. Soc.*, 107, 1985, 5844-5849
- Banerjee K., Kumar S., Bremmell K., Griesser H., *J. Hosp. Infection*, 76, 2010, 234-242
- Barraud N., Hassett D., Hwang S., Rice S., Kjelleberg S., Webb J., *J. Bacteriology*, 188(21), 2006, 7344-7353
- Barth C., Dunning M., Bretscher L., Woehlck H., *Anesth. Analg.*, 101, 2005, 748-752
- Beltran F., *Ozone Sci.&Eng.*, 19, 1997, 13-38
- Benitez F., Beltran J, Gonzalez T., Pascual A., *Chem. Eng. Commun.*, 119, 1993, 151-165
- Benstaali B, Cheron B., Addou A., Brisset J.L., *Proc. 14th Int. Symp. on Plasma Chemicals*, Praga, Czech Republic, II, 1999, 939-44
- Benstaali B., Addou A., Brisset J.L., *Materials Chemistry and Physics*, 78, 2002, 214-221
- Benstaali B., Moussa D., Addou A., Brisset J. L., *Eur. Phys. J.* 4, 1998, 171-179
- Beroual A., Aka-N'Gnui T., *Conference on Electrical Insulation and Dielectric Phenomena 2002*, 248-241

- Beroual A., Zahn M., Badent A., Kist K., Schwabe A., Yamashita H., Yamazawa K., Danikas M., Chadband W., Torshin Y., *IEEE Electrical Insulation Magazine*, 14(2), 1998, 6-17
- Bertrand A., Robitaille G., Nadeau P., Castonguay Y., *Tree Physiology*, 19, 1999, 527-534
- Bhakta A., Ruckenstein E., *Adv. Colloid and Interfaces Sci.*, 70, 1997, 1-124
- Bian W., Ying X., Shi J., *J. Hazard. Mat.*, 162, 2009, 906-912
- Bian W., Zhou M., Lei L., *Plasma Chem. Plasma Process.*, 27, 2007, 337-348
- Birhanli A., Ozmen M., *Drug Chem Toxicol.*, 28(1), 2005, 51-65
- Bistroń S., Sarre P., Szymonik B., *Chemik*, 3, 1978, 81-83
- Braun A., Oliveiros E., *Wat. Sci. Tech.*, 35(4), 1997, 17-23
- Bremner D., Mitchell S., Staines H., *Ultrasonics Sonochemistry*, 3(1), 1996, 47-52
- Brisset J. L., *J. Appl. Electrochem.* 27(2), 1997, 179-183
- Bruggeman P., Leys C., *J. Phys. D: Appl. Phys.* 42(5), 2009, 053001
- Burlica R., Kirkpatrick M., Locke B., *J. Electrostat.*, 64, 2006, 35-43
- Burlica R., Kirkpatrick M., Finney W., Clark R., Locke B., *J. Electrostat.*, 62, 2004, 309-321
- Busca G., Berardinelli S., Resini C., Arrighi L., *J. Hazard. Mat.*, 160, 2008, 265-288
- Buxton G., Greenstock C., Helman W., Ross A., *J. Phys. Chem. Ref. Data*, 17, 1988, 513-882
- Calabrese E., Kenyon E., *Air Toxics and Risk Assessment.*, Lewis Publishers, Chelsea, MI, 1991
- Castellanos, A., *Electrohydrodynamics*, Springer, Wien - New York, 1998
- Ceccato P., *Filamentary plasma discharge inside water: initiation and propagation of a plasma in a dense medium*, Ecole Polytechnique Palaiseau (Paris), France, 2009
- Chang J. In: Penetrante B, Schultheis S, Eds., *Non-thermal plasma techniques for pollution control*, NATO ASI series, Berlin: Springer, 34, 1992, 1-32
- Chang J., *J. Aerosol. Sci.*, 20(8), 1989, 1087-90
- Chen C., Lee H., Chang M., *J. Electrostat.*, 67, 2009, 703-708
- Chen C., Phillips J., *J. Phys. D: Appl. Phys.*, 35, 2002, 998-1009
- Chen G., *Separation and Purification Technology*, 38, 2004, 11-41
- Chen L., *Wat. Res.*, 34(3), 2000, 974-982
- Chen Y., Zhang X., S. Chang, Dai Y., Yuan W., *Acta Scientiae Circumstantiae*, 25(1), 2005, 113-116
- Cheng T., Kao H., Chan C., Chang W., *Env. Res.*, 93, 2003, 279-284
- Choi H. Shikova T., Titov V., Rybkin V., *J. Colloid and Interface Sci.*, 300, 2006, 640-647.
- Choi H., Kim Y., Lim H., Cho J., Kang J., Kim K., *Water Sci. Tech.* 43(5), 2001, 349-356
- Choi I., Wiesmann U., *Ozone Sci.&Eng.*, 26, 2004, 539-549

- Choi J., Han I., Baik H., Lee M., Han D., Park J., Lee I., Song K., Lim Y., *J. Electrostat.*, 64, 2006a, 17-22
- Christophorou L., Siomos K., *Electron-molecule interactions and their applications*, Academic press, Harcourt Brace Jovanivich, Publishers, 1984
- Chrostowski P. C., Dietrich A. M., Suffet I. H., *Water Res.* 17 (11), 1983, 1627-1633
- Chu W., Kwan C., *Wat. Res.*, 36, 2002, 2187-2194
- Clements J., Sato M., Davis R., *IEEE Trans. Ind. Appl.*, IA23, 1987, 224-235
- Crompton, D. *Adv. in Parasitology*, 48, 2001, 285-375
- Czernichowski A., *Pure Appl. Chem.*, 66, 1994, 1301-1310
- Daia Q., Upadhyaya M., *Weed Sci.*, 50(5), 2002, 611-615
- De Laat J., Berger, P., Poinot T., Karpel Vel Leitner N., Dore M., *Ozone: Sci. Eng.* 19, 1997, 395-408
- Demirev A., Nenov V., *Ozone: Sci. Eng.*, 27, 2005, 475-485
- DEPA, Danish Environmental Protection Agency, „Azocolorants in Textiles and Toys”, Environmental Project, no. 416, ISBN 87-7909-048-6, 1998
- Depenyou F. Doubla A., Laminsi S. Moussa D., Brisset J. L., *Le Breton J., Corrosion Sci.*, 50, 2008, 1422-1432
- Destailats H., Turjanski A., Estron D., Hoffman M., *J. Phys. Org. Chem.* 15, 2002, 287-292
- Diatczyk J., Giżewski T., Kapka L., Komarzyniec G., Pawłat J., Stryczewska H. D., 7th Int. Conference Electromagnetic Devices and Processes in Environment Protection - ELMECO-7 joint with 10th Seminar Applications of Superconductors - AoS-10, Nałęczów, Poland, 2011, 23-24
- Dickenson E., *Introduction to Food Colloids*, Oxford University, Press 1992
- Dojcinovic B., Roglic G., Obradovic B., Kuraica M., Kostic M., Nesi J., Manojlovic D., *J. Hazard. Mat.*, 192, 2011, 763-771
- Dors M., Metel E., Mizeraczyk J., *Int. J. Plasma Env. Sci. & Tech.* 1(1), 2007, 76-81
- Dors M., Mizeraczyk J., Mok Y., *JAOTs*, 9(2), 2006, 139-143
- Dors M., Nichipor G., Mizeraczyk J., *Dielectric Liquids*, IEEE Int. Conference, Portugal, Coimbra 2005, 95, (10.1109/ICDL.2005.1490035)
- Doubla A. Laminsi S., Nzali S., Njoyim E., Kamsu-Kom J., Brisset J. L., *Chemosphere*, 69, 2007, 332-337
- Doubla A., Bouba Bello L., Fotso M., Brisset J. L., *Dyes and Pigments*, 77, 2008, 118-124
- Dubeau H., Chung Y., *Mol. Gen. Genet.*, 197(1), 1984, 120-124
- Dutta R., Chowdhury R., Bhat S., Gokturk S., Tuncay M., *J. Surf. Detergents*, 6(4), 2003, 325-330
- Ebihara K, Mitsugi F., Ikegami T., Nakamura N., Hashimoto Y., Yamashita Y., Baba S., Stryczewska H. D., Pawłat J., Teii S., Sung T., *The European Physical Journal Applied Physics*, 2013, doi:10.1051/epjap/2012120420

- Ebihara K., Ikegami T., Mitsugi F., Ikegami T., Stryczewska H. D., Gyoutoku Y., Symp. on the Appl. of Plasma to Bio-Medical Eng., Lunghwa Univerisity of Sci. and Tech., Taiwan, 2008, 21-24
- Ebihara K., Stryczewska H. D., Ikegami T., Mitsugi F., Pawłat J., Przegląd Elektrotechniczny, 7, 2011, 148-152
- Ebihara K., Stryczewska H. D., Mitsugi F., Ikegami T., Sakai T., Pawłat J., Teii S., 7th Int. Conference Electromagnetic Devices and Processes in Environment Protection - ELMECO-7 joint with 10th Seminar Applications of Superconductors - AoS-10, Nałęczów, Poland, 2011a, 29-30
- Ebihara K., Sugimoto S., Ikegami T., Mitsugi F., Stryczewska H. D., 6th Int. Conference on Electromagnetic Devices and Processes in Environment Protection (ELMECO-6), Naleczów, Poland, 2008a
- Ebihara K., Sugimoto S., Ikegami T., Mitsugi F., Stryczewska H. D., Przegląd Elektrotechniczny, 5, 2009, 113-114
- Ebihara K., Takayama M., Ikegami T., Ogata K., Stryczewska H. D., Gyoutoku Y., Sakai T., JAOTs, 9(2), 2006a, 170-173
- Ebihara K., Takayama M., Ikegami T., Stryczewska H. D., Gyoutoku Y., Yokoyama T., Gunjikake N., Tachibana M., Sakai T., Proc. 17th Int. Symp. on Plasma Chemistry; Toronto, Canada, 2005, CD(1201).
- Ebihara K., Takayama M., Stryczewska H. D., Ikegami T., Gyoutoku Y., Tachibana M., IEEJ Trans., 125(10), 2006, 963-969
- Ebihara, K., Workshop on the Appl. of Plasma to Green Env. Tech., Taoyuan, Taiwan, 2006, 86-90
- Eliasson B.; Kogelschatz U., IEEE Trans. Plasma Sci., 19, 1991, 1063-1077
- Elles C., Shkrob I., Crowell R., Bradforth S., J. Chem. Phys., 126, 2007, 164503
- El-Sayed Y., Bandosz T., J. Colloid and Interface Sci., 242, 2001, 44-51
- Favero M., Developing indicators for sterilization. In: Rutala, W., Disinfection, sterilization and antisepsis in health care. Washington, DC: Association for Professionals in Infection Control and Epidemiology, Inc., 1998, 119-132
- Favero M., Sterility assurance: concepts for patient safety. In: Rutala W, editor. Disinfection, sterilization and antisepsis: principles and practices in healthcare facilities. Washington, DC: Association for Professionals in Infection Control and Epidemiology, Inc. 2001, 110-119
- Feng J., Zheng Z., Luan J., Li K., Wang L., Feng J., J. Hazard. Mat., 164, 2009, 838-846
- Foffana I., Beroual A., JJAP, 37, 1998, 2540-2547
- Fukawa F., Rokkaku K., Suzuku S., Yazawa Y., Itoh H., IEEJ Transactions on Fundamentals and Materials, 132(8), 2012, 664-669
- Fukawa F., Rokkaku K., Teranishi K., Shimomura N., Suzuki S., Itoh H., IEEE Transactions on Plasma Science, 39(11), 2011, 2662-2663
- Gallagher T., Simple Dielectric Liquids: Mobility, Conduction, Breakdown, Clarendon Press, Oxford, 1975
- Gao Z., Yang S., Ta N., Sun C., J. Hazard. Mat., 145, 2007, 424-430

- Gehring P., Szinovatz W., Eschweiler H., Barberl R., *Ozone Sci. & Eng.*, 19, 1997, 157-168
- Ghosal S., *Electrophoresis*, 25, 2004, 214-228
- Gierżatowicz R., Pawłowski L., *Nadtlenek wodoru w sozotechnice*, WU, Lublin, Poland, 1996
- Glaze, H., Kang, J., *J. AWWA*, 80(5), 1988, 57-63
- Goi A., Trapido M., *JAOTs*, 13(1), 2010, 50-58
- Golota V., Dindorogo V., Zavada L., Kyrychenko V., Petrenkova V., Pugach S., Sukhomlin E., Taran G., *Proc. 4th Int. Symp. on Ozone Appl.*, Cuba, 2004
- Gordon G., Bubnis B., *Ozone Sci.&Eng.*, 21(5), 1999, 447-464
- Grabowski L., Veldhuizen E., Pemen A., Rutgers W., *Plasma Chem. Plasma Process.*, 26, 2006, 3-17
- Grabowski R., Veldhuizen E., Pemen A., Rutgers W., *Plasma Sources Sci. Tech.*, 16, 2007, 226-232
- Grymonpre D., Finney W., Clark R., Locke B., *Ind. Eng. Chem. Res.*, 43, 2004, 1975-1989
- Grymonpre D., Finney W., Clark R., Locke B., *Industrial & Eng. Chem. Res.*, 42, 2003, 5117-5134
- Grymonpre D., Finney W., Locke B., *Chem. Eng. Sci.*, 54, 1999, 3095-3105
- Grymonpre D., Sharma A., Finney W., Locke B., *Chem. Eng. J.*, 82, 2001, 189-207
- Guideline for Disinfection and Sterilization in Healthcare Facilities 2008, <http://www.cdc.gov>
- Guo Y., Liao X., Ye D., *J. Env. Sci.*, 20, 2008, 1429-1432
- Hamelin C., Chung Y., *Mol. Gen. Genet.*, 184, 1981, 560-561
- Hamelin, C., *Int. J. Radiat. Oncol. Biol. Phys.*, 11, 1985, 253-257
- Hancock P., Curry R., McDonald K., *14th IEEE*, 2, 2003, 1128-1131
- Hayashi D., Hoeben W., Dooms G., van Veldhuizen E., Rutgers W., Kroesen G., *J. Phys. D: Appl. Phys.* 33(21), 2000, 2769-2774
- He Z., Liu J., Cai W., *J. Electrostat.*, 63, 2005, 371-386
- Henn G., Birkinshaw C., Buggy M., Jones E., *J. Mat. Sci. (Mater. Med.)* 7, 1996, 591-595
- Hensel K., Pawłat J., Mizuno A., *Proc. 16th Int. Symp. on Plasma Chem.*, Taormina, Italy, 2003
- Hensel K., Pawłat J., Takashima K., Mizuno A., *Proc. 30th IEEE Int. Conference on Plasma Sci. ICOPS 2003*, Cheju, Korea, 2003b
- Hensel K., Pawłat J., Takashima K., Mizuno A., *Proc. Int. Joint Power Generation Conference IJPGC 2003*, Georgia, USA, 2003a
- Hermann H., Henins I., Park J., Selwyn G., *Phys. Plasmas*, 6, 1999, 2284-2289
- Hickling A., *Electrochemical processes in glow discharge at the gas-solution interface* in Bockris J., Conway B. (Eds.), *Modern Aspects of Electrochemistry*, Butterworths, London, 1971
- Hobler T., *Dyfuzyjny ruch masy i absorberia*, WNT, Warszawa, Poland, 1978

- Hochnadel C., *Radiat. Res.* 17, 1962, 286-301
- Hoeben W., Veldhuizen E., Rutgers W., Kroesen G., *J. Phys. D: Apl. Phys.*, 32(24), 1999, 133-137
- Hoeben W., Velhduizen E., Rutgers W., Cramers C., Kroesen G., *Plasma Sources Sci. Tech.*, 9, 2000, 361-369
- Hsu M., Masten S., *Env. Eng. Sci.* 1997, 14(4), 207-218
- <http://chemicalland21.com>
- <http://saujanya.com>, 2005
- <http://stainsfile.info>, 2005
- <http://www.cerionx.com>
- <http://www.h2o2.com>
- <http://www.mpbio.com>
- <http://www.neoplas.eu>
- <http://www.sigmaaldrich.com>
- <http://www.sterrad.com>
- Hutzler N., Murphy B., Gierke J., *J. Hazard. Mater.*, 26, 1991, 225-230
- Ibrahim M., Mizuno H., Yasuda Y., Fukunaga K., Nakao K., *BioChem. Eng. J.* 8, 2001, 9-18
- Ihara S., Kobayashi A., Miichi T., Satoh S., Yamabe C., Sakai E., Furube T., *Proc. 13th Ozone World Congress, Kyoto, Japan, 1997*, 883-888
- Imasaka K., Kato Y., Suehiro J., *Surface and Coatings Tech.*, 202(22-23), 2008, 5271-5274
- Ince N., Gonenc D., *Env. Tech.*, 1997, 18, 179-185
- Int. Agency for Research on Cancer. IARC Monographs on the Evaluation of the Carcinogenic Risk of Chemicals to Humans. Alkyl Compounds, Aldehydes, Epoxides, and Peroxides., Lyon, France: IARC, 36, 1985
- Int. Agency for Research on Cancer. IARC Monographs on the Evaluation of Carcinogenic Risks to Humans. Re-evaluation of Some Organic Chemicals, Hydrazine, and Hydrogen Peroxide., Lyon, France: IARC, 71, 1999
- Int. Agency for Research on Cancer. IARC Monographs on the Evaluation of Carcinogenic Risks to Humans. Overall Evaluations of Carcinogenicity., Lyon, France: IARC, 7, 1987
- Ishizaki K., Sawadaishi K., Miura K., Shinriki N., *Wat. Res.*, 21(7), 1987, 823-827
- Ito K., Inoue S., Hiraku Y., Kawanishi S., *Mutation Research/Genetic Toxicology and Environmental Mutagenesis*, 585(1-2), 2005, 60-70
- Janknecht P., Wilderer P., Picard C., Larbot A., *Separation and Purification Tech.* 25, 2001, 341-346
- Jans U., Hoigné J., *Atmospheric Env.*, 34(7), 2000, 1069-1085
- Jodzis S., *Ozone Sci. & Engineering*, 34(5), 2012, 378-386
- Jodzis S., Smoliński T., Sówka P., *IEEE Transactions on Plasma Science*, 39(4), 2011, 1055-1060

- Jones H., Kunhardt E., *IEEE Trans. Dielectrics Electr. Insul.*, 1(6), 1994, 1016-1025
- Jones H., Kunhardt E., *J. Appl. Phys.*, 77, 1995, 795-805
- Joseph J., Destailhats H., Hung H., Hoffmann M., *J. Phys. Chem.*, 104, 2000, 301-307
- Joshi A., Locke B., Arce P., Finney W., *J. Hazard. Mat.*, 41, 1995, 3-30
- Joshi R., Qian J., Kolb J., Schoenbach K., *IEEE Trans. on Dielectrics and Electrical Insulation*, 2003, 293-296
- Joshi R., Qian J., Zhao G., Kolb J., Schoenbach K., Schamiloglu E., Gaudet J., *J. Appl. Phys.*, 96(9), 2004, 5129-5139
- Kabasawa Y., Kanzaki T., *Contact Dermatitis*, 20(5), 1989, 378-379
- Kamgang-Youbi G., Briandet R., Herry J., Brisset J. L., Naitali M., *J. Appl. Microbiology*, 103, 2007, 621-628
- Kamgang-Youbi G., Herry J., Bellon-Fontaine M., Brisset J. L., Doubla A., Naitali M., *Appl. Env. Microbiology.*, 73(15), 2007a, 4791-4796
- Kamgang-Youbi G., Herry J., Meylheuc T., Brisset J. L., Bellon-Fontaine M., Doubla A., Naitali M., *Let. Appl. Microbiology* 48(1), 2008, 13-8
- Kamgang-Youbi G., Naitali M., Herry J., Hnatiuc E., Brisset J. L., 12th Int. Conference on Optimization of Electrical and Electronic Equipment (OPTIM), Basov 2010, 1336 - 1342
- Karmi A., Redman J., Glaze W., Stolarik G., *J. IAWWA*, 89(8), 1997, 41-53
- Kim H., Prieto G., Takashima K., Katsura S., Mizuno A., *J. Electrostat.*, 55(1) 2002, 25-41
- Kim K., Ihm S., *J. Hazard. Mat.*, 186(1), 2011, 16-34
- Kim Y., Hong S., Cha M., Song Y., Kim S., *JAOTs*, 6, 2003, 17-22
- Kirkpatrick M., Locke B., *Ind. Eng. Chem. Res.*, 44, 2005, 4243-4248
- Kirkpatrick M., Plasma-catalyst interactions in treatment of gas phase contaminants and in electrical discharge in water, College of Engineering, Florida State University, Tallahassee, FL, USA, 2004
- Kogelschatz U., Eliasson B., Egli W., *Pure Appl. Chem.* 71, 1999, 1819-1828
- Kogelschatz U., *Plasma Chem. & Plasma Proc.*, 23(1), 2003, 1-46
- Kogelschatz U., *Proc. 10th Int. Conference on Gas Discharges and their Applications*, Swansea, 1992, 1-9
- Kołaciński Z., Szymański Ł., Raniszewski G., *Eur. Phys. J. Appl. Phys.*, 61(2), 2013, 24314(1)-24314(7)
- Kołaciński Z., Szymański Ł., Raniszewski G., *JAOT*, 13(1), 2010, 89-98
- Komanapalli I., Lau B., *Appl. Microb. and Biotechnology*, 46(5-6), 1996, 610-614
- Komarzyniec G., Janowski W., Stryczewska H. D., Pawłat J., Diatczyk J., *Przegląd Elektrotechniczny*, 7, 2011, 32-35
- Kovscek A., Patzek T., Radke C., *Chem. Eng. Sci.* 50, 1995, 3783-3799
- Kozakova Z., Nejezchleb M., Krcma F., Halamova I., Caslavsky J., Dolinova J., *Desalination*, 258, 2010, 93-99

- Kozlov K., Tatarenko P. Samoilovich V., Proc. Hakone XI, Oléron Island, 2008
- Kunitomo S. Sun B., J. Pulsed Power Plasma Sci., IEEE, 6, 2001, 1138-1141
- Kurniawan T., Lo W., Chan G., Chem. Eng. J., 125, 2006, 35-57
- Kusic H., Koprivanac N., Locke B., J. Hazard. Mat. B, 125, 2005, 190-200
- Kuzhekin I., Proc. 9th Int. Symp. High Voltage Eng., Graz, Austria 1995, 8073-1-8073-3
- Kwon B., Kim E., Lee J., Chemosphere, 74(10), 2009, 1335-1339
- Langlais B., Reckhow D., Brink D., Ozone in Water Treatment, Lewis Publ. Chelsea, 1991
- Laroussi M., Leipold F., Int. J. Mass Spectrom. 233, 2004, 81-86
- Laroussi, M., IEEE Trans. Plasma Sci., 27, 1999, 69-70
- Lee S., Mills A., Chem. Commun., 8, 2003, 2366-2367
- Li A., Schoonover T., Zou Q., Norlock F., Scheff P., Wadden R. NUATRC Research Report, 6, 2005
- Li N., Huang J., Lei K., Chen J., Zhang Q., J. Electrostat., 69, 2011, 291-295
- Lide D., CRC Handbook of Chemistry and Physics, CRC Press, Taylor and Francis, Group, Boca Raton, FL, 2006
- Lim H., Choi H., Hwang T., Kang J., Wat. Res., 36(1), 2002, 219-229
- Line S., Daniel B., Luc V., Jane M., Anal. Biochem., 241, 1996, 67-74
- Liu H., Chen J., Yang L., Zhou Y., Appl. Surface Sci., 254(6), 2008, 815-1821
- Liu W., X., Env.Sci. Tech., 39, 2005, 8512-8517
- Liu Y., J.Hazard. Mat., 166, 2009, 1495-1499
- Locke B., Sato M., Sunka P., Hoffmann M., Chang J., Ind. Eng. Chem. Res., 45, 2006, 882-905
- Lubicki P., Cross J., Jayaram S., Proc. IEEE International Symposium on Electrical Insulation, Montreal, Canada, 1996, 882-886
- Lukes P., Appleton A., Locke B., Conference Record IEEE, 37, 2002, 1816-1821
- Lukes P., Clupek M., Sunka P., Babický V., Winterová G., Janda V. Acta Phys. Slovaca 53(6), 2003, 423-430
- Lukes P., Clupek M., Sunka P., Peterka F., Sano T., Negishi N., Matsuzawa S., Takeuchi K., Res. Chem. Intermediat. 31(4-6), 2005, 285-294
- Lukes P., Locke B., Industrial & Eng. Chem. Res., 44, 2005, 2921-2930
- Lukes P., Water treatment by pulsed streamer corona discharge”, Institute of Chemical Technology, Prague, 2001
- Luster-Teasley S., Ubaka-Blackmoore N., Masten S., J. Hazard. Mat., 167(1-3), 2009, 701-706
- Machala Z., Jedlovsky I., Chladekova L., Pongrac B., Giertl D., Janda M., Sikurova L., Polcic P., Eur. Phys. J. D 54, 2009, 195-204
- Machala Z., Jedlovsky I., Hensel K., Martisovits V., Foltin V., Proc. Hakone X, Saga, Japan, 2006, 277-283
- Magureanu M., Piroi D., Mandache N., David V., Medvedovici A., Bradu C., Parvulescu V., Wat. Res., 45(11), 2011, 3407-3416

- Magureanu M., Piroi D., Mandache N., Parvulescu V., *J. Appl. Phys.*, 104, 2008, 103306-103307
- Mah T., Pitts B., Pellock B., Walker G., Stewart P., O'Toole G., *Nature* 426, 2003, 306-310
- Maier, D., *Ozone et ozonation des eaux*, Tec & Doc, Paris, 1991
- Malik M., Ghaffar A., Malik S., *Plasma Sources Sci. Tech.*, 10, 2001, 82-91
- Malik M., Kolb J., Sun Y., Schoenbach K., *J. Hazard. Mat.*, 197, 2011, 220-228
- Malik M., *Plasma Sources Sci. Tech.* 12, 2003, 26-32
- Malik M., Rehman U., Ghaffar A., Ahmed K., *Plasma Sources Sci. Tech.*, 11, 2002, 236-240
- Marouf-Khelifa K., Abdelmalek F., Khelifa A., Belhadj M., Addou A., Brisset J. L., *Separation and Purification Tech.*, 50(3), 2006, 373-379
- Masten S., Davies S., *J. Contaminant Hydrology*, 28(4), 1997, 327-335
- Matzing H., *Adv. Chem. Phys.*, 80, 1994, 315-402
- McLean P., Reid E., Gurney M., *Biochem. J.*, 91(3), 1964, 464-473
- Meek T. *Introduction to Spectroscopy, Atomic Structure And Chemical Bonding*, Canoe Press, University of West Indies, 1998
- Melke J., Uziak S., Klimowicz Z., *Annales UMCS, Sec. E*, 58, 2003, 111-126
- Menashi W., *Treatment of surfaces*, US Patent 3 383 163, 1968
- Metcalf W., *Br. J. Pharmacol. Chemother.* 19(3), 1962, 492-497
- Mikula M., Panak J., Dvonka V., *Plasma Sources Sci. Tech.* 6, 1997, 179-184
- Miller C., Valentine R., Roehl M., Alvarez P., *J. Hazard. Mat.*, 158(2-3), 2008, 478-484
- Mills A., Wang J., *J. Photochem. Photobiol.*, 127, 1999, 123-134
- Moisan M., Barbeau J., Crevier M., Pelletier J., Philip N., Saudi B., IUPAC, *Pure and Applied Chemistry*, 74, 2002, 349-358
- Moisan M., Barbeau J., Moreau S., Pelletier J., Tabrizian M., Yahia L., *Int. J. Pharm.*, 226, 2001, 1-21
- Moisan M., Barbeau J., Pelletier J., Philip N., Saudi B., *Proc.13th CIP*, 2001a, 12-18
- Mok Y., Jo J., Whitehead C., *Chem. Eng. J.*, 142, 2008, 56-64
- Mok Y., *Plasma Chem. Plasma Process.*, 20, 2000, 495-509
- Montie T, Kelly-Wintenberg K., Roth J., *IEEE Trans Plasma Sci.*, 28(1), 2000, 41-50
- Morar R., Munteanu R., Simion E., Munteanu I., Dascalescu L., *IEEE Trans. On Industry Applications*, 35(1), 1999, 208-212
- Moreau M., Feuilloley M., Orange N., Brisset J. L., *J. Appl. Microbiol.*, 98, 2005, 1039-1046
- Morvova M., Morva I., Hensel K., Pawlat J., Kosutova Z. *Int. COE Forum on Plasma, Sci&Tech.*, Nagoya, Japan, 2004
- Moussa D., Abdelmalek F., Benstaali B., Addou A., Hnatiuc E., Brisset J.-L., *Eur. Phys. J. Appl. Phys.*, 29(2), 2005, 189-199
- Mun S., Cho S., Kim T., Oh B., Yoon J., *Chemosphere*, 77(2), 2009, 285-290

- Naitali M., Kamgang-Youbi G., Herry J., Bellon-Fontaine M., Brisset J.L., Appl. Env. Microbiol., 76, 2010, 7662-64
- Natal-Santiago J., Hill M., Dumesic J., J. Molecular Catalysis A: Chemical, 140, 1999, 199-214
- Nawrocki J., Ochrona Srodowiska, 3(74), 1999, 31-36
- Neagoe G., Brablec A., Rahel J., Slavicek P., Hakone XI, Oléron Island, 2008
- Niewulis A., Podliński J., Kocik M., Barbucha R., Mizeraczyk J., Mizuno A., J. Electrostat. 65(12), 2007, 728-734
- NIST Chemical Kinetics Database, <http://kinetics.nist.gov>
- Njatawidjaja E., Sugiarto A., Ohshima T., Sato M., J. Electrostat., 63, 2005, 353-359
- Njoyim-Tamungang E., Laminsi S., Ghogomu P., Njopwouo D., Brisset J. L., Chem. Eng. J., 173, 2011, 303-308
- Nozaki T., Agiral A., Yuzawa S., Gardeniers J., Okazaki K., Chem. Eng. J., 166(1), 2011, 288-293
- O'Mahony M., Dobson A., Barnes J., Singleton I., Chemosphere, 63(2), 2006, 307-314
- Ohgiyama T., Sato M., Kimura K., Proc. Institute of Electrostatics, Japan, 1991, 253
- Ohkawa H., Akitsu T., Tsuji M., Kimura H., Kogoma M., Fukushima K., Surface and Coatings Tech., 200 (20-21), 2006, 5829-5835
- Onishchenko A., Kamardin I., Radjabov A., Avtonomov T., Golota V., Ibragimov V., Taran P., G., Химическая и биологическая безопасность, 6, 2005, 26-34
- Özkayhan M., J. Helminthology, 80(1), 2006, 15-18
- Ozmen G., Kayana B., Gizir A., Hesenov A., J. Hazard. Mat., 168, 2009, 129-136
- Ozonek J., Ekoinżynieria, 4, 1996, 20-24
- Ozonek J., Laboratorium syntezy ozonu: podstawy procesowe: pomiary elektryczne: ekotechnologie, Lublin, Wydawnictwo Politechniki Lubelskiej, 1993
- Patino J., Delgado M., Fernandez J., Colloids and Surfaces: A, 99, 1995, 65-78
- Pawłat J., Hensel K., Ihara S., Proc. 15th SAPP, Podbanske, Slovakia, 2005b
- Pawłat J., Yamabe C., Pollo I., Proc. Hakone IX, Padua, 2004c
- Pawłat J., 7th Int. Conference Electromagnetic Devices and Processes in Environment Protection - ELMECO-7 joint with 10th Seminar Applications of Superconductors - AoS-10, Nałęczów. Poland, 2011b, 123-124.
- Pawłat J., C. Yamabe, I. Pollo, Appl. Plasma Sci., 7, 1999, 45-51
- Pawłat J., C. Yamabe, I. Pollo, Proc. 2000 National Convention IEEJ, Tokyo, Japan, 1, 2000, 232
- Pawłat J., Diatczyk J., Komarzyniec G., Giżewski T., Stryczewska H. D., Ebihara K., Mitsugi F., Aouqi S., Nakamiya T., IEEE Region 8 UROCON

- 2011 - Int. Conference on Computer as a Tool joint with the Conference on Telecommunications, Lisbon, Portugal, 2011a
- Pawłat J., Diatczyk J., Stryczewska H. D., *Przegląd Elektrotechniczny*, 1, 2011, 245-248
- Pawłat J., Foaming system properties, generation of oxidants for environmental purposes using electrical discharge in foam, PhD Thesis, Saga University, 2001
- Pawłat J., Gizewski T., Stryczewska H. D., Samoń J., *Proc. ICPM4*, Orléans, France, 2012, 187-187
- Pawłat J., Gizewski T., Stryczewska H. D., *Proc. AOTs-17*, San Diego, California, 2011e, 54-54
- Pawłat J., Hayashi N., Ihara S., Yamabe C., Pollo I., *Adv. Env. Res.*, 8, 2004, 351-358
- Pawłat J., Hayashi N., Ihara S., Yamabe C., Pollo I., *Colloids and Surfaces A: Phys.& Eng. Asp.*, 220(1-3), 2003a, 179-190
- Pawłat J., Hayashi N., Ihara S., Yamabe C., Pollo I., *Plasma Chem. & Plasma Proc.*, 23(3), 2003, 569-583
- Pawłat J., Hayashi N., Yamabe C., 7th APCPST & 17th SPSM, Fukuoka, Japan, 2004f, 30P-94
- Pawłat J., Hayashi N., Yamabe C., Pollo I., *Ozone Sci. & Engineering*, 24(3), 2002, 181-191
- Pawłat J., Hensel K., Ihara S., 22nd Symp. Plasma Physics and Technology, Prague, Czech Republic, 2006b
- Pawłat J., Hensel K., Ihara S., *Acta Physica Slovaca*, 55(5), 2005a, 479-485
- Pawłat J., Hensel K., Ihara S., *Czechoslovak J. Physics, Suppl. D*, 56, 2006, B1174-B1178
- Pawłat J., Hensel K., Ihara S., Yamabe C., *Chem. Listy*, 102(16), 2008, 1494-1497
- Pawłat J., Hensel K., Yamabe C., *Czech. J. Phys.*, 54, 2004b, Suppl.C SPPT 332-1
- Pawłat J., Hensel K., Yamabe C., Mizuno A., *Proc. 16th Int. Symp. on Plasma Chemistry*, Taormina, Italy, June, 2003c
- Pawłat J., Hensel K., Yamabe C., Mizuno A., *Proc. 30th IEEE Int. Conference on Plasma Sci. ICOPS 2003*, Cheju, Korea, 2003f
- Pawłat J., Hensel K., Yamabe C., Mizuno A., *Proc. Int. Joint Power Generation Conference IJPGC 2003*, Georgia, USA, 2003d
- Pawłat J., Hensel K., Yamabe C., *Proc. 21th SPPT*, Praha, Czech Republic, 2004g
- Pawłat J., Ihara S. *Plasma Process. Polym.*, 4(7-8), 2007, 753-759
- Pawłat J., Ihara S., Hensel K., Yamabe C., 2nd Central European Symp. on Plasma Chemistry CESPC, Brno (Czech Republic), 2008b
- Pawłat J., Ihara S., Hensel K., Yamabe C., *Proc. HAKONE XI*, Oleron Island, France, 2008c

- Pawłat J., Ihara S., Proc. HAKONE X, Saga, Japan, 2006c
- Pawłat J., Ihara S., Yamabe C., Pollo I., Plasma Proc. Polym., 2(3), 2005, 218-221
- Pawłat J., Ihara S., Yamabe C., Proc. 15th Symp. on Applications of Plasma Processes Liptovský Ján, Slovakia, 2009
- Pawłat J., Ihara S., Yamabe C., Proc. 6th Int. Conference Electromagnetic Devices and Processes in Environment Protection, 2008
- Pawłat J., Inaba T., IEEJ Trans. PE, 123(7), 2003b, 844-851
- Pawłat J., Ishii J., Mineshima H., Inaba T., Proc. 14th National Convention of IEE of Japan, Tokyo, Japan, 2002f, 124
- Pawłat J., Ishii J., Mineshima H., Inaba T., Proc. Workshop on Plasma Diagnostics and Industrial Applications of Plasmas, the Abdus Salam Int. Centre for Theoretical Physics, Miramare, Trieste, Italy, 2002a
- Pawłat J., Ishii J., Mineshima M., Inaba T., Proc. 5th Symp. on Super High Temp. Plasma Characteristics and its Applications to the Environmental Processes, Tokyo, 2002e, 117-126
- Pawłat J., Matsuo T., Ihara S., Proc. 28th ICPIG, Prague, Czech Republic, 2007
- Pawłat J., Mizuno A., Yamabe C., Pollo I. JAOTs, 7(1), 2004a, 59-64
- Pawłat J., Mizuno A., Yamabe C., Pollo I., Proc. 26th Conference of Institute Electrostatics Japan, Toyohashi, Japan, 2002g, 249-252
- Pawłat J., Mizuno A., Yamabe C., Pollo I., Proc. Joint conference of ACED & K-J Symp. on ED and HVE, Seoul, Korea, 2002d, 340-343
- Pawłat J., Mizuno A., Yamabe C., Proc. Conference of Institute Electrostatics Japan, Tokyo, Japan, 2003h
- Pawłat J., Mizuno A., Yamabe C., Proc. ELMECO-4 2003, Nałęczów, Poland, 2003g
- Pawłat J., Mizuno A., Yamabe C., Proc. IEEJ Conference, Saga, Japan, 2002h, 11-15
- Pawłat J., Proc. 5th Seminar on Applications of Superconductivity, Nałęczów, Poland, 2004
- Pawłat J., Proc. First Centr.European Symp. On Plasma Chem., Gdansk, Poland, 2006a
- Pawłat J., Proc.17th Int. Colloquium on Plasma, Marseille, France, 2009a
- Pawłat J., Przegląd Elektrotechniczny, 1, 2005, 17-19
- Pawłat J., Przegląd Elektrotechniczny, 10b, 2012, 139-140
- Pawłat J., Stryczewska H. D., Diatczyk J., Ebihara K., Mitsugi F., Gdańsk Workshop - Progress in New Methods of Water and Waste Water Cleaning, Gdańsk, Poland, 2011f, 9
- Pawłat J., Stryczewska H. D., Ebihara K., Mitsugi F., Aoqui S., Nakamiya T., NATO Advanced Research Workshop - Plasma for Bio-decontamination, Medicine and Food Security, Jasna, Slovakia, 2011d, 109-110

- Pawłat J., Stryczewska H. D., Ebihara K., Proc. 15th Int. Conf. on Advanced Oxidation Technologies for Treatment of Water, Air and Soil, Niagara Falls, New York, USA, 2009b
- Pawłat J., Stryczewska H. D., Int. J. Sci. Eng. & Tech., 2011c, 1002-1007
- Pawłat J., Stryczewska H. D., Mitsugi F., Ebihara K., Aoqui S., Proc. APCPST, Cheju, Korea, 2010
- Pawłat J., Stryczewska H. D., Solar energy for water conditioning, W Ac.. Sci. Eng. Tech. T, 58, 2011g, 872-877
- Pawłat J., The European Physical Journal Applied Physics, 2013, doi:10.1051/epjap/2012120431
- Pawłat J., Yamabe C., 21st Symp. on Plasma Processing, Sapporo, Japan, 2004d, 274-275
- Pawłat J., Yamabe C., Int. COE Forum on Plasma, Sci&Tech., Nagoya, Japan, 2004e
- Pawłat J., Yamabe C., Mizuno A., Pollo I., Proc. 26th Int. Conference on Phenomena in Ionized Gases, Greifswald, Germany, 2003e
- Pawłat J., Yamabe C., Pollo I., Proc. VII Ogólnopolskie Sympozjum Chemii Plazmy, Kazimierz, Polska, 2002c
- Pawłat J., Yamabe C., Pollo I., Proc. VIIIth Int. Symp. on High Pressure Low Temperature Plasma Chemistry, Puhajarve, Estonia, 2002b, 327-331
- Pawłat J., Yamabe C., Pollo I., VIII Ogólnopolskie Sympozjum Chemii Plazmy, Słok, Poland, 2004h
- Petri B., Watts R., Teel A., Huling S., Brown R., in "In Situ Chemical Oxidation for Groundwater Remediation" Siegrist R., Crimi M., Simpkin T. (Eds), SERDP/ESTCP Environmental Remediation Technology, 3, 2011, Springer Science+Business Media, ISBN: 978-1-4419-7825-7
- Peyrous R., Held B., Pignolet P., Papers of Technical Meeting on Electric Discharges, Tokyo, ED, 87-63, 1987, 95-109
- Pierpoint A., Hapeman C., Torrents A., Chemosphere, 50(8), 2003, 1025-1034
- Pollo I., BOSE, 21(2), 1999, 177-186
- Pollo I., Jagkiewicz Z., Malicki J., Nuclear and Chemical Waste Management, 1981, 315-317
- Pongrác B., Machala Z., IEEE Trans. Plasma Sci. 39, 2011, 2664-2665
- Pozin M., Muchlenow I., Tarat E., Pianowe oczyszczalniki gazu, wymienniki ciepła i absorbery, WNT, Warszawa, Poland, 1962.
- Pryor A., Method for treatment of top soil of a field with ozone gas to increase growth of plants, United States Patent 6173527
- Pschera S., Abwasserbehandlung mit Ozon (R. Oldenbourg) Verlag, München, Germany, 1997
- Pugh R., Adv. in Colloid and Interface Sci., 64, 1996, 67-142
- Randorn C., Wongnawa S., Boonsin P., Sci. Asia, 30, 2004, 149-156
- Raniszewski G., Kołaciński Z., Szymański Ł., Electrical Review, 88(8), 2012a, 1-5

- Raniszewski G., Kołaciński Z., Szymański Ł., JAOT, 15(1), 2012, 34-40
- Rauf M., Ashraf S., J. Hazard. Mater., 166, 2009, 6-16
- Rinaldi L., Biggeri A., Carbone S., Musells V., Catelan D., Veneziano V., Cringoil G., BMC Vet. Res., 2(29), 2006, 1-6
- Ristenpart W., Aksay I., Saville D., Langmuir 23, 2007, 4071-4080
- Rivas J., Gimeno O., de la Calle R., Beltrán F., J.Hazard. Mat., 169(1-3), 2009, 509-515
- Rokkaku K., Fukawa F., Suzuki S., Itoh H., IEEJ Transactions on Fundamentals and Materials, 2012- in print
- Rosenfeldt E., Linden K., Canonica S., Gunten U., Wat. Res., 40, 2006, 3695-3704
- Ross P., Nelson P., Richard J., Osweiler G., Rice L., Plattner R., Wilson T., Appl. & Env. Microbiol, 56(10), 1990, 3225-3226
- Samoń R., Pawłat J., Prace Instytutu Elektrotechniki, 249, 2011, 191-204
- Sano N., Yamamoto D., Kanki T., Ind. Eng. Chem. Res., 42, 2003, 5423-5428
- Schaper L., Deilman M., Graham W., Stalder K., Hakone XI, Oléron Island, 2008
- Schmidt-Szałowski K., Krawczyk K., Sentek J., Ulejczyk B., Górská A., Młotek M., Chem. Eng. Research and Design, 89, 2011, 2643-2651
- Segvic M., Pepeljnjak S., Vet. Arhiv., 71(5), 2001, 299-323
- Sengupta S., Srivastava A., Singh R., J. Electroanalytical Chem., 427(1-2), 1997, 23-27
- Sentek J., Krawczyk K., Młotek M., Kalczewska M., Kroker T., Kolb T., Schnek A., Gericke K., Schmidt-Szałowski K., Appl. Catalysis B: Environmental, 94, 2010, 19-26
- Shang K. Wang F., Li J., Proc. 4th Int. Conference on Bioinformatics and Biomedical Engineering (iCBBE), 2010
- Sharma A., Josephson G., Camaioni D., Goheen S., Environ. Sci. Technol. 34(11), 2000, 2267-2272
- Shen Y., Lei L., Zhang X., Zhou M., Zhang Y., J. Hazard. Mat., 150, 2008, 713-722
- Shi J., Bian W., Yin X., J. Hazard. Mat., 171, 2009, 924-931
- Shin S., Kim S., Kim H., Park C., J. Photochemistry and Photobiology A: Chemistry, 143, 2001, 11-16
- Shiratori S., Inami Y., Kikuchi M., Thin Solid Films, 393, 2001, 243-248
- Shubo H., Ralin D., Jun W., Xin L., Zhou F., Langmuir, 19, 2003, 8943-8950
- Spaulding E., Chemical disinfection of medical and surgical materials. In: Lawrence, C., Block SS, eds. Disinfection, sterilization, and preservation. Philadelphia: Lea & Febiger, 1968, 517-531
- Spaulding E., E. J. Hosp. Res. 9, 1972, 5-31
- Srinivasan B., Palanki S., Grymonpre D., Locke B., Chem. Eng. Sci., 56(3), 2001, 1035-1039

- Stahelin, J., Hoigne, J. *Environmental Science and Technology*, 19, 1985, 1206-13
- Stara Z., Krcma F., Nejezchleb M., Skalny J., *Desalination*, 239, 2009, 283-294
- Steelman V., *Aorn J.* 55, 1992, 773-787
- Stryczewska H. D., Diatczyk J., Pawłat J., *JAOTs*, 14(2), 2011, 276-281
- Stryczewska H. D., Ebihara K., Takayama M., Gyoutoku Y., Tachibana M., *Plasma Process. Polym.*, 2, 2005, 238-245
- Stryczewska H. D., Pawłat J., Ebihara K., Ikegami T., Mitsugi F., Sakai T., Teiji S., *Przegląd Elektrotechniczny*, 88(6), 2012, 92-94
- Stryczewska H. D., *Technologie Plazmowe w Energetyce i Inżynierii Środowiska*, Wydawnictwo Politechniki Lubelskiej, Lublin, 2009
- Suarasan I., Ghizdavu L., *J. Electrostat.*, 54, 2002, 207-214
- Sugiarto A., Ito S., Ohsima T., Sato M., Skalny J., *J. Electrostat.*, 58, 2003, 135-145
- Sugiarto A., Sato M., *Thin Solid Films* 386, 2001, 295-299
- Sun B., Sato M., Clements J., *J. Env. Sci.*, 34, 2000, 509-513
- Sun B., Sato M., Clements J., *J. Phys. D: Appl. Phys.*, 32, 1999, 1908-1915
- Sunka P., Babicky V., Clupek M., Lukes P., Simek M., Schmidt J., Cernak M., *Plasma Sources Sci. Tech.*, 8, 1999, 258-265
- Sunka P., Fuciman M., Babickj V., Clupek M., Benes J., Pouckova P., Soucek J., *Czechoslovak J. Physics, Suppl. D.*, 52, 2002, 397-405
- Sunka, P., *Phys. Plasmas*, 8, 2001, 2587-2594
- Swamy H., Smith T., MacDonald E., *J. Anim. Sci.*, 82, 2004, 2131-2139
- Tajima R., Ehara Y., Kishida H., Ito T., *Proc. 2000 National Convention I.E.E. of Japan*, Tokyo, Japan, 1, 2000, 214
- Takahashi T., Mizuno T., Ayabe M., Yamamoto K., *Proc. 13th Ozone World Congress*, Kyoto, Japan, 1997, 449-454
- Takayama M., Ebihara K., Stryczewska H. D., Ikegami T., Gyoutoku Y., Kubo K., Tachibana M., *Thin Solid Films*, 506-507, 2006, 396-399
- Temnikov A., Sokolova M., Orlov A., *Hakone XI*, Oléron Island, 2008
- Tomizawa S., Tezuka M., *Plasma Chem. Plasma Process.*, 27, 2007, 486-495
- Tremblay L., Kohl S., Rice J., Gagne J., *Marine Chem.*, 96, 2005, 21-34
- Tsagou-Sobze E., Moussa D., Doubla A., Hnatiuc E., Brisset J. L., *J. Hazard. Mat.*, 152, 2008, 446-449
- Tuhkanen T., Kainulainen T., Vartiainen T., Kalliokoshi P., *Ozone Sci. & Eng.*, 16, 1994, 367-383
- Tzortzakis N., Singleton I., Barnes J., *Postharvest Biology and Technology*, 47, 2008, 1-9
- U.S. Department of Health and Human Services. *Registry of Toxic Effects of Chemical Substances (RTECS, online database)*. National Toxicology Information Program, National Library of Medicine, Bethesda, MD, 1993
- Ushakov V., *Impulse Breakdown of Liquids Power Systems*, Springer, 2007

- Van Der Zee F., Dubbelman T., Van Steveninck J., *Free Radical Research*, 2(4-6), 1987, 279-284
- Van der Zee F., Lettinga G., Field J., *Chemosphere*, 44(5), 2001, 1169-1176
- Vandenberk S., Peeters J., *J. Photochemistry and Photobiology A: Chemistry*, 6272, 2003, 1-6
- Venkatadri R., Peters R., *Hazard. Waste Hazard. Mater.*, 10(2), 1993, 107-148
- Vinogradov I., Wieseemann K., *Proc. HAKONE VI Conference, Cork, Ireland*, 1998, 221-224
- Vladimirova T., Morgunova E., *J. Chem. Soc. Faraday Trans.*, 91, 1995, 681-686
- Vleugels M., Shama G., Deng X., Greenacre E., Brocklehurst T., Kong M., *IEEE Trans Plasma Sci.*, 33, 2005, 824-828
- Voloshin A., Sharipov G., Kazkov V., Tolstikov G., *Bulletin of the Academy of Sci. USSR Division of Chemical Sci.*, 35(11), 1986, 2397-2399
- Walling C., *Accounts Chem. Res.*, 8, 1975, 125-131
- Walling C., Weil T., *Int. J. Chem. Kin.*, 6, 1974, 507-516
- Wan J., Coventry J., Swiergon P., Sanguansri P., Versteeg C., *Trends in Food Sci.&Tech.* 2009, 1-11
- Wang F., Li J., Yan W., Wang W., Li G., *High Voltage Eng.*, 33, 2007, 124-127
- Wang L., *J. Hazard. Mat.*, 171, 2009, 577-581
- Watanabe K., Imai S., Mori Y., *Jap. Chem. Eng. Sci.* 60(17), 2005, 4846-4857
- Watts R., *J. Remediation*, 2(4), 1992, 413-425
- Watts R., Udell M., Rauch P., Leung S., *Hazard. Waste and Hazard. Mat.*, 7(4), 1990, 335-345
- Wing N., Lauren D., Bryden W., Burgess L., *Nat. Toxins.*, 1(4), 1993, 229-34
- Wirtz K., *US/German Environmental Chamber Workshop Riverside*, 1999
- Wolcott R., Ehrlich G., *JAMA*, 299(22), 2008, 2682-2684
- Wüthrich R., Mandin P., *Electrochimica Acta*, 54, 2009, 4031-4035
- Yamatake A., Angeloni D., Dickson S., Emelko M., Yasuoka K., Chang J., *JJAP*, 45(10B), 2006, 8298-8301
- Yang B., Lei L., Zhou M., *Chinese Chemical Letters*, 15(10), 2004, 1215-1218
- Yang B., Zhou M., Lei L., *Chemosphere*, 60, 2005, 405-411
- Yang H., Tezuka M., *J. Environmental Sci.*, 23(6), 2011, 1044-1049
- Yang Y., Cho Y., Fridman A., *Plasma Discharge in Liquid: Water Treatment and Applications*, CRC Press Taylor & Francis Group, 2012
- Yang Y., *Plasma Discharge in Water and Its Application for Industrial Cooling Water Treatment*, Drexel University, USA, 2011
- Yerokhin A., Nie X., Leyland A., Matthews A., Dowey S., *Surface and Coatings Tech.*, 122, 1999, 73-93
- Yerokhin A., Pilkington A., Matthews A., *J. Materials Proces. Tech.*, 210, 2010, 54-63
- Yu D., Kang N., Bae W., Banks K., *Chemosphere*, 66(5), 2007, 799-807

-
- Yu H., Perni S., Shi J., Wang D., Kong M., Shama G., *J. Appl. Microbiology*, 101, 2006, 1323-1330.
- Yvin J., Coste C., Method and system for the treatment of seeds and bulbs with ozone, United States Patent 5703009
- Zhang J., Chen J., Li X., *J. Wat. Res. and Protection*, 1(2), 2009, 99-109
- Zhang L., Sun B., Zhu X., *J. Electrostat.*, 67, 2009a, 62-66
- Zhang R., Wang L., Zhang C., Nie Y., Wu Y., Guan Z., *IEEE Trans. Plasma Sci.*, 34, 2006, 1033-1037
- Zhang Y., Zheng J., Qu X., Chen H., *Chemosphere*, 60, 2008, 1518-1524
- Zhang Y., Zhou M., Hao X., Lei L., *Chemosphere*, 67, 2007, 702-711
- Zhang Y., Zhou M., Lei L., *Chem. Eng. J.*, 132, 2007a, 325-333
- Zhao L., Adamiak K., *IEEE Trans. on Industry Applications*, 45(1), 2009, 16-21
- Zhao W., Shi W., Wang D., *Chemosphere*, 57, 2004, 1189-1199
- Zhou T., Lu X., Wang J., Wong F., Li Y., *J. Hazard. Mat.*, 165, 2009, 193-199
- Zollinger H., *Color Chemistry*, VCH, Weinheim, 1987

Figures

- Fig. 2.1. Possible initiation mechanisms at the metal/liquid interface: avalanches in the liquid phase (A), ion conduction and nucleation by joule heating (B), cavity or crack created by electrostatic pressure (C), breakdown of an oxide layer or local electrode melting and plasma spot formation (D) (Ceccato, 2009)
- Fig. 2.2. Summary of the physical processes at the plasma/liquid interface (Ceccato, 2009)
- Fig. 2.3. Main molecular species in humid air plasma (Doubla et al., 2008)
- Fig. 2.4. Chemical radical production path in water plasma discharges (Bruggeman and Leys, 2009)
- Fig. 2.5. Plasma underwater, overwater, inside bubbles (Bruggeman and Leys, 2009; Ceccato, 2009)
- Fig. 2.6. Capillary discharge reactor configurations (Bruggeman and Leys, 2009; Ceccato, 2009)
- Fig. 2.7. Diaphragm discharge reactor configuration (Bruggeman and Leys, 2009; Ceccato, 2009; Neagoe et al. 2008)
- Fig. 2.8. Configurations of plasma overwater reactor (Bruggeman and Leys, 2009; Ceccato, 2009)
- Fig. 2.9. Gas injection reactor configuration (Bruggeman and Leys, 2009; Ceccato, 2009)
- Fig. 2.10. Glow discharge electrolysis reactors (Bruggeman and Leys, 2009; Ceccato, 2009)
- Fig. 2.11. Experimental set-ups of the glidarc plasma (E-electrodes) (Abdelmalek, 2003; Abdelmalek et al., 2004; Burlica et al, 2006)
- Fig. 2.12. Glow discharge electrolysis (GDE) (Choi et al., 2006a)
- Fig. 2.13. Contact glow discharge electrolysis (CGDE) (Wang, 2009)
- Fig. 2.14. Typical appearance of plasma discharge during EPP treatment. The optical emission from the discharge is characteristic of electrolyte composition (e.g. Zn^{2+} in this illustration) (Yerokhin et al., 2010)
- Fig. 2.15. The schematic diagram of corona above water reactor (Bian et al., 2009; Grabowski et al., 2006)
- Fig. 2.16. Experimental set-up with corona-liquid reactor (Dors et al., 2006)
- Fig. 2.17. The schematic diagram of electrostatically atomized ring-mesh reactor (Njatawidjaja et al., 2005; Shi et al., 2009)
- Fig. 2.18. The schematic diagram of cylindrical wetted-wall reactor (Sano et al., 2003; Shi et al., 2009)
- Fig. 2.19. Illustration of brush-plate electrical discharge reactor (Chen et al., 2009)
- Fig. 2.20. Diagram of DBD experimental apparatus (Mok et al., 2008)

- Fig. 2.21. The schematic diagram of dielectric barrier gas-liquid discharge reactors: DBD with mesh (A) and water falling DBD (B) (Zhang et al., 2008; Dojcinovic et al., 2011)
- Fig. 2.22. Configuration of diaphragm discharge. Schema of set-up (A), ideogram of process (B), reactor (C) (Kozakova et al., 2010; Stara et al., 2009)
- Fig. 2.23. Photographs of liquid phase discharge at different voltage. From left to right, the peak voltages are 22, 24, 26kV, Q_{air} 200ml/min (Zhang et al., 2009a)
- Fig. 2.24. Schematic diagram of HDBW reactor (A), HDAW reactor (B) and GD reactor (C) (Zhang et al., 2007; 2007a). HDBW-reactor with both electrodes submerged into liquid phase, HDAW-reactor with high voltage hollow electrodes immersed in water whereas the ground electrode placed over water, GD-reactor with pulsed high voltage electrodes in the gas phase above water level and the ground electrode submerged into liquid
- Fig. 2.25. Discharge modes in HDBW reactor (A), HDAW reactor (B) and GD reactor (C) (Zhang et al., 2007; 2007a)
- Fig. 2.26. Schemat of reactor configurations: (A) reference reactor, (B) series reactor and (C) parallel reactor (Kusic et al., 2005)
- Fig. 2.27. Streamer discharge with electrode gap 45mm (A), spark with streamer discharge with electrode gap 15mm (B) spark discharge with electrode gap 6mm (C) (Sugiarto and Sato, 2001) cited by (Ceccato, 2009; Locke et al., 2006)
- Fig. 2.28. Schematic representation of the plasma microreactor (A), microplasma generated in the glass tube (B), thermal image of the reactor during reaction conditions without external cooling (C) (Agiral et al., 2011)
- Fig. 2.29. Examples of microplasma reactors working in humid environments, (A) - (Nozaki et al., 2011), (B) - (Imasaka et al., 2008)
- Fig. 2.30. Foaming column
- Fig. 2.31. Cylindrical foaming column
- Fig. 2.32. Pulse power sources: schematic wiring (A), set-up with rotary spark-gap (B), set-up with coaxial cable (C)
- Fig. 2.33. Regimes of cylindrical plasma reactor: (A) - for discharge in water (submerged electrodes), (B) - bubbling, (C) - foaming
- Fig. 2.34. The bubble structure while departing from the diffuser
- Fig. 2.35. Photographs of spatial development of the discharge in flat foaming column taken by ICCD camera in dependence on charging voltage for the NP electrode (A) and ND electrode (B), airflow rate 10l/min
- Fig. 2.36. Digital photo of the electrical discharge in cylindrical foaming column

- Fig. 2.37. The electrical waveforms (A, B, D, E) and instantaneous power (C, F) of the discharges in the NP (I) and ND electrode (II) set-ups. Airflow rate: 8l/min, 14kV of applied voltage
- Fig. 2.38. Typical applied voltage and current waveforms of the discharge in oxygen (A), air (B). Electrical supply with rotary spark gap, gas flow rate 5l/min, input power 40W
- Fig. 2.39. Cross section of the single foam bubble with the proceeding processes
- Fig. 2.40. Emission intensity in foam, applied voltage: 15kV, substrates: argon and pure water
- Fig. 2.41. Hydrogen peroxide concentration in dependence on frequency and time (for water submerged electrodes, bubbling and foaming)
- Fig. 2.42. Dissolved ozone concentration in dependence on frequency and time (water submerged electrodes, bubbling and foaming)
- Fig. 2.43. Gaseous ozone concentration in cylindrical foaming column in dependence on the gas flow. Total power 40W
- Fig. 2.44. The comparison of the instantaneous input energy versus $O_{3(aq)}$ concentration obtained in the flat type reactor in dependence on electrode configuration at 8l/min oxygen flow rate (NP - needle-to-metal plate electrode, ND - needle-to-dielectric covered metal plate electrode, PD - metal plate-to-dielectric covered metal plate electrode)
- Fig. 3.1. Degradation pathways of phenol by pulsed electrical discharges under conditions of oxygen-containing ozone gas bubbling. $V=25kV$, $f=60Hz$, discharge gap 30mm, $[Phenol]_0=50mg/l$. (A) Attack of oxygen on phenol; (B) ozone addition to phenol (Joshi et al., 1995; Shen et al., 2008; Zhang et al., 2009)
- Fig. 3.2. Concentrations of phenol and dihydroxyphenols in the aqueous phase during DC positive corona discharge processing. Discharge current $75\mu A$. Gas flow rate 1l/min. Initial phenol concentration 0.027mM (Dors et al., 2006)
- Fig. 3.3. Positive pulse streamer corona reactor for phenol treatment (Dors, 2007)
- Fig. 3.4. Concentrations of phenol in phenol-polluted water of different conductivities: $1\mu S/cm$, $200\mu S/cm$, $600\mu S/cm$. Initial phenol concentration 0.62mM, without addition of iron salts (A) and with initial concentration of Fe_2SO_4 0.08mM (B). Water amount $500cm^3$. Pulse energy 0.7J (Dors et al., 2007)
- Fig. 3.5. Comparison of 4-CP removal in each electrical reactor, input voltage 16kV, pulsed repetition rate 100Hz, electrode distance 20mm, oxygen flow rate $0.2m^3/h$, initial pH 5.4, initial conductivity at $1.5\mu S/cm$ (Zhang et al., 2007a)

- Fig. 3.6. Formation of byproducts in each electrical reactor: 4-chlorocatechol and hydroquinone (Zhang et al., 2007a)
- Fig. 3.7. Effect of bubbling gas on 4-CP degradation and yields of formic, acetic, oxalic, propanoic and maleic acid (Bian et al., 2009)
- Fig. 3.8. Decolourisation rate (in %) of BTB with the treatment time (with and without added azide) (Doubla et al., 2008)
- Fig. 3.9. pH evolution of the plasma treated BTB solutions against the treatment time (with and without added azide) (Doubla et al., 2008)
- Fig. 3.10. Temporal variations of the absorbance at 484 (chromaticity) and 310nm (vibration of naphthalene rings in the dye molecules) for three degradation conditions (Mok et al., 2008)
- Fig. 3.11. Absorption spectra of dye solution (Direct Red 79, initial concentration 12 mg/dm^3) recorded during the diaphragm discharge treatment in the anode (A) and cathode part (B) of the reactor (input power of 160W) (Kozakova et al., 2010)
- Fig. 3.12. Comparison of dye decomposition by diaphragm discharge and pure electrolysis in the 5M NaCl solution, (Direct Red 79, initial concentration of 12 mg/dm^3 , conductivity of $600 \mu\text{S/cm}$, discharge current of 100mA, electric power in discharge regime of 160W, electric power in electrolysis regime of 40W) (Stara et al., 2009)
- Fig. 3.13. Relative concentration decrease of organic dyes with various chemical structure: according to the dye class (A), and according to the dye colour (B) during the negative discharge treatment (initial dye concentration of approximately 12 mg/dm^3 in a 4mM NaCl solution, input power of 160W) (Stara et al., 2009)
- Fig. 3.14. PBB decolourisation in different electrolytic solutions (Wang, 2009)
- Fig. 3.15. Reactive Black: effect of initial pH value on the decolourisation efficiency (A), visible absorption spectra (initial dye concentration 40.0 mg/dm^3 , initial pH 9.00, after 24h of treatment time) (B), change in the solution pH and conductivity values during the reaction process for different initial pH (after 5min of treatment time) (C), effects of residence time on absorbance for λ_{max} after introduction the energy density in the solution of 45 and 90 kJ/dm^3 (absorbance of initial solution, before the plasma treatment 0.475, $c_0=40.0 \text{ mg/dm}^3$, initial pH 9.00) (D) (Dojcinovic et al., 2011)
- Fig. 3.16. Cylindrical foaming column (A). The photograph of foaming reactor (EV foam) (B) and MO foam (C). Oscillograms of the discharge in EV foam (substrate gas: oxygen) (D)

- Fig. 3.17. Ethyl Violet: molecular structure (A), absorbance peak (B), purification of EV solution (C), removal of COD (dodecyl solution and Ethyl Violet, substrate gas- oxygen) (D)
- Fig. 3.18. Methylene Blue: molecular structure (A), the decomposition of MB in dependence on supplied gas (30 Hz) (B) and frequency (air) (C)
- Fig. 3.19. Indigo Blue: molecular structure (A), decomposition of IB in water, bubbling and foaming systems at 60 Hz (B). Foam: decomposition of IB in dependence on supplied gas (30Hz) (C) and frequency (air) (D)
- Fig. 3.20. Molecular structure of MO (A) and removal of color caused by MO in dependence on electrical discharge frequency in foam
- Fig. 3.21. Removal rate of MB, IB and HA versus total discharge power, frequency 30Hz
- Fig. 3.22. Chemical structure of TWEEN-20 (A), TRITON-100 (B), polyoxyethylene nonylphenyl ether (C), dodecyl sodium sulfate (D). Photograph of the foaming process in P5NPE solution (E) (<http://chemicaland21.com>; www.sigmaaldrich.com; www.mpbio.com)
- Fig. 3.23. Change of COD in dependence on the treatment time
- Fig. 3.24. Absorption of acetaldehyde within foam with addition of Triton X-100 versus time (A) and change in acetaldehyde concentration after application of electrical discharge to the saturated solution (power with losses included, [W]) (B)
- Fig. 3.25. COD in dependence on the treatment time at the lower pulse energy (P5NPE)
- Fig. 4.1. Photographs of the plasma jet generated in RF powered device with different flow of air. P=80W, 12.98MHz frequency
- Fig. 4.2. Block diagram of integrated system for soil treatment
- Fig. 4.3. Ozone generators used in the soil sterilization system: screw type ozonizer (A), OP-20W ozonizer (B)
- Fig. 4.4. Ozonized water distribution system
- Fig. 4.5. Experimental set-up for general soil treatment (A), ceramic diffuser (B), multi-electrode injection system (C), set-up for sterilization of pathogens within soil (D)
- Fig. 4.6. Ozone diffusion into soil
- Fig. 4.7. Changes of pH and electrical conductivity during and after soil ozonation
- Fig. 4.8. Average DRO concentrations from the soil column as a function of ozone injection time and cumulative ozone mass (A). Relative concentrations of diesel range alkanes as a function of ozone injection time at the (B) former (near the gas inlet), and (C) later (near post-reaction gas outlet) part of the soil column (the initial concentrations of C₁₀, C₁₂, C₁₄, C₁₆, C₁₈, C₂₀, C₂₂, and C₂₄ were 228, 223, 273, 225, 189, 160, 110, and 78mg/kg soil, respectively) (Yu et al., 2007)

- Fig. 4.9. Comparison of percent pyrene removal in pH 6 for dry soils (blue), 5% moisture (black), and 10% moisture (white) at various ozone doses (Luster-Teasley et al., 2009)
- Fig. 4.10. Set up for ozone treatment of DNA solution
- Fig. 4.11. AFM image of DNA sample prepared on mica substrate (A) before ozonation, (B) after ozonation
- Fig. 4.12. Ozone concentration vs. efficiency for screw-type ozonizer, (10kHz, 15°C) (A), sterilization rate as a function of ozone amount (B)
- Fig. 4.13. Influence of soil pre-ozonation on spinach

Tables

- Tab. 2.1. Summary of the characteristics of pulsed corona, pulsed arc and pulsed spark discharge in water (Yang, 2011; Yang et al., 2012)
- Tab. 2.2. Advanced oxidation processes (Anotai et al., 2010; Bremner et al., 1996; Kwon et al., 2009; Nawrocki, 1999; Venkatadri and Peters, 1993)
- Tab. 2.3. Basic reactions involving oxidative compounds in humid environment (Dors et al., 2005; Chen et al., 2002; 2009; Grymonpre et al., 2001; Mok et al., 2008)
- Tab. 2.4. Properites of selected species involved in AOPs (Buxton et al., 1988; Lide, 2006; Petri et al., 2011)
- Tab. 2.5. Selected chemical and physical phenomena due to the electrical discharge in dense medium
- Tab. 3.1. Examples of most absorbed wavelengths for selected dyes (saujanya.com; stainsfile.info; Stara et al., 2009; Van der Zee et al., 2001)
- Tab. 3.2. Basic reactions induced by corona discharge directly involved in phenol decomposition (Dors et al., 2005)
- Tab. 3.3. Typical images, voltage and current pulses of pulsed positive streamer discharge in phenol-polluted water of different conductivities: (A) 1 μ S/cm, (B) 200 μ S/cm, (C) 600 μ S/cm. Initial phenol concentration 0.62mM. Pulse energy 0.7J (Dors et al., 2007)
- Tab. 3.4. Treatment of phenol solution in corona reactors (Kusic et al., 2005)
- Tab. 3.5. Decolourisation in diaphragm discharge (Kozakova et al., 2010; Kuzhekin, 1995; Stara et al., 2009).
- Tab. 4.1. *Fusarium* mycotoxins
- Tab. 4.2. Soil sterilization by in-situ ozone treatment

Streszczenie

Wyładowania elektryczne w środowiskach wilgotnych: generatory, zjawiska, zastosowania

Rozwój przemysłu niesie za sobą ryzyko powstania zanieczyszczeń chemicznych i mikrobiologicznych powietrza, wody i gleby. Mimo ustalenia dopuszczalnych norm emisji polutantów, wysiłków kadry naukowo-badawczej oraz nakładów finansowych często spotyka się przypadki przekraczania chwilowych dopuszczalnych ich stężeń, zwłaszcza w przypadku dużych zakładów produkcyjnych lub oczyszczalni ścieków. Konieczne jest prowadzenie badań nad nowymi, efektywnymi technologiami kontroli zanieczyszczeń, pozwalającymi tanio i skutecznie rozwiązać problem ich rozkładu, m.in. w przypadku związków wielkocząsteczkowych i trudnobiodegradowalnych; gdy klasyczne oczyszczanie chemiczne i biologiczne nie jest wystarczające. Coraz bardziej popularną alternatywą, lub niejednokrotnie koniecznym etapem procesu puryfikacji mediów stają się procesy zaawansowanego utleniania (ang. advanced oxidation processes - AOP). W procesach tych głównym czynnikiem aktywnym są biodegradowalne, silne utleniacze, które nie przyczyniają się do powstania zanieczyszczeń wtórnych. Do kategorii AOP zaliczyć można symultaniczne stosowanie takich związków jak ozon, woda utleniona, rodniki hydroksylowe, promieniowanie UV, promieniowanie gamma, katalizatory, itd.

Ozon (O_3) nie może być przechowywany ze względu na krótki czas rozpadu oraz wysoką reaktywność i musi być wytwarzany na miejscu jego stosowania. Zwykle ozon generowany z suchego gazu substratowego (powietrze, tlen), w reaktorach plazmowych (najczęściej na drodze wyładowań barierowych) jest następnie transportowany do miejsca wykorzystania i dystrybuowany w komorze reakcyjnej poprzez sieć rur i dyfuzorów. W ciągu ostatniej dekady poszukiwano rozwiązań, które pozwoliłyby uniknąć strat wynikających z konieczności przesyłu utleniaczy a także umożliwiły uproszczenie budowy układów oczyszczania. Istnieje wiele zanieczyszczonych mediów (w tym również wilgotne gazy oraz ciecze), w których, dzięki zastosowaniu reaktorów o specjalnej konstrukcji byłoby możliwe jednoczesne prowadzenie obydwu procesów: generacji utleniaczy i usuwania zanieczyszczeń w tej samej przestrzeni reakcyjnej, min. przy użyciu wyładowań elektrycznych zachodzących bezpośrednio w oczyszczanym ośrodku. Badania wzajemnych interakcji w układach ciecz-gaz oraz zachodzące w nich podczas wyładowań elektrycznych zjawiska stały się dziś ważnym działem inżynierii elektrycznej i chemicznej.

Prezentowana monografia ma na celu przybliżenie i popularyzację wyładowań elektrycznych generowanych w cieczach, pianach i wilgotnych gazach, jako faktycznego i potencjalnego środowiska przebiegu różnorodnych procesów

technologicznych, jak również prezentację możliwości poszczególnych układów w aspekcie generowania utleniaczy i usuwania zanieczyszczeń. W pracy omówiono podstawowe procesy inicjujące wyładowania elektryczne w środowiskach wilgotnych oraz kolejne etapy ich przebiegu. Ponadto podano podstawowe kryteria klasyfikacji wyładowań pod względem parametrów fizykochemicznych oraz rodzaju ośrodka, w którym przebiega proces.

Prezentowana monografia przybliży również istniejącą wiedzę na temat generowania środków utleniających, podaje ich ogólną charakterystykę a także wiele przykładów zastosowań technik zaawansowanego utleniania. Omówiono nowe rodzaje plazmotronów, zwanych hybrydowymi, których geometria oraz układ zasilania pozwalają na otrzymanie wyładowania elektrycznego w wilgotnym medium.

Szczególną uwagę poświęcono w pracy dziedzinie badań zainicjowanych przez autorkę - wyładowaniom elektrycznym w pianach. Piany uzyskane poprzez dodatek surfaktantów lub też bez ich użycia (w reaktorach, gdzie zachowane są odpowiednie parametry przepływu gazu i cieczy), pozwalają na zwiększenie transportu masowego na granicy faz ciecz-gaz i powinny one znaleźć się w centrum uwagi badaczy. To nowatorskie rozwiązanie umożliwia otrzymanie kilku utleniaczy w jednej komorze reakcyjnej, zaś zanieczyszczenia mogą być zawarte zarówno w fazie gazowej jak i w ciekłej. W monografii przedstawiono wyniki badań własnych nad konstrukcją plazmotronów pianowych, ich zasilaniem, charakterystyką zachodzących w nich wyładowań elektrycznych oraz ich ścisłą zależnością od parametrów fizycznych pian i składu chemicznego substratów pianowych. Zaprezentowano również wyniki pomiarów substancji utleniających generowanych w pianach takich jak ozon gazowy i rozpuszczony, nadtlenek wodoru, rodniki OH oraz możliwości usuwania wybranych zanieczyszczeń organicznych: barwników, substancji powierzchniowo czynnych, kwasów humusowych oraz substancji lotnych. Dokonano porównania skuteczności systemu pianowego z innymi eksperymentalnymi systemami wyładowań elektrycznych w układach ciecz-gaz na podstawie danych literaturowych i badań własnych. Wilgotne środowisko, stworzone przez system pianowy jest interesującą i stosunkowo tanią alternatywą dla konwencjonalnych metod generowania utleniaczy. W pianie możliwe jest poprawienie procesu oczyszczania chemicznego poprzez zwiększenie powierzchni kontaktu między poszczególnymi fazami. Obecność różnych rodzajów utleniaczy prowadzi do metod AOP, co potencjalnie zapewnia intensyfikację procesów rozkładu i neutralizacji zanieczyszczeń. Kolumna pianowa łączy więc ideę generatora związków utleniających oraz komory reakcyjnej. Transport utleniaczy do miejsca zastosowania i spowodowane tym straty mogą być pominięte, ponieważ system pianowy umożliwia generowanie utleniaczy *In situ*, nawet w oczyszczanym medium. Należy zaznaczyć, że nigdy dotąd nie prowadzono badań dotyczących wyładowań elektrycznych w pianie oraz ich praktycznego zastosowania do rozkładu polutantów.

W ostatniej części monografii wskazano nowe kierunki wykorzystania plazmy w środowiskach wielofazowych takie jak medycyna, biotechnologia, rolnictwo i przemysł spożywczy. Szczególną uwagę poświęcono zastosowaniu ozonu i technik plazmowych do kondycjonowania gleby. Na przykładzie badań prowadzonych przez grupę badawczą, do której należy autorka omówiono wpływ ozonu na parametry fizykochemiczne gleby, wybrane mikroorganizmy chorobotwórcze przynoszące straty w rolnictwie a także na wzrost niektórych gatunków roślin.

Wprowadzenie reaktorów hybrydowych do poszczególnych gałęzi przemysłu wymaga jednak dalszych badań nad ich bezpieczeństwem, standaryzacją i optymalizacją parametrów zasilania elektrycznego tak, by zmaksymalizować efektywność energetyczną.